Supporting Information

Rapid Non-Invasive Skin Monitoring by Surface Mass Recording and Data Learning

Yingdi Zhu,[1] Andreas Lesch,[2] Xiaoyun Li,[3,4] Tzu-En Lin,[5] Natalia Gasilova,[1] Milica Jović,[1] Horst Matthias Pick,[6] Ping-Chih Ho,[3,4] Hubert H. Girault[1]*

[1]Institute of Chemical Sciences and Engineering, School of Basic Science, École Polytechnique Fédérale de Lausanne, 1015 Lausanne, Switzerland.

[2]Department of Industrial Chemistry "Toso Montanari", Universita degli Studi di Bologna, 40136 Bologna, Italy.

[3]Department of Fundamental Oncology, Université de Lausanne, 1066 Epalinges, Switzerland.

[4]Ludwig Institute for Cancer Research, Université de Lausanne, 1066 Epalinges, Switzerland.

[5]Institute of Biomedical Engineering, College of Electrical and Computer Engineering, National Chiao Tung University, 30010 Hsinchu, Taiwan.

[6]Environmental Engineering Institute, School of Architecture, Civil and Environmental Engineering, École Polytechnique Fédérale de Lausanne, 1015 Lausanne, Switzerland.

*Correspondence: hubert.girault@epfl.ch

Table of Content

Supplementary Methods 3
Algorithm Description 4
Figure S1. A photo of the sampling discs 5
Figure S2. Influence of the sampling disc on MALDI-TOF MS measurement 5
Figure S3. MALDI-TOF mass spectra of blank sampling discs 6
Figure S4. Skin surface mass fingerprints from human volunteers 7
Figure S5. Classification of mass fingerprints from normal skins 8
Figure S6. Influence of sampling repetition times 9
Figure S7. Microscopic image of mouse skin cells collected from a fourth sampling 10
Figure S8. Skin surface mass fingerprints from six healthy mice 11
Figure S9. Bright field images of melanoma skin lesions at early progression stages 12
Figure S10. Microscopic images of mouse skin cells collected by adhesive sampling 13
Figure S11. Hierarchical clustering dendrogram of mouse skin surface mass fingerprints 14
Figure S12. Comparison of mass fingerprints by Jaccard index 15
Figure S13. Comparison of mass fingerprints by Euclidean distance 16
Figure S14. Statistical analysis of the mouse skin surface mass fingerprint PCA scores 17
Figure S15. Summary of mouse skin surface mass fingerprint peaks 18
Figure S16. Label-Free Quantitative Proteomic Data 20
Figure S17. Images of cells collected from healthy skin and adjacent non-tumor skin 21
Figure S18. Analysis of mass fingerprints from adjacent non-tumor skin surface 22
Figure S19. MALDI-TOF mass spectra of mouse blood-circulating exosomes 23
Figure S20. Hierarchical clustering dendrogram from the mouse blood test 24
Figure S21. Statistical analysis of the mouse blood test PCA scores 25
Figure S22. Comparison of mass fingerprints by intensity-weighted Euclidean distance 26
Figure S23. Mass fingerprints from normal skins, skin moles and melanoma cells 27
Table S1. Human skin sample information 29
Table S2. Human skin surface mass fingerprint peak information 30
Table S3. Cosine similarities of mouse skin surface mass fingerprints 34
Table S4. Comparison of peak intensities between healthy and speckle skins from mice 36
Table S5. A list of all investigated machine learning classification algorithms 37
Table S6. PCA scores of mouse skin surface mass fingerprints 38
Table S7. One-way ANOVA test of mouse skin surface mass fingerprint PCA scores 39
Table S8. Mass spectral cosine similarities of mouse blood-circulating exosomes 40
Table S9. PCA scores of the mouse blood test 42
Table S10. One-way ANOVA statistic of the mouse blood test PCA scores 43
Data File S1. Proteomic data for peak assignment on mouse skin surface mass fingerprints 44
Data File S2. Quantitative proteomic data of mouse skin tissues 49
Data File S3. Quantitative proteomic data of melanoma biomarkers 51
Data File S4. Proteomic data for the assignment of exosomal mass spectral peaks 54
References 58

Supplementary Methods

Cell culture

Human cell lines SBCL2 and WM239 obtained from American Type Culture Condition (ATCC®, Virginia, USA) were cultured in Dulbecco's modified Eagle's medium supplemented with 10% of newborn fetal calf serum and 1% of 100× penicillin/streptomycin (Gibco Life Technologies, Basel, Switzerland) at 37 °C in a humidified atmosphere filled with 5% CO_2. When reaching 80% flask confluency, the cells were harvested by trypsinization. Around 10^3 cells were pipetted on MALDI target and covered with MALDI matrix for MALDI-TOF MS measurement.

Isolation of blood exosomes

Mouse blood was collected in EDTA-treated tubes. The tubes were kept upright at 37 ℃ for 30 min, followed by centrifugation at 1500 *g* at 4 ℃ for 12 min. Blood plasma present on the top layer was collected. Exosomes were isolated from the blood plasma using ExoQuick™ Plasma prep and Exosome precipitation kit (Catalog # EXOQ5TM-1, System Bioscience, Palo Alto, Canada) according to the user manual. The obtained exosomes were suspended in ice-cold deionized water or phosphate-buffered saline, purified using 100 kDa cut-off centrifugal filters to remove the co-precipitated blood plasma proteins, and stored in -80 ℃ for later measurements. The exosome concentration was measured by nanoparticle tracking analysis using NanoSight NS300 (Malvern Panalytical Ltd, United Kingdom). 1 µL of exosomes (~$5 \cdot 10^7$ exosome particles) was pipetted on MALDI target and covered with MALDI matrix for MALDI-TOF MS measurement.

Top-down proteomic analysis

Skin tissues excised from mice were flashily frozen on dry ice, crushed in the frozen state, and homogenized for 2 h in ice-cold protein extraction buffer, *i.e.* Laemmli 2× buffer (pH 6.8) containing 4% SDS, 20% glycerol, 10% 2-mercaptoethanol, 0.004% bromphenol blue and 0.125 M Tris HCl. As for mouse blood exosomes, they were homogenized in ice-cold Laemmli 2× buffer for 20 min. The tissue or exosome samples were incubated at 95 ℃ for 10 min to denature the proteins. After centrifugation at 10,000 *g* for 10 min, the supernatants were collected for protein isolation through methanol-chloroform precipitation. After enrichment using 30 kDa-cut off Amicon® Ultra centrifugal filters, proteins smaller than 30 kDa were subjected to top-down proteomic analysis using liquid chromatograph-tandem mass spectrometry (Thermo Fisher UPLC Ultimate 3000 – Q Exactive HF Hybrid Quadrupole Orbitrap Mass Spectrometer), with the analysis conducted in ISIC Mass Spectrometry Facility in École Polytechnique Fédérale de Lausanne.

Quantitative proteomic analysis

Proteins were extracted from the excised mouse skin tissues in the same way as described in the above *Top-down proteomic analysis* section. After methanol-chloroform precipitation, the proteins were digested in trypsin/Lys-C protease mix to generate short peptides. After peptide quantification using a colorimetric assay kit (Pierce™, Thermo Fisher), an identical amount of peptides were analyzed for each mouse sample using liquid chromatography-tandem mass spectrometry (Thermo Fisher Ultimate 3000 RSLC nano –Q Exactive HF Orbitrap mass spectrometer). Proteins were identified through the observation of unique peptides by using Scaffold and MaxQuant proteome software. The relative quantity of each protein was determined by the spectral counting data, mainly the normalized total spectrum count, *i.e.* the normalized total number of peptide spectra identified for a protein group. The proteins were also performed label-free quantification (LFQ) by using MaxQuant software based on the LFQ intensity. This quantitative bottom-up proteomic analysis was conducted in Proteomics Core Facility in École Polytechnique Fédérale de Lausanne.

Algorithm Description

In the present work, mass spectral similarity scores were calculated by using one of the four algorithms, *i.e.* cosine correlation, Jaccard index, relative Euclidean distance, and intensity-weighted Euclidean distance. The algorithm details are described below.

1) The cosine similarity (or cosine correlation) between mass spectrum *A* and *B* is calculated as:

$$\cos(A,B) = \frac{A \cdot B}{\|A\| \cdot \|B\|} = \frac{\sum_{k=1}^{n_{AB}} y_{Ak} \cdot y_{Bk}}{\sqrt{\sum_{i=1}^{N_A} y_{Ai}^2} \cdot \sqrt{\sum_{j=1}^{N_B} y_{Bj}^2}} \quad (1)$$

In this algorithm, N_A *or* N_B is the peak number in spectrum *A* or *B*, and $n_{AB}$is the number of identical peaks shared by the two spectra, while y_A *or* y_B is the relative intensity of a peak measured from spectrum *A* or *B*.[3]

2) Jaccard index, also known as Jaccard similarity coefficient or Intersection over Union, considers only the number of identical peaks between two spectra. It defines the similarity between spectrum *A* and *B* as:

$$J(A,B) = \frac{(A \cap B)}{(A \cup B)} = \frac{n_{AB}}{N_A + N_B - n_{AB}} \quad (2)$$

In this algorithm, N_A or N_B is the peak number in spectrum *A* or *B*, while n_{AB} is the number of identical peaks between the two spectra.

3) The relative Euclidean (*Eu*) similarity considers the *Eu* distance in *m/z* value and intensity of each pair of identical peak in two spectra. *Eu* distance of the *k*th pair of identical peak between spectrum *A* and *B* is defined as

$$Eu_k = \frac{\sqrt{(x_{Ak} - x_{Bk})^2 + (y_{Ak} - y_{Bk})^2}}{\sqrt{[\max(x_{Ak}, x_{Bk})^2 \cdot tolerance^2 + \max(y_{Ak}, y_{Bk})^2]}} \quad (3)$$

Here, x_{Ak} or x_{Bk} is the *m/z* value of the identical peak *k* in spectrum *A* or *B*, while y_{Ak} or y_{Bk} is the relative intensity of peak *k* in spectrum *A* or *B*, and the $tolerance$ is the mass tolerance allowing the definition of identical peaks (1000 ppm here). The *Eu* similarity between spectrum *A* and *B* is then defined as

$$Eu = 1 - \frac{\sum_{k=1}^{n_{AB}} Eu_k + N_A + N_B - 2n_{AB}}{N_A + N_B - n_{AB}} \quad (4)$$

Here, N_A or N_B is the peak number in spectrum *A* or *B*, while n_{AB} is the number of their identical peaks. This algorithm has been described in detail by Yang Y. *et al.*[4]

4) As for the intensity-weighted relative Euclidean (*iEu*) similarity, the above mentioned relative *Eu* distance is weighted by the peak intensity, and is defined as below.

$$iEu = 1 - \frac{\sum_{k=1}^{n_{AB}} Eu_k(y_{Ak} + y_{Bk}) + \sum_{i=1}^{N_A} y_{Ai} + \sum_{j=1}^{N_B} y_{Bj} - \sum_{k=1}^{n_{AB}}(y_{Ak} + y_{Bk})}{\sum_{i=1}^{N_A} y_{Ai} + \sum_{j=1}^{N_B} y_{Bj}} \quad (5)$$

Supplementary Figures, Tables and Data Files

Figure S1. A photo of the sampling discs. D-Squame® brand sampling discs were used in this work.

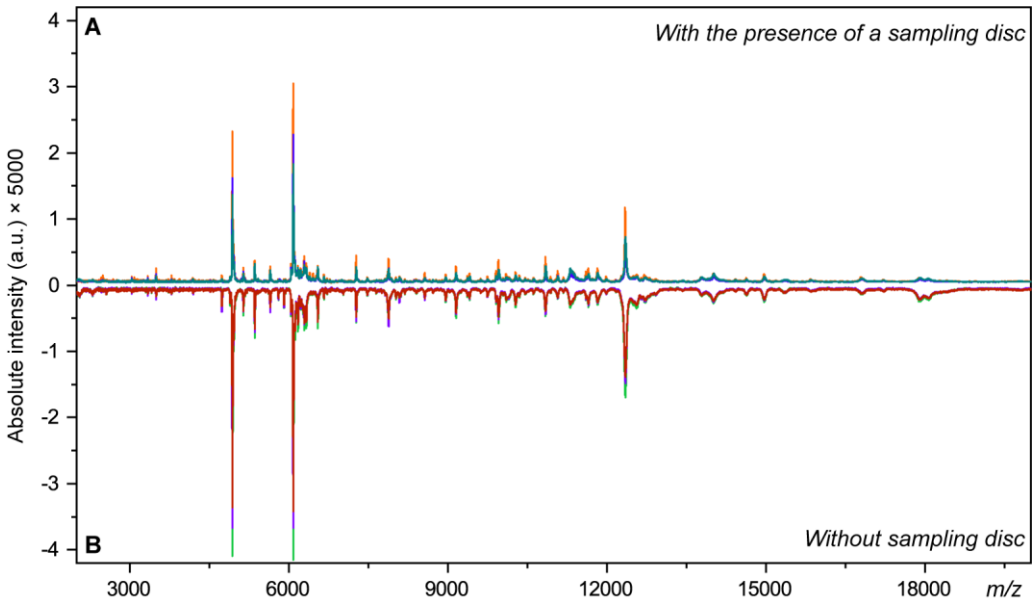

Figure S2. Influence of the sampling disc on MALDI-TOF MS measurement. Comparison of MALDI-TOF mass spectra generated from human melanoma cells WM239 under two different conditions: (**A**) with the presence of a sampling disc (*i.e.*, the cells were prepared on a sampling disc, and the disc thereafter was fixed on the MALDI target for MS measurement, (**B**) without the sampling disc (*i.e.*, the cells were directly prepared on the MALDI target for the measurement). The cells were *in vitro* grown in Petri dishes and harvested by trypsinization. Each of the spectra was generated from ~1000 cells, and each assay was repeated three times. Sinapinic acid was used as the matrix.

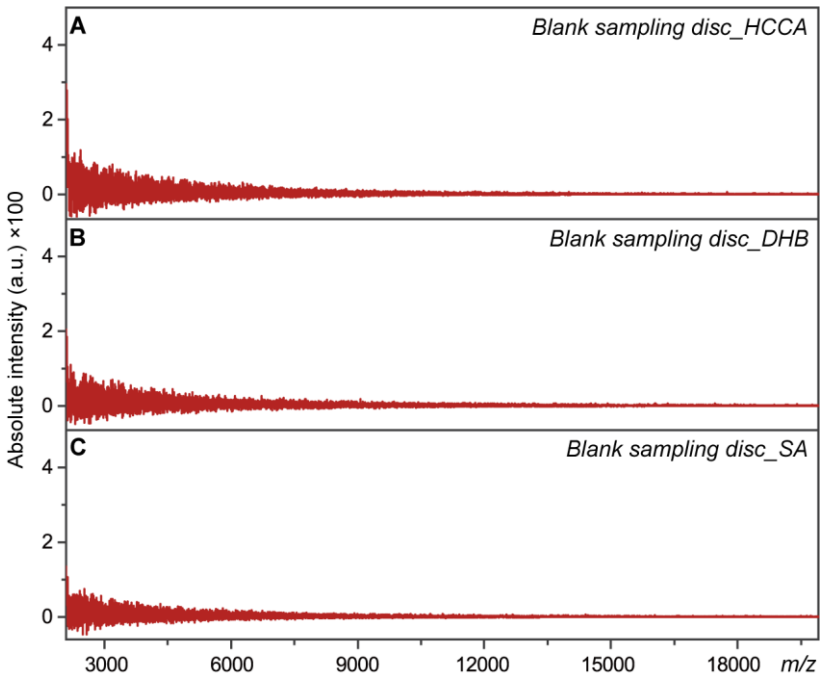

Figure S3. MALDI-TOF mass spectra of blank sampling discs. The matrix used for the measurement was (**A**) α-cyano-4-hydroxycinnamic acid (HCCA), (**B**) 2,5-dihydroxybenzoic acid (DHB), and (**C**) sinapinic acid (SA), respectively. The matrix was prepared with the concentration of 10 mg·mL^{-1} (for HCCA and DHB) or 15 mg·mL^{-1} (for SA) in the mixture of 50/49.9/0.1% (volume percentage) acetonitrile/water/trifluoroacetic acid.

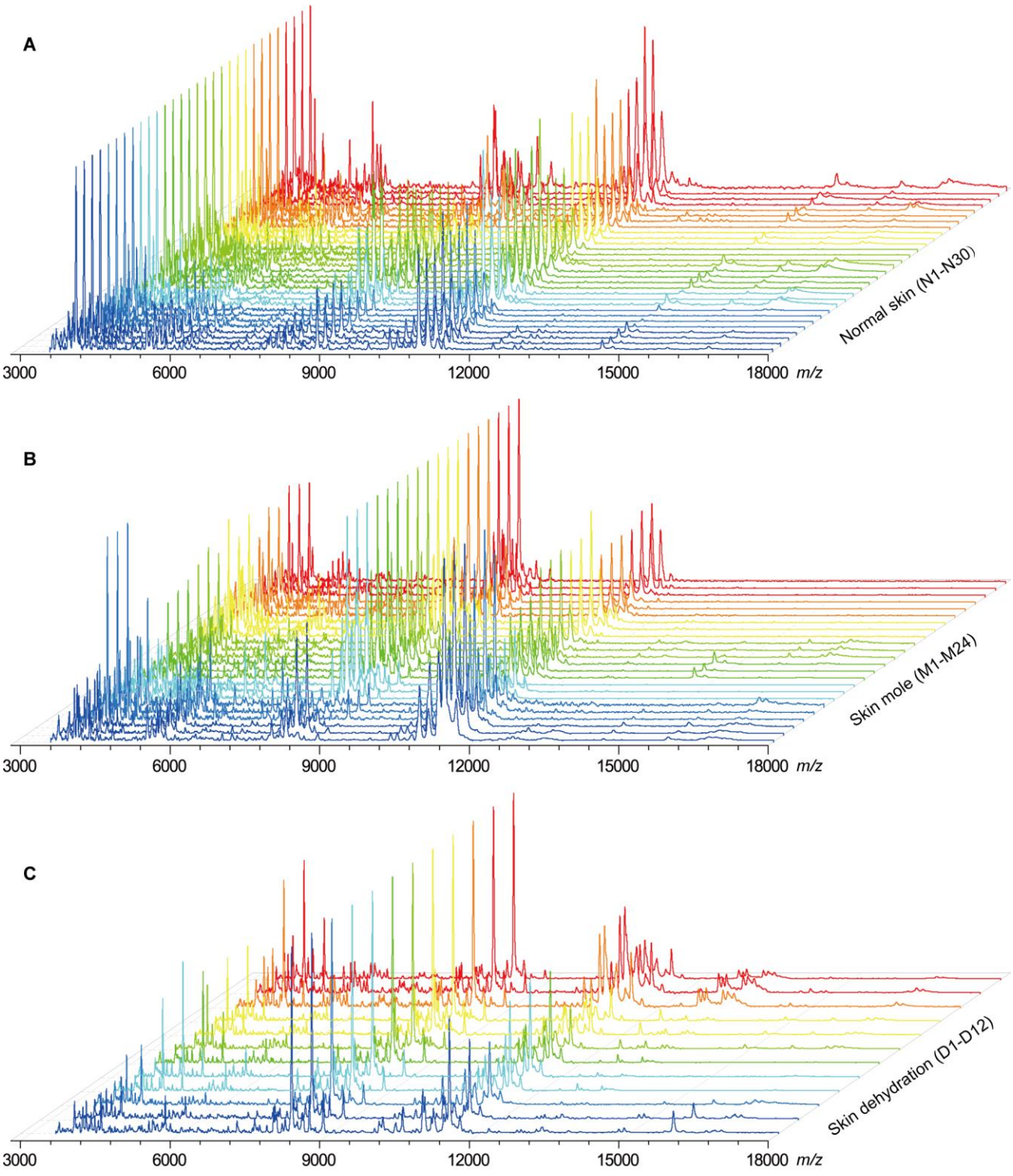

Figure S4. Skin surface mass fingerprints from human volunteers. The skin conditions are (**A**) normal healthy skins on different body sites, (**B**) black skin moles on different body sites, and (**C**) dry-itchy dehydrated skins on different body sites. Nine healthy volunteers from different districts were involved in the test, and all the spectra were obtained from the third samplings on each selected skin region.

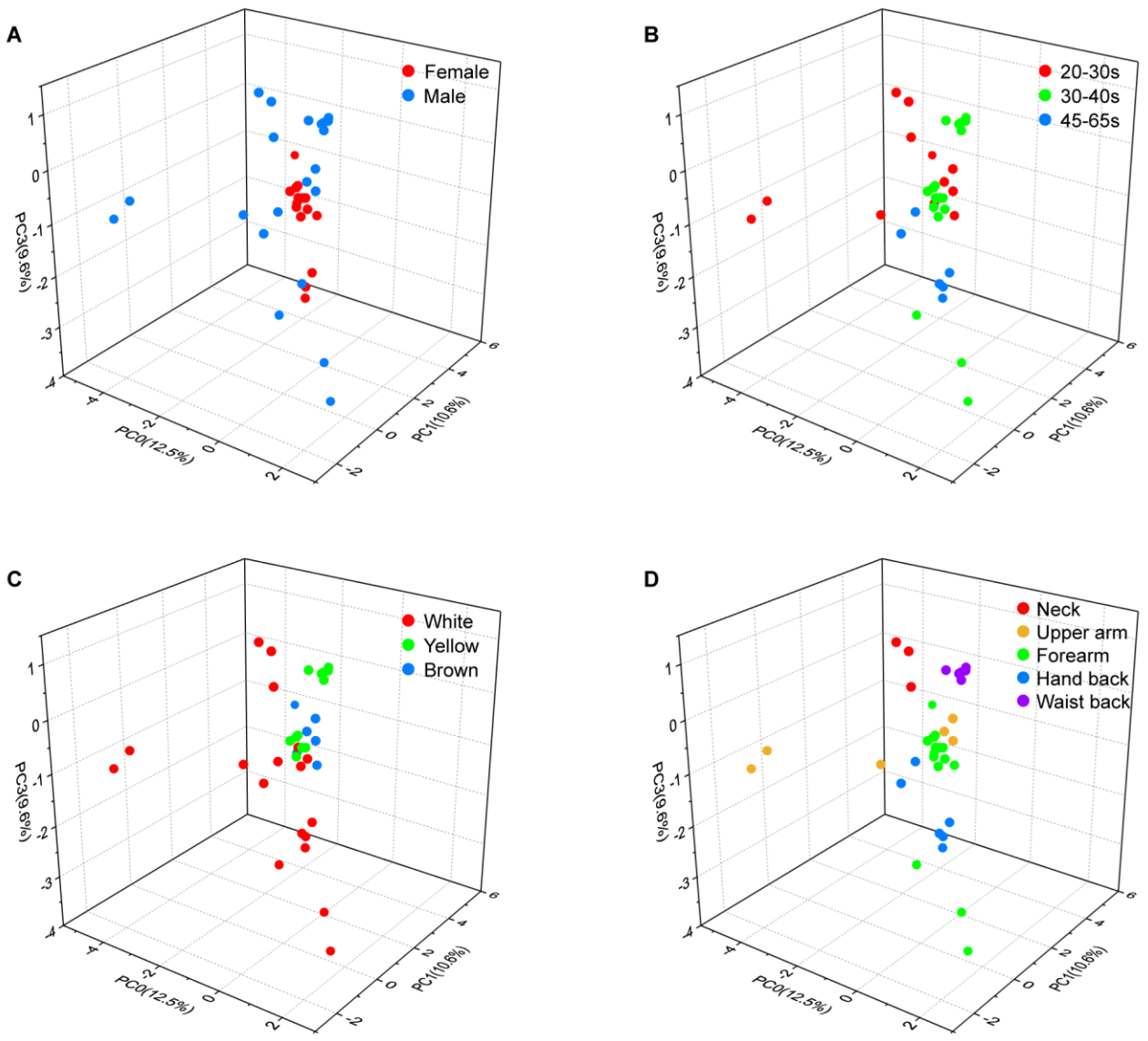

Figure S5. Classification of mass fingerprints from normal skins. The normal skin surface mass fingerprints obtained from healthy volunteers were classified according to factors including (**A**) the host gender (female or male), (**B**) the host age (here 20 to 30 years old, 30 to 40 years old, and 45 to 65 years old) (**C**) skin tone (here including white, yellow, and brown), and (**D**) body site (here including neck, upper arm, forearm, the back of hand, and the back of waist).

More information about the volunteers was provided in **Table S1**. The classification was conducted by using principal component analysis according to the first three principal components. The classification results shown in **Figure S5** indicate that the skin surface mass fingerprints could be influenced by all these factors together.

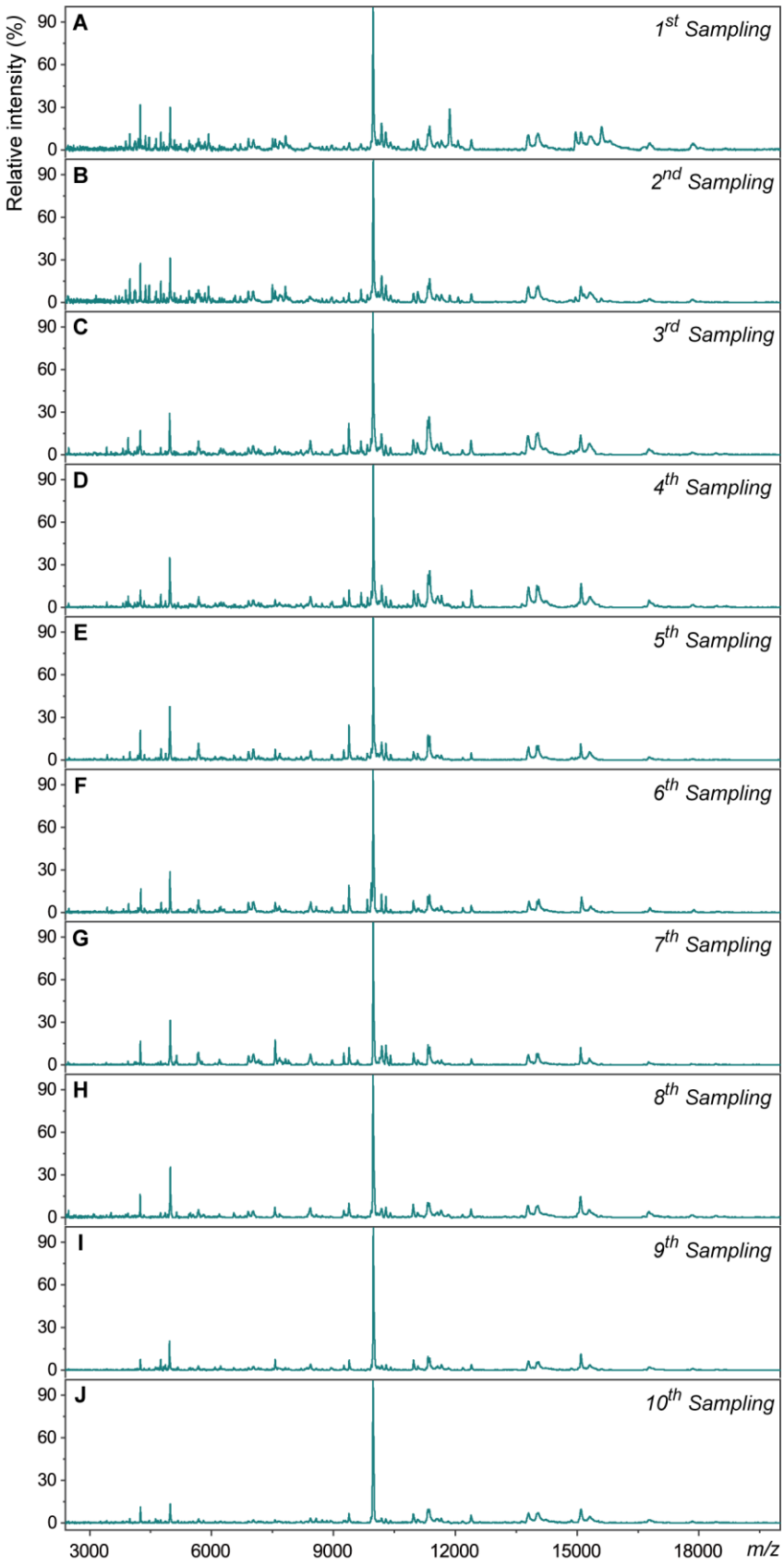

Figure S6. Influence of sampling repetition times. (**A-J**) MALDI-TOF mass spectra generated from ten sequential samplings from an individual normal skin region on the back of a 7-week-old healthy mouse, using a new sampling disc each time.

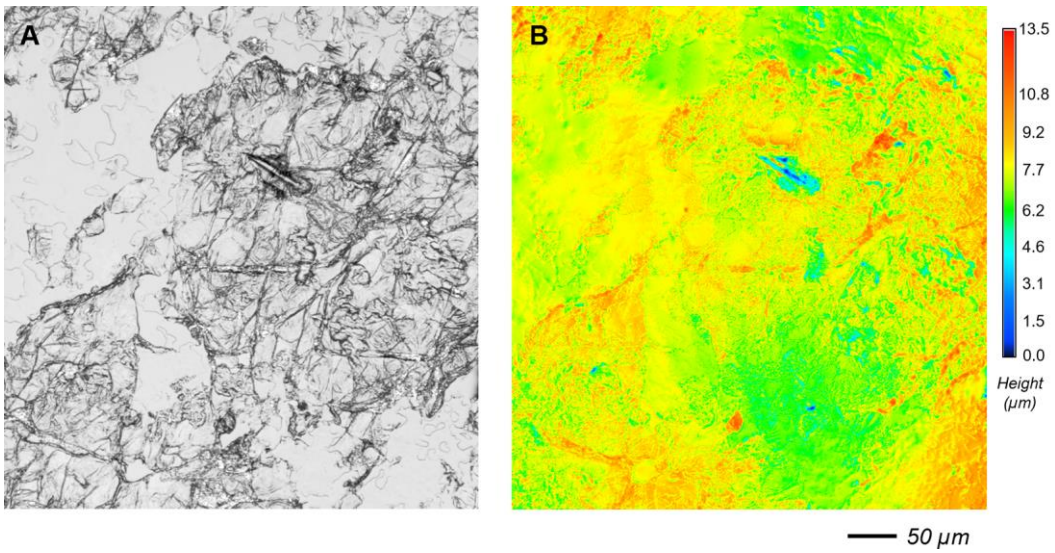

Figure S7. Microscopic image of mouse skin cells collected from a fourth sampling. Epidermal cells were collected from the back skin of an arbitrary healthy mouse using the adhesive sampling discs. (**A**) 3D laser scanning microscopy image of the epidermal cells generated from the fourth sampling. (**B**) Height profile of the epidermal cells collected on the sampling disc.

In order to optimize the sampling procedure, a healthy mouse was repetitively sampled on an individual normal skin region ten times for MALDI-TOF MS measurements. Results show that the first three samplings produced slightly more mass spectral peaks than the last three (**Figure S6**). The first few samplings were more likely suffering from interferences caused by dander, hair or dust on the skin surface, while the last few could harvest a smaller amount of skin cells due to the more adhering skin layers in depth.[5] Following this, each skin region tested below was sampled four times in a row and the fourth sample was analyzed. The examination using laser scanning microscopy confirms that the fourth sampling can collect enough skin cells with a cell layer thickness around 3 μm (**Figure S7**). With this unified sampling procedure, the collected samples are comparable among mouse individuals. During mass spectrometry measurements, in order to diminish the 'sweet spots' effect caused by the heterogeneous distribution of cells and the MALDI matrix, each sample was measured three times, each being an accumulation from 2×300 laser shots all over the lesion area.

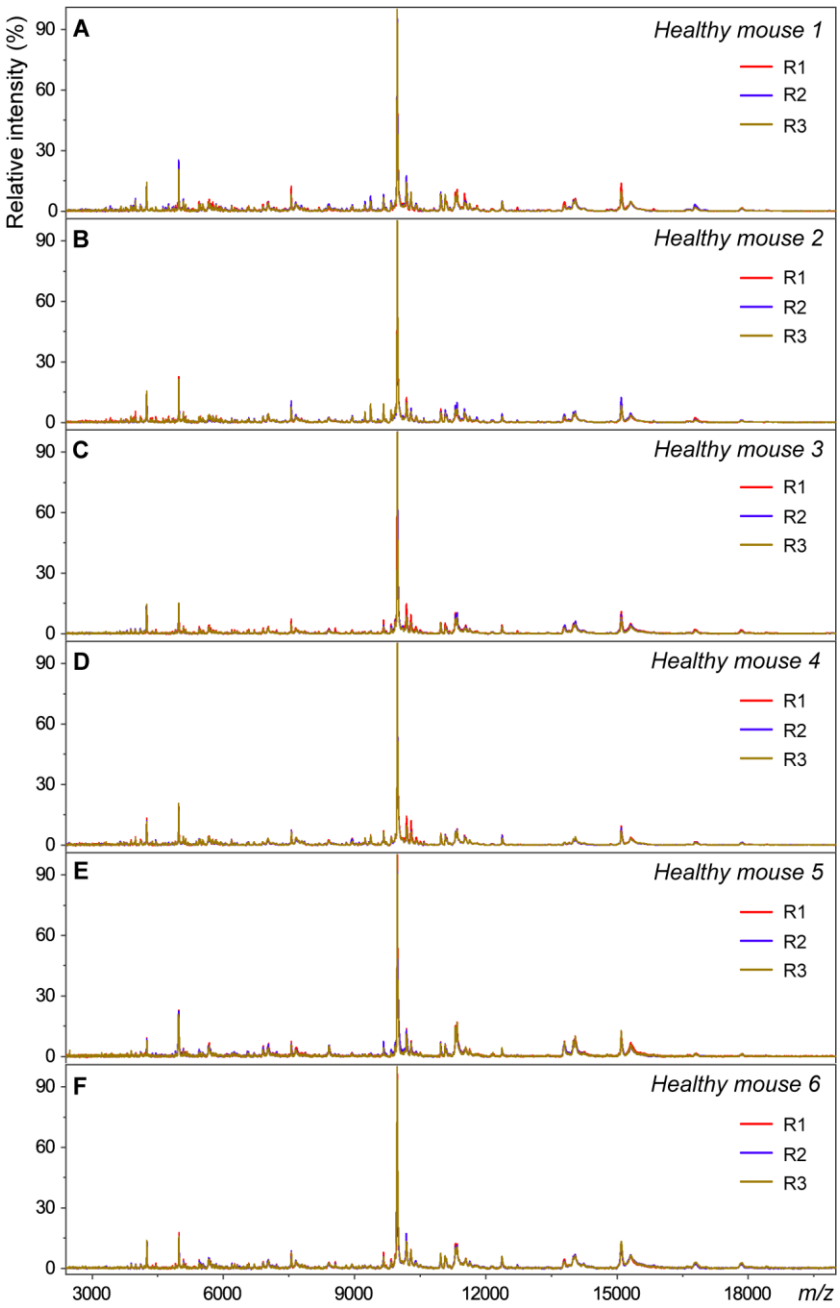

Figure S8. Skin surface mass fingerprints from six healthy mice. The mice were at different ages, *i.e.* (**A**, **B**) 7-week-old, (**C**, **D**) 10-week-old and (**E**, **F**) 12-week-old. All the mice were sampled on their back skin, and skin cells collected from the fourth adhesive samplings were analyzed by MALDI-TOF MS.

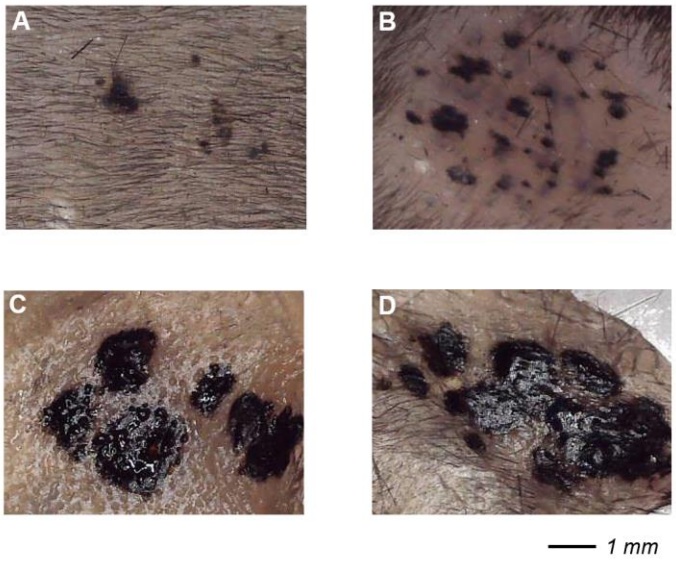

Figure S9. Bright field images of melanoma skin lesions at early progression stages. The skin lesions on four mouse individuals are imaged as representatives. (**A**) A mouse developed a few black speckles on the skin four weeks after the 4-HT administration (speckle number <10). (**B**) A mouse developed more black speckles on the skin four weeks after the 4-HT administration (speckle number >20). (**C**) A mouse developed tumor nodules with ~15 mm^2 total superficial surface area on the skin six weeks after the 4-HT administration. (**D**) A mouse developed tumor nodules with ~24 mm^2 total superficial surface area on the skin six weeks after the 4-HT administration. The skin lesions at later progression stages had no significant change in the physical appearance except for the increase of the tumor nodule size. The images were taken with DNT Digimicro Profi digital microscope.

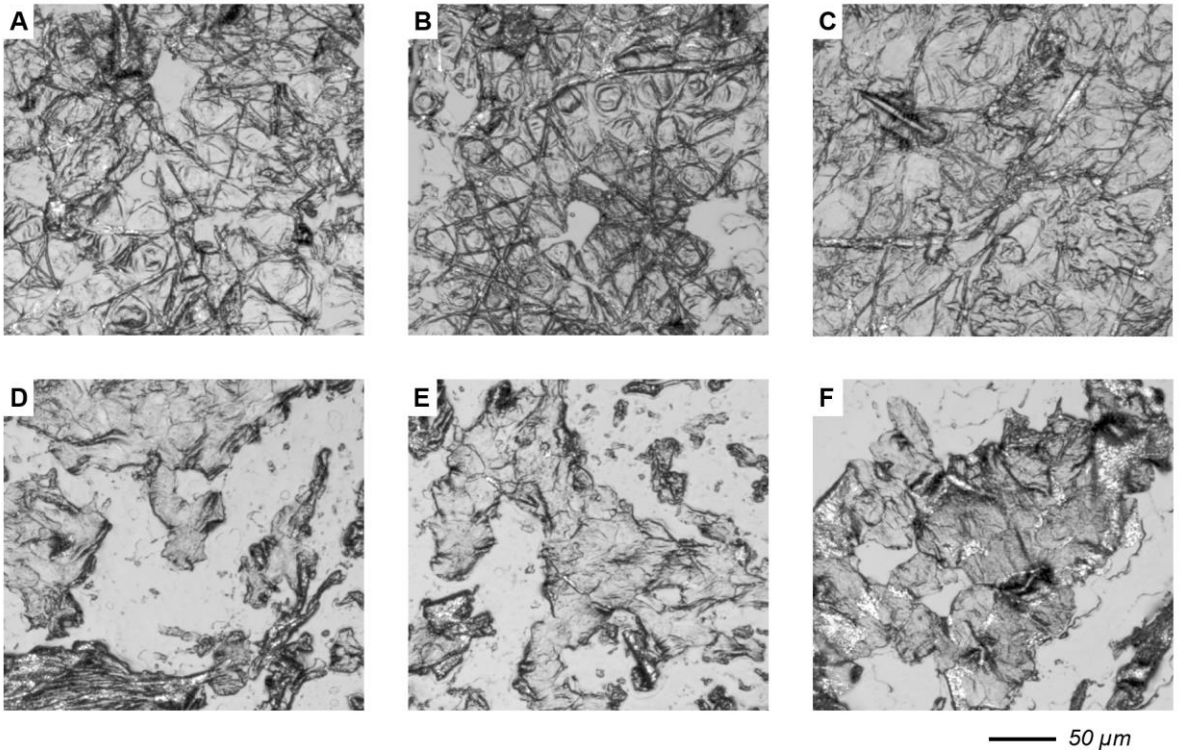

Figure S10. Microscopic images of mouse skin cells collected by adhesive sampling. 3D laser scanning microscopy images of mouse epidermal cells collected from: (**A-C**) a normal skin region on three healthy mice, (**D-F**) the skin tumor region on three cancerous mice. The three healthy mice were at different ages, *i.e.* (**A**) 7-week-old, (**B**) 10-week-old and (**C**) 12-week-old. The three cancerous mice carried different size of skin tumor, *i.e.* (**D**) 70 mm^2, (**F**) 130 mm^2 and (**F**) 182 mm^2 of superficial surface area. In each image, the cells were collected from the fourth adhesive samplings.

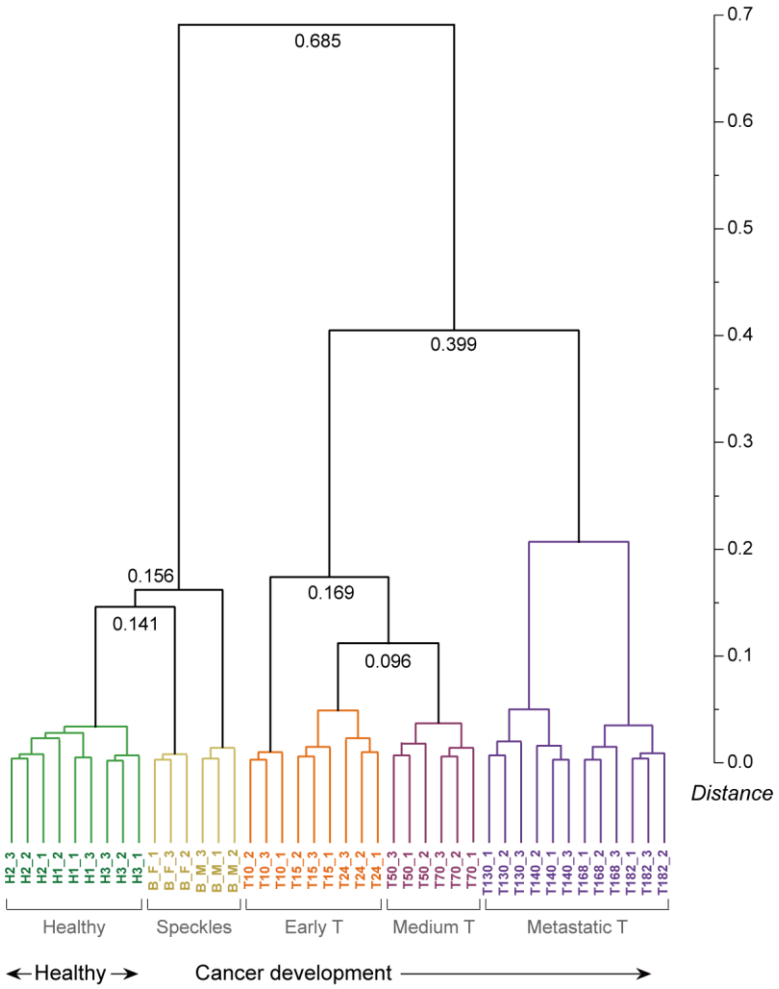

Figure S11. Hierarchical clustering dendrogram of mouse skin surface mass fingerprints. Hierarchical cluster analysis (HCA) was conducted with the mouse skin surface mass fingerprints by using the cosine similarity and the average linkage. The inter-group distance is determined based on the mean distance between all objects in one group and all objects in the other group, and each single-pair distance is calculated as one minus the single-pair cosine similarity (*i.e.* 1-cosine similarity).

The cosine similarity (or cosine correlation) between mass spectrum *A* and *B* is calculated as:

$$\cos(A,B) = \frac{A \cdot B}{\|A\| \cdot \|B\|} = \frac{\sum_{k=1}^{n_{AB}} y_{Ak} \cdot y_{Bk}}{\sqrt{\sum_{i=1}^{N_A} y_{Ai}^2} \cdot \sqrt{\sum_{j=1}^{N_B} y_{Bj}^2}} \quad (1)$$

In this algorithm, N_A *or* N_B is the peak number in spectrum *A* or *B*, and $n_{AB}$is the number of identical peaks shared by the two spectra, while y_A *or* y_B is the relative intensity of a peak measured from spectrum *A* or *B*.[3]

HCA is an unsupervised machine learning method to group objects in such a way that the objects in the same group are more similar to each other than to those in other groups. The average linkage method (*i.e.* unweighted pair group method with arithmetic mean) determines the inter-group distance based on the mean distance between all objects in one group and all objects in the other group, and thus helps to avoid problems caused by the chaining effect or outlying data.

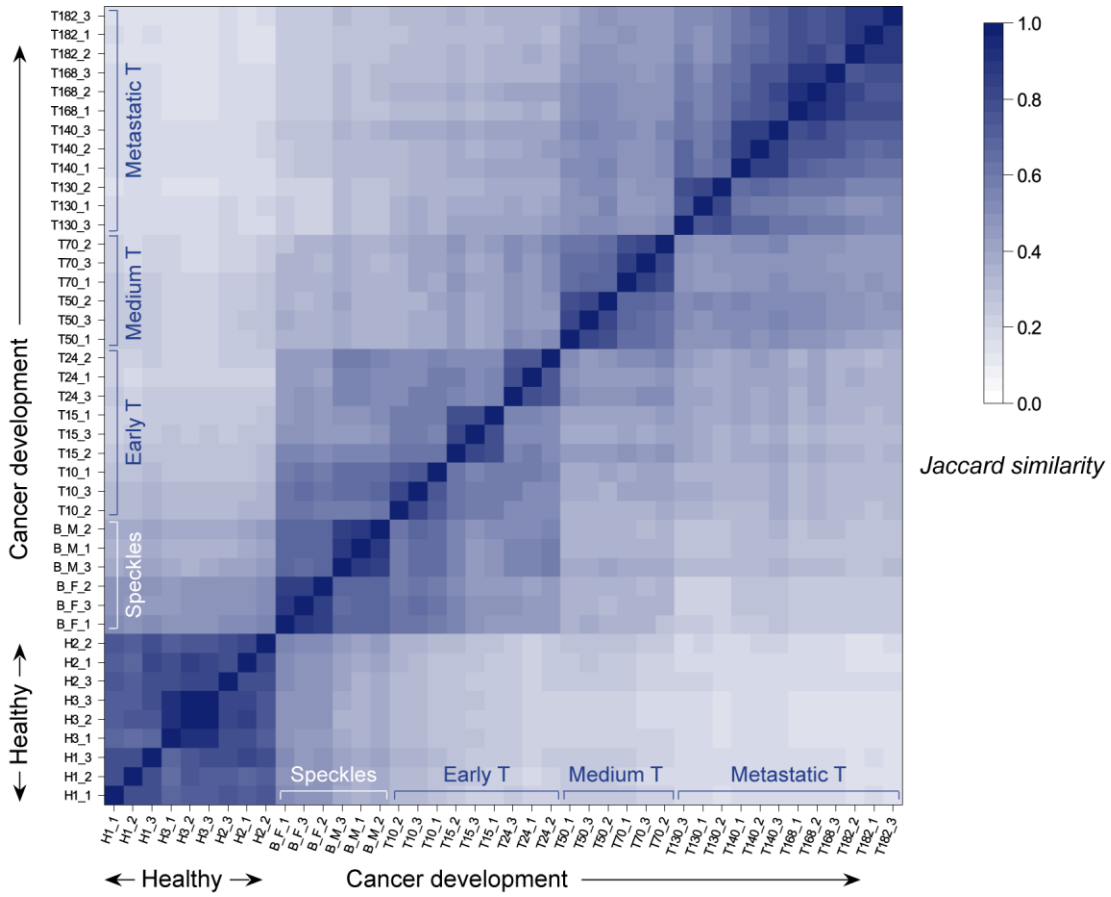

Figure S12. Comparison of mass fingerprints by Jaccard index

Jaccard index, also known as Jaccard similarity coefficient or Intersection over Union, considers only the number of identical peaks between two spectra. It defines the similarity between spectrum *A* and *B* as

$$J(A,B) = \frac{(A \cap B)}{(A \cup B)} = \frac{n_{AB}}{N_A + N_B - n_{AB}} \tag{2}$$

where N_A or N_B is the peak number in spectrum *A* or *B*, while n_{AB} is the number of identical peaks between the two spectra.

Figure S12 shows the hierarchal clustering heat map of the mouse skin surface mass fingerprints according to the fingerprint Jaccard similarity with the average linkage method.

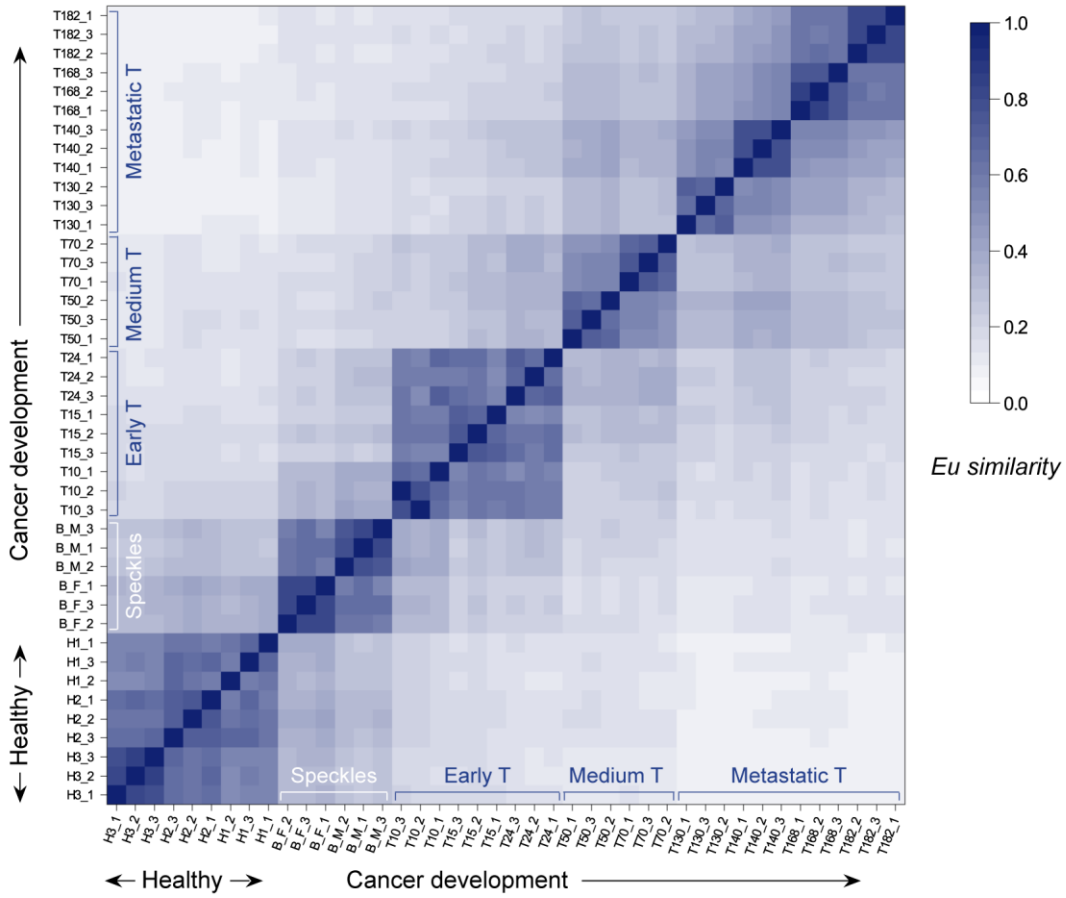

Figure S13. Comparison of mass fingerprints by Euclidean distance

The relative Euclidean (*Eu*) similarity considers the *Eu* distance in *m/z* value and intensity of each pair of identical peak in two spectra. *Eu* distance of the *k*th pair of identical peak between spectrum *A* and *B* is defined as

$$Eu_k = \frac{\sqrt{(x_{Ak} - x_{Bk})^2 + (y_{Ak} - y_{Bk})^2}}{\sqrt{[\max(x_{Ak}, x_{Bk})^2 \cdot tolerance^2 + \max(y_{Ak}, y_{Bk})^2]}} \quad (3)$$

where x_{Ak} or x_{Bk} is the *m/z* value of the identical peak *k* in spectrum *A* or *B*, while y_{Ak} or y_{Bk} is the relative intensity of peak *k* in spectrum *A* or *B*, and the $tolerance$ is the mass tolerance allowing the definition of identical peaks (1000 ppm here). The *Eu* similarity between spectrum *A* and *B* is then defined as

$$Eu = 1 - \frac{\sum_{k=1}^{n_{AB}} Eu_k + N_A + N_B - 2n_{AB}}{N_A + N_B - n_{AB}} \quad (4)$$

where N_A or N_B is the peak number in spectrum *A* or *B*, while n_{AB} is the number of their identical peaks. This algorithm has been described in detail by Yang Y. *et al.*[4]

Figure S13 shows the hierarchal clustering heat map of the mouse skin surface mass fingerprints according to the fingerprint *Eu* similarity with the average linkage method.

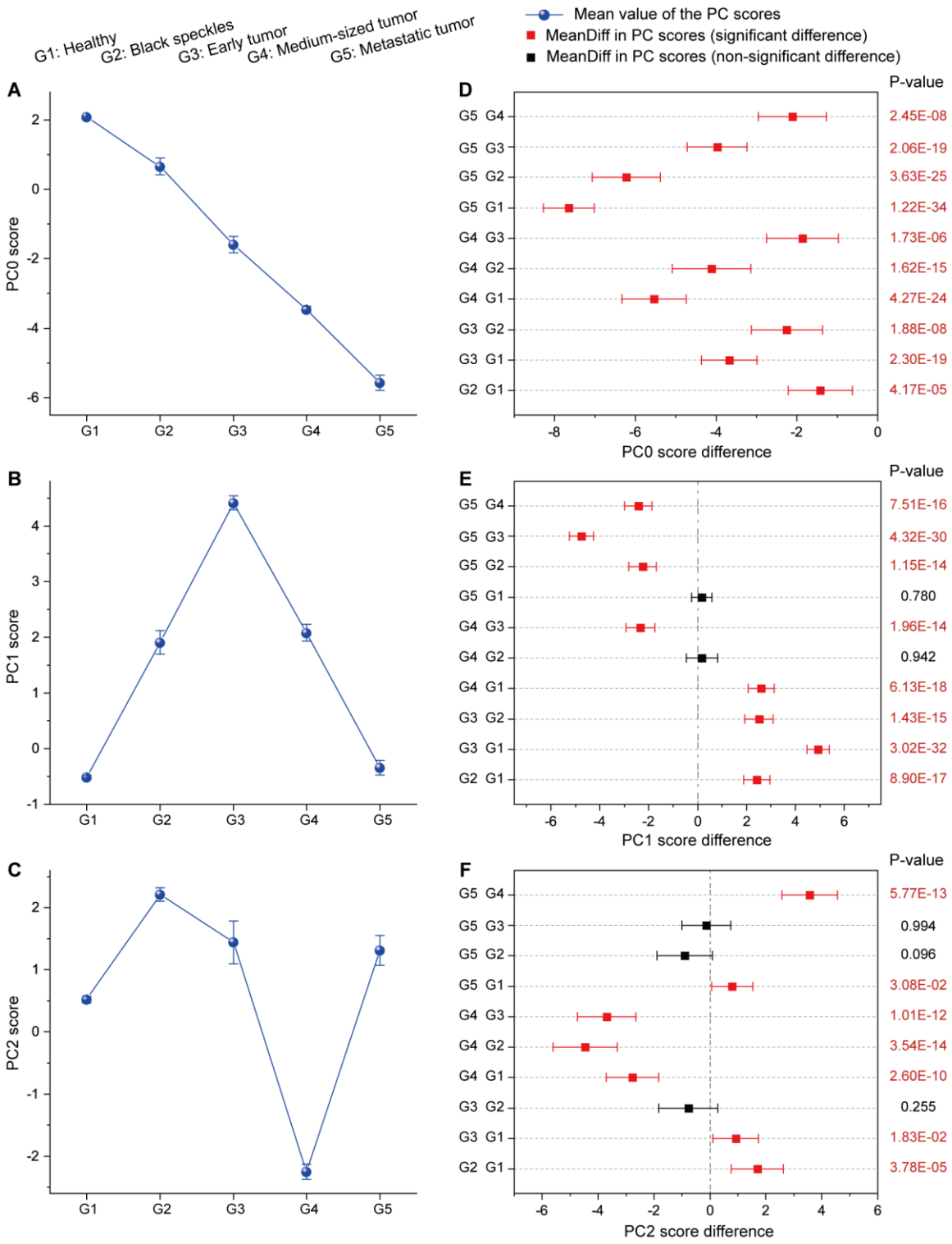

Figure S14. Statistical analysis of the mouse skin surface mass fingerprint PCA scores. Changes in the PCA scores along with the cancer development are plotted in (**A**) for PC0, (**B**) for PC1 and (**C**) for PC2. Differences in the PCA scores between each two skin groups are plotted in (**D**) for PC0, (**E**) for PC1 and (**F**) for PC2, with the level of statistical significance (P-value) from one-way ANOVA statistical labeled on each plot.

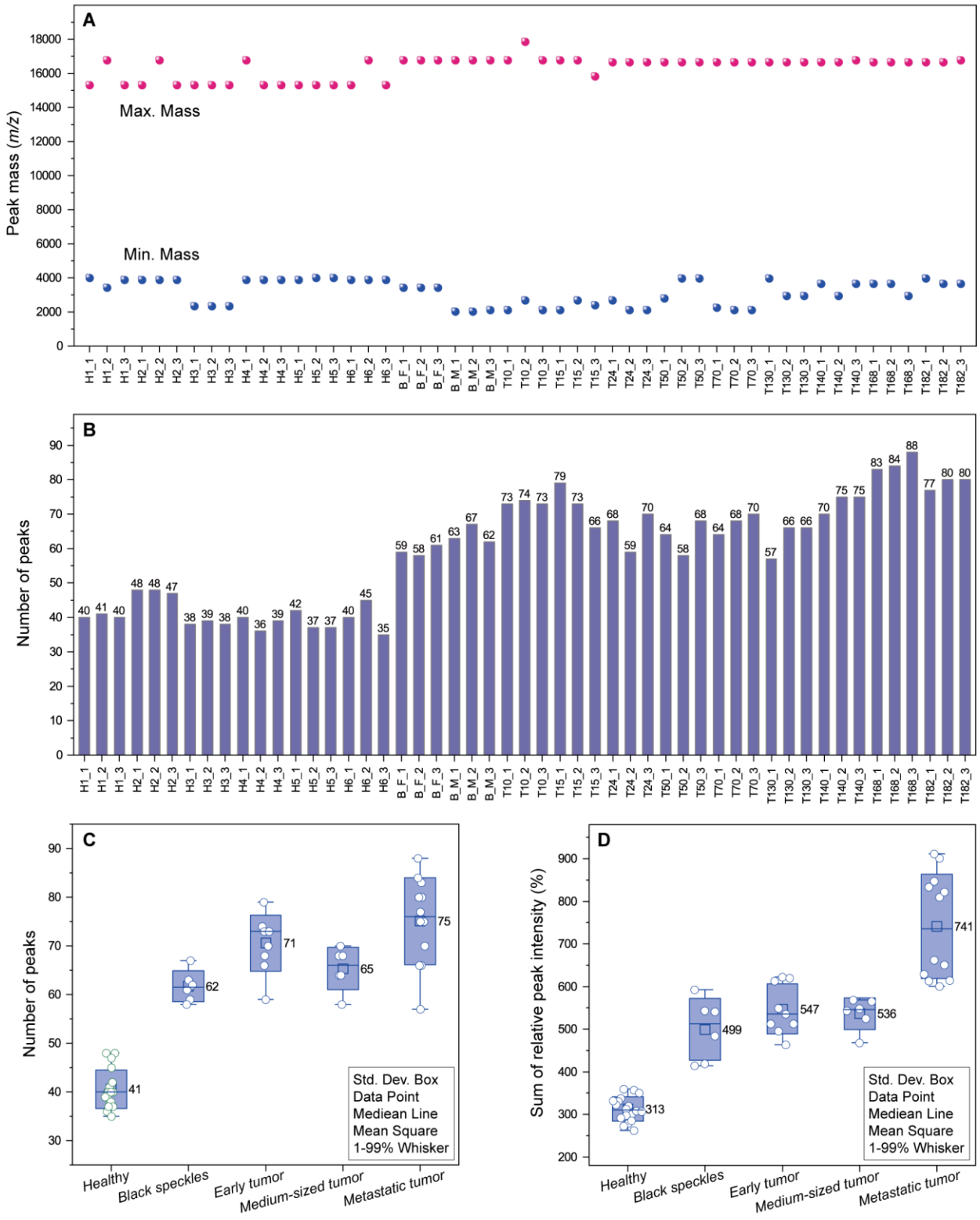

Figure S15. Summary of mouse skin surface mass fingerprint peaks. (A) The minimum and maximum peak mass (*m/z*) detected from each mouse skin. (**B**) The peak number detected from each mouse skin. (**C**) Statistical analysis of the peak number per fingerprint at different skin stages. (**D**) Statistical analysis of the sum of relative peak intensity per fingerprint at different skin stages. The peaks were extracted from the mass fingerprints by using MALDIquant algorithm on the Mass-Up software platform, with the peak-picking parameters set as relative peak intensity threshold 2%, *signal-to-noise* ratio threshold 3.0, and half window size 60.

Mass fingerprints derived from the mouse skins during the malignancy growth were compared in terms of peak mass (*m/z* value), peak number and relative peak intensity. The minimum and maximum peak masses were observed as 2,018 *m/z* and 17,860 *m/z*, respectively, not significantly changed during the cancer development (**Figure S15A**). The number of well-resolved peaks per fingerprint was increased from 41(±4) to 62(±3), 71(±6), 65(±4) and 75(±9) respectively when the skins turned from healthy state to lesions with speckles, early tumors, medium-size tumors and further metastatic tumors (**Figure S15B-C**). At the same time, the sum of relative peak intensity per fingerprint increased from 3.13(±0.28) to 4.99(±0.73), 5.47(±0.59), 5.36(±0.37) and 7.41(±1.22), respectively (**Figure S15D**). Such increases should be related with the disorder progression.

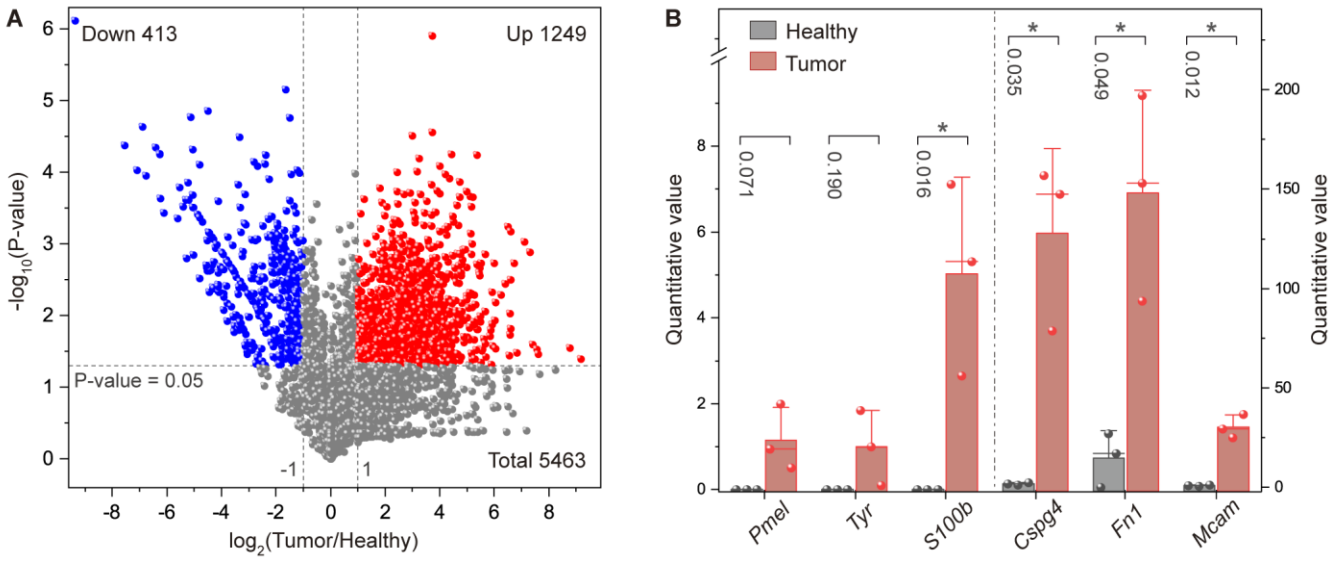

Figure S16. Label-Free Quantitative Proteomic Data. Label-free quantitative (LFQ) bottom-up proteomics was performed with the excised mouse skin tissues, with the data processed using MaxQuant proteome software. Three tumor lesions (70, 130 and 182 mm^2) were analyzed as representatives, with the quantitative value (*i.e.* LFQ intensity $\times 10^7$) of each identified protein statistically compared to the healthy controls. (**A**) A comparison of all the protein quantitative values between skin tumors and healthy skins, with the paired t-test statistical significance (P-value) plotted versus the magnitude of log2 fold change. (**B**) A comparison of quantitative values from six well-established melanoma biomarkers between skin tumors and healthy skins, with the displaying of mean value bars, median value lines, data dot distribution and paired t-test P-values (star rating: * P-value $\leq$0.05). A significant difference was conditioned by the absolute log2 fold change absolute value $\geq$1 and the paired t-test P-value $\leq$0.05.

Two procedures were employed for the quantitative proteomic analysis, *i.e.* spectral counting by using Scaffold proteome software (results in **Figure 6**), and label-free quantification (LFQ) by using MaxQuant proteome software (results in **Figure S16**). Generally, the results provided by the two procedures were consistent with each other. Both results were thus presented in this manuscript to serve as a support to each other.

With the MaxQuant LFQ, altogether 5,463 proteins were identified. Compared to the healthy controls, the tumor lesions had more than 30% of proteins differently expressed, including 23% up-regulated (1,249/5,463) and 8% down-regulated (413/5,463), as shown in **Figure S16A**. These values were close to the Scaffold values in **Figure 6A**. Among the differently expressed proteins, the two quantification procedures shared 795 common up-regulated proteins and 253 common down-regulated proteins (**Data File S2**). This proteomic quantification outcome confirmed a significant difference in the protein expression between the healthy and tumorous skins. It coincided with the change of the skin surface mass fingerprint patterns.

The six well-known melanoma biomarkers were all detected from the tumor lesions, but not detected or detected with much lower quantity from the healthy controls, as shown in both **Figure S16B** by MaxQuant LFQ and in **Figure 6B** by Scaffold spectral counting (details in **Data File S3**). The melanoma diagnostic sensitivity and specificity provided by the six biomarkers have been reported as 72-100% and 91-100% by *Pmel*, 90-100% and 97-100% by *Tyr*, 89% (specificity not available) by *Cspg4*, 89-100% and 70-79% by *S100b*, 95-99% and 100% by *Fn1*, respectively; and the *Mcam* has been suggested as an independent prognostic predictor with a higher expression associated with a worse prognosis.[6] This result confirmed that the tumor lesions we developed in the mouse skin were indeed melanoma-type skin cancer.

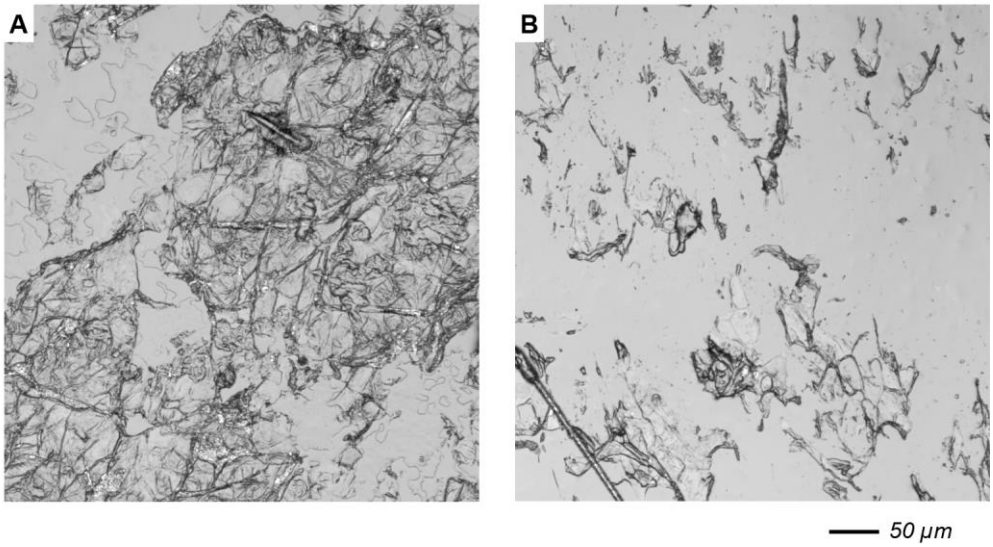

Figure S17. Images of cells collected from healthy skin and adjacent non-tumor skin. 3D laser scanning microscopy images of epidermal cells collected from the skin surface of: (**A**) a healthy mouse, (**B**) an adjacent non-tumor skin region of the T182 mouse (the mouse carrying 182 mm^2 tumor). The non-tumor skin region was located 15 mm away from the tumor lesion. The cells were collected using the adhesive discs with the same sampling protocol, both from the fourth samplings.

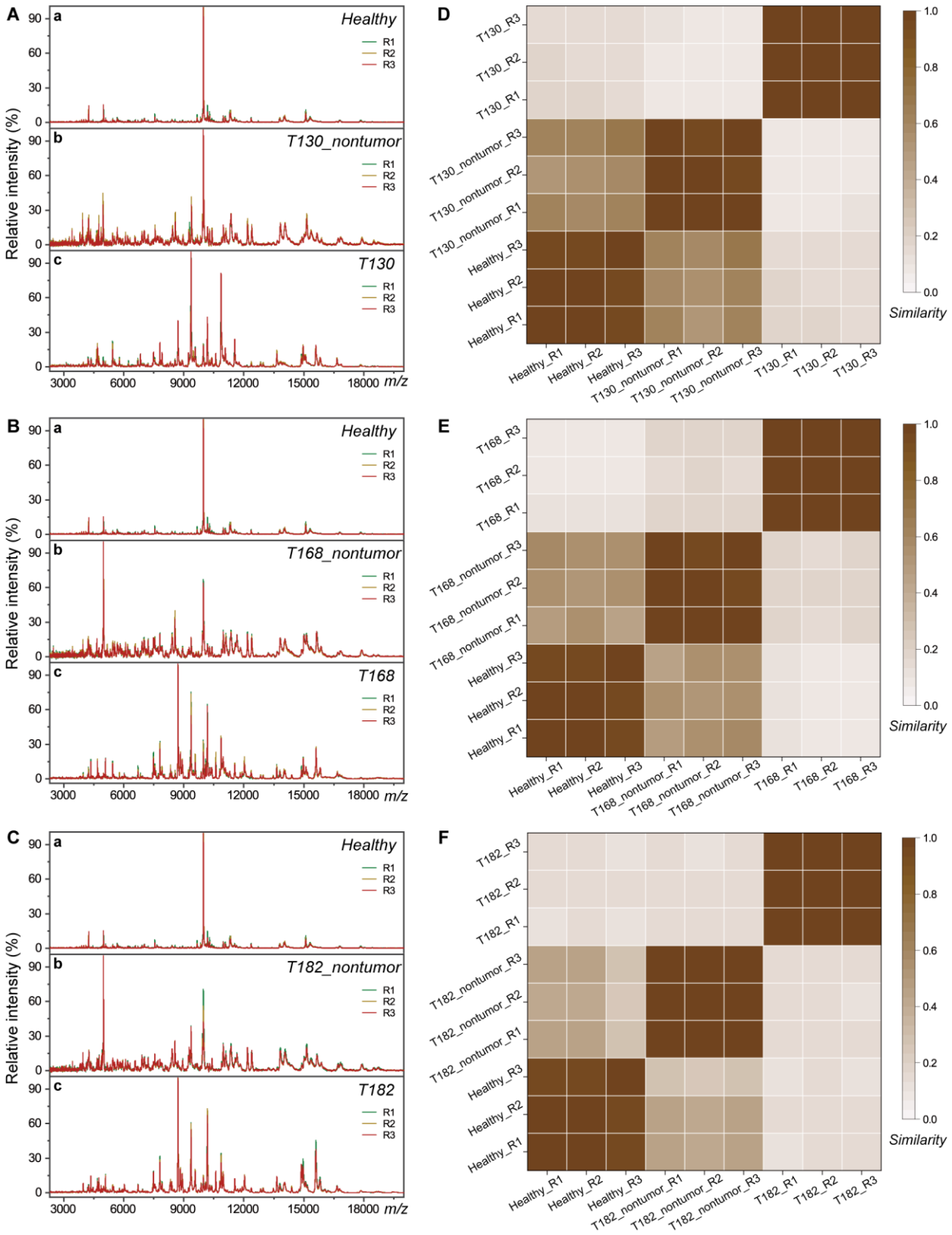

Figure S18. Analysis of mass fingerprints from adjacent non-tumor skin surface. The fingerprints were compared to the corresponding tumor regions as well as the healthy controls. The test was conducted on three cancerous mice: (**A**) T130 mouse, (**B**) T168 mouse, (**C**) T182 mouse, with the fingerprint cosine similarity heat map shown in (**D**), (**E**), (**F**), respectively. All the fingerprints came from the fourth samplings.

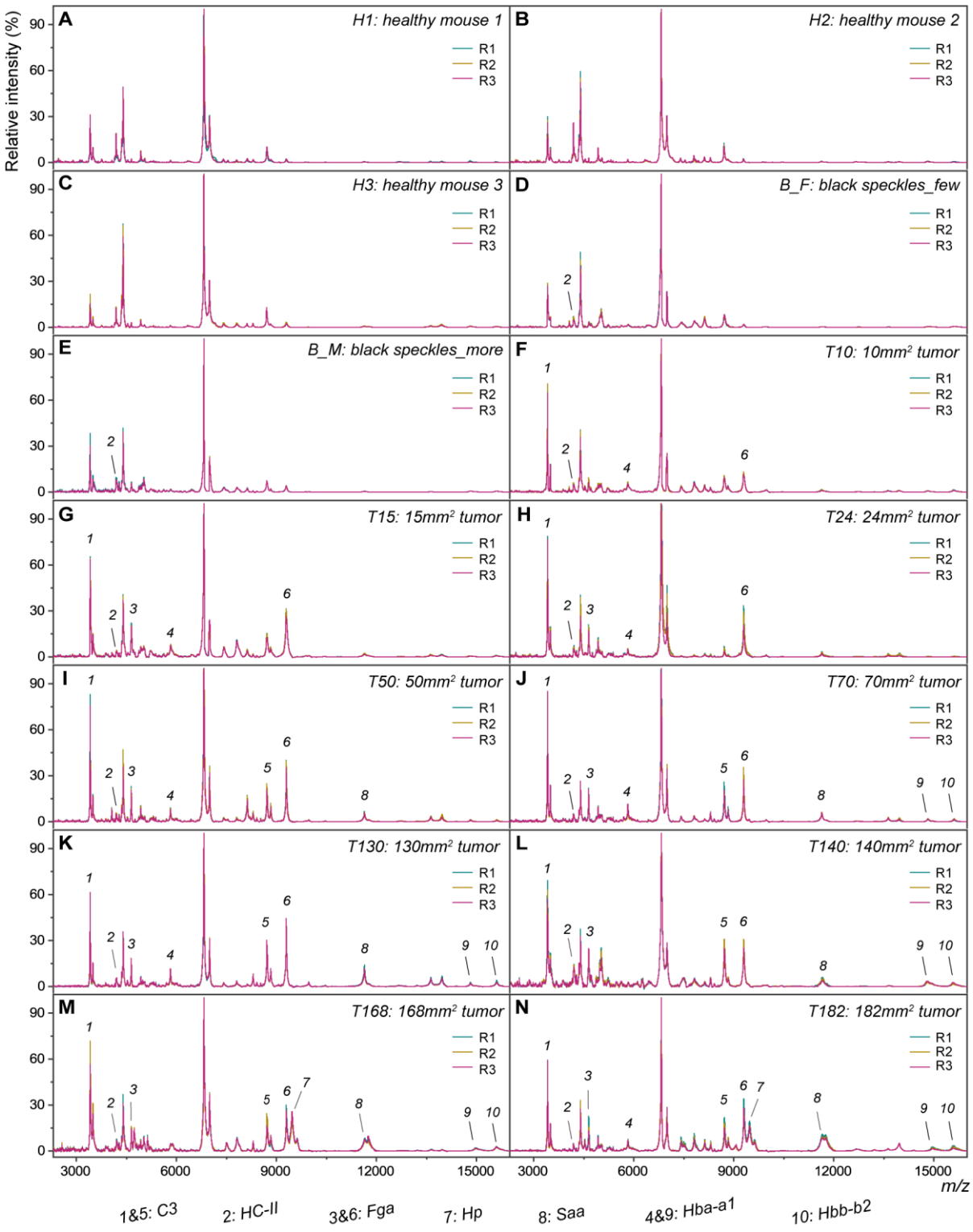

Figure S19. MALDI-TOF mass spectra of mouse blood-circulating exosomes. (A-N) The mouse skins progress from healthy state (*H1*, *H2*, *H3* for three healthy mouse individuals) to the lesions with different numbers of black speckles (*B_F* for few speckles, *B_M* for more speckles), and to skin tumors with the superficial surface area increased from *10* to *182* mm^2 (*T10*, *T15*, *T24*, *T50*, *T70*, *T130*, *T140*, *T168*, *T182*). Each spectrum was generated from ~5·10^7 intact exosomes, using the matrix of sinapinic acid. The peaks differently detected from cancerous mice are marked out, with their possible protein identities list on the bottom. The protein identities were tentatively clarified through a correlation of the MALDI-TOF mass spectra with the exosomal top-down proteomic data, as explained in **Data File S4** with details.

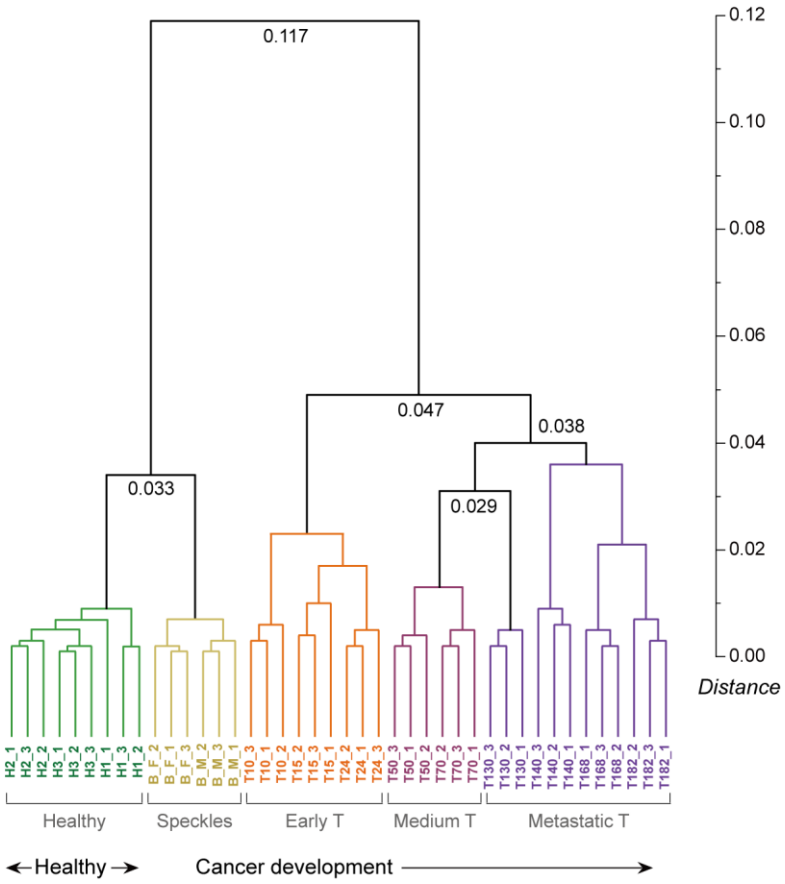

Figure S20. Hierarchical clustering dendrogram from the mouse blood test. Hierarchical cluster analysis (HCA) was conducted with the mass spectra generated from the mouse blood-circulating exosomes by using the cosine similarity and the average linkage. The inter-group distance is determined based on the mean distance between all objects in one group and all objects in the other group, and each single-pair distance is calculated as one minus the single-pair cosine similarity (*i.e.* 1-cosine similarity).

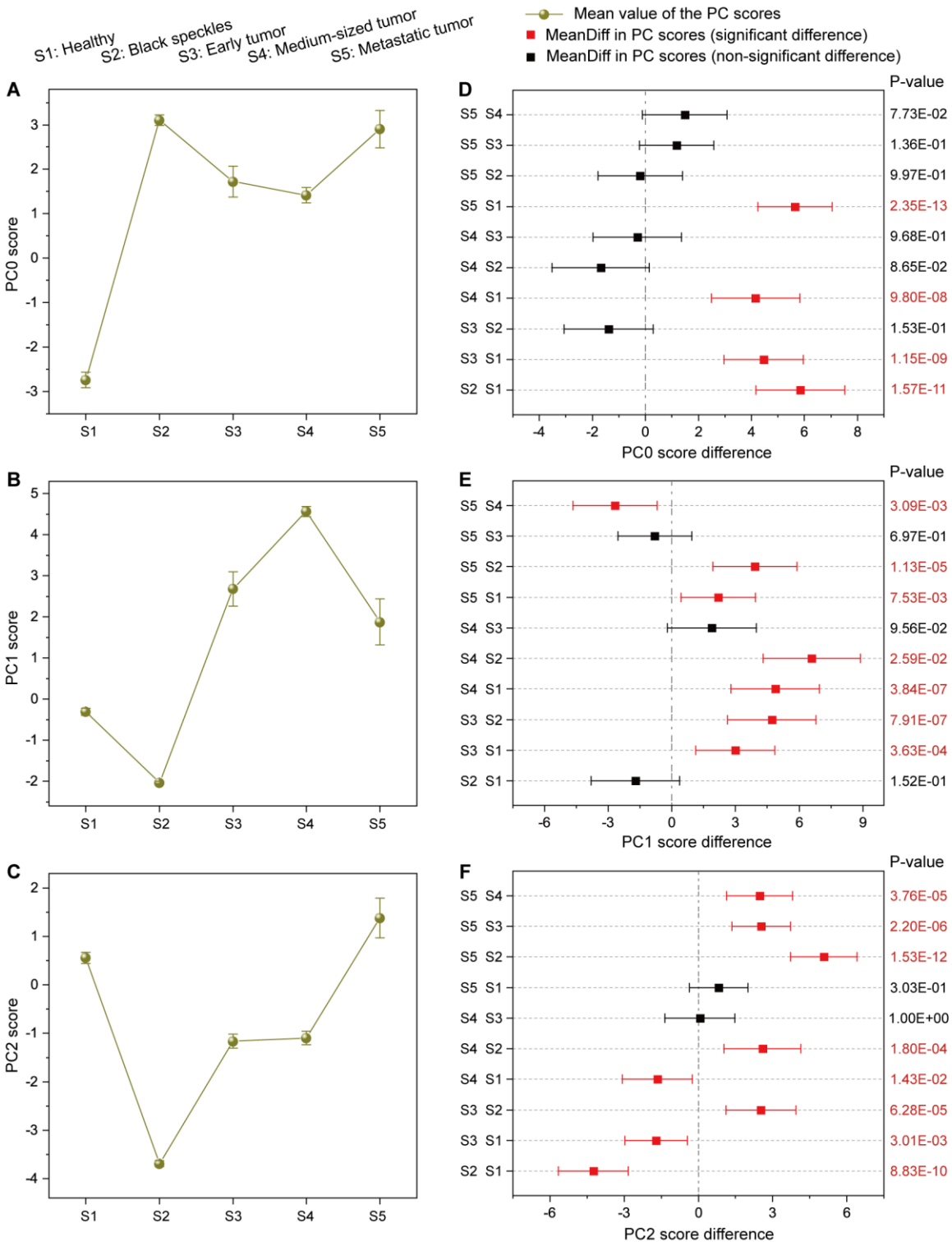

Figure S21. Statistical analysis of the mouse blood test PCA scores. Changes in the PCA scores along with the cancer development are plotted in (**A**) for PC0, (**B**) for PC1 and (**C**) for PC2. Differences in the PCA scores between each two skin groups are plotted in (**D**) for PC0, (**E**) for PC1 and (**F**) for PC2, with the level of statistical significance (P-value) from one-way ANOVA statistical labeled.

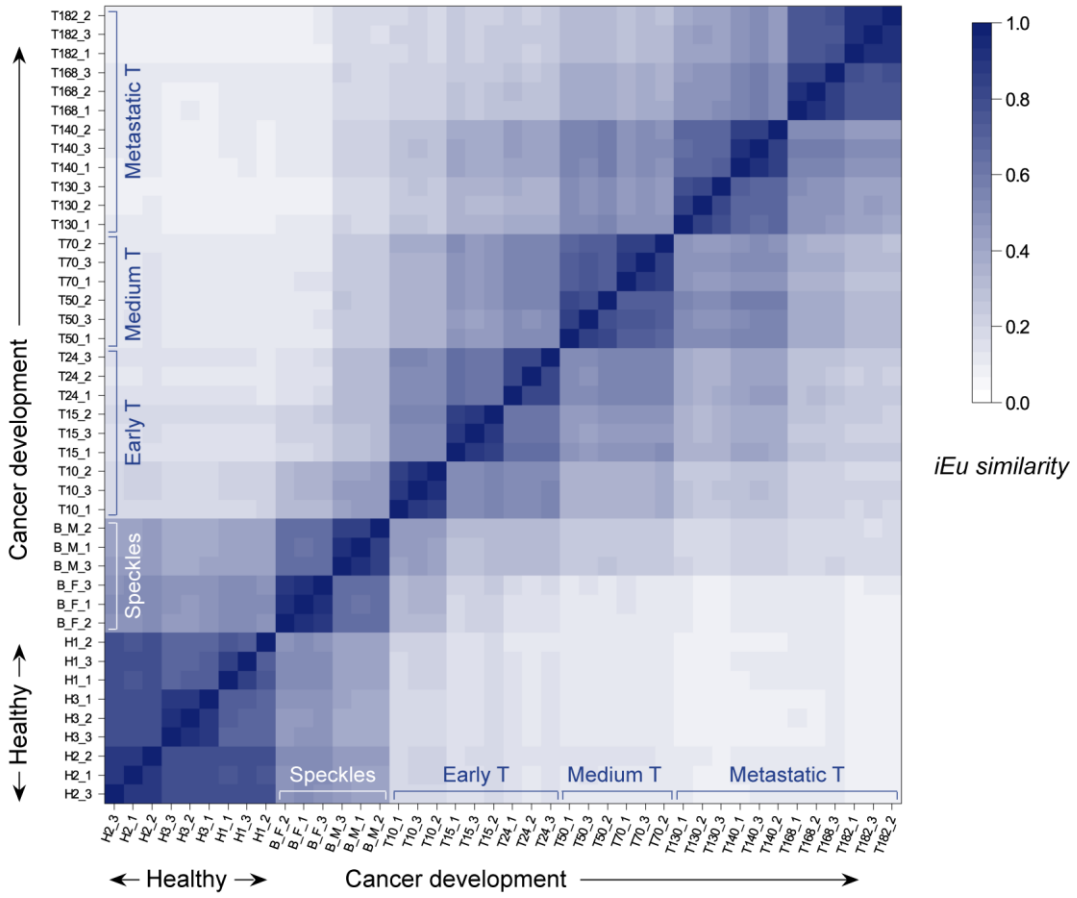

Figure S22. Comparison of mass fingerprints by intensity-weighted Euclidean distance

As for the intensity-weighted relative Euclidean (*iEu*) similarity, the previously mentioned relative *Eu* distance (**Figure S13**) is weighted by the peak intensity, and is defined as below.[4]

$$iEu = 1 - \frac{\sum_{k=1}^{n_{AB}} Eu_k(y_{Ak} + y_{Bk}) + \sum_{i=1}^{N_A} y_{Ai} + \sum_{j=1}^{N_B} y_{Bj} - \sum_{k=1}^{n_{AB}} (y_{Ak} + y_{Bk})}{\sum_{i=1}^{N_A} y_{Ai} + \sum_{j=1}^{N_B} y_{Bj}} \quad (5)$$

Figure S22 shows the hierarchal clustering heat map of the mouse skin surface mass fingerprints according to the fingerprint *iEu* similarity with the average linkage method.

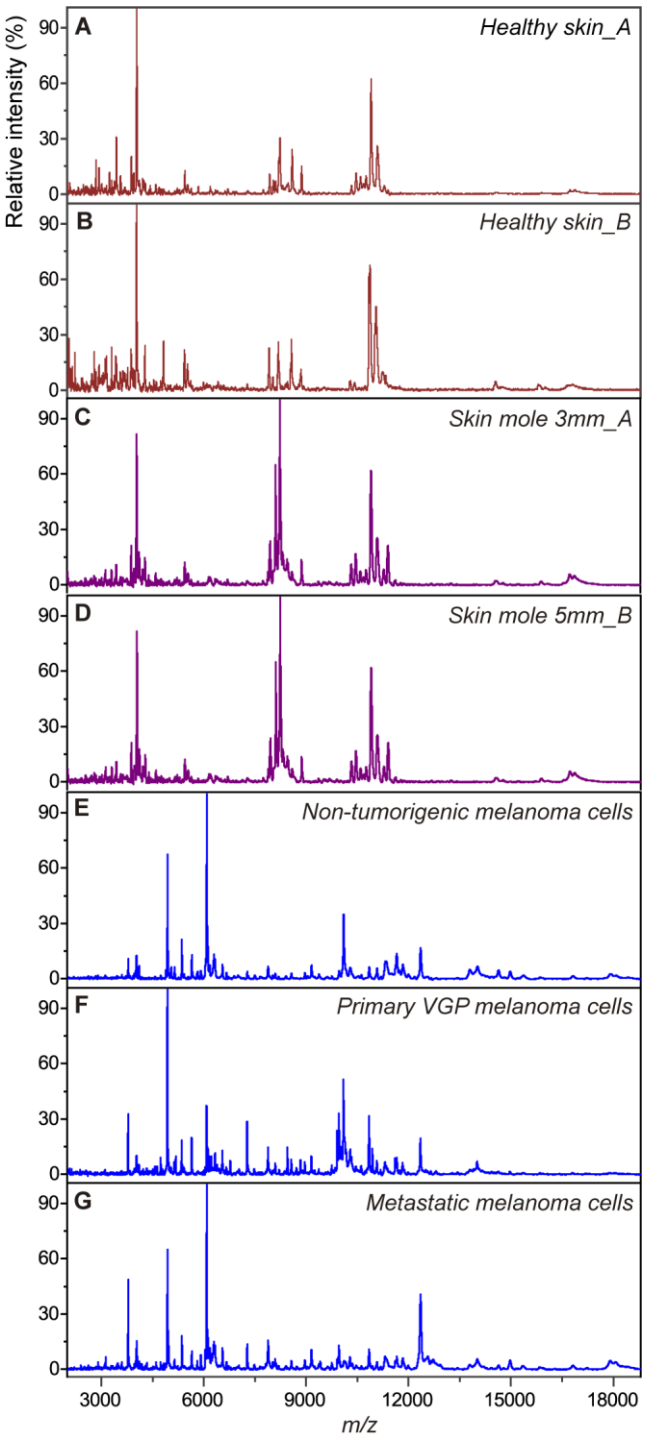

Figure S23. Mass fingerprints from normal skins, skin moles and melanoma cells. A normal skin region or a dark skin mole (with a lateral diameter of 3 mm and 5 mm, respectively) on the forearm of two healthy adult volunteers *A* and *B* were adhesively sampled three times in a row, with mass fingerprints obtained from the third samplings shown in (**A-D**), respectively. In (**E-G**), the mass fingerprints were obtained from human melanoma-mimic samples, prepared with human primary non-tumorigenic melanoma cells SBCL2, primary tumorigenic vertical growth phase (VGP) melanoma cells WM115, and metastatic melanoma cells WM239, respectively.

The mass fingerprints in **Figure S23** were obtained from two healthy volunteers, one female with yellow skin (healthy volunteer *A*) and one male with white skin (healthy volunteer *B*). Both individuals were in their early

30s and tested on a normal skin region on the right forearm. Their mass fingerprints displayed a mutual cosine similarity of 0.823±0.005, a value considerably high (**Figure S23 A-B**). The fingerprints in **Figure S23 C-D** were derived from black skin moles on the forearm of volunteer *A* (3 mm lateral diameter) and volunteer *B* (5 mm lateral diameter), displaying 0.749±0.027 and 0.503±0.037 cosine similarity to their corresponding healthy skins, and shared a mutual similarity of 0.556±0.026. The two moles had been confirmed as benign by a local dermatologist in Valais, Switzerland. A skin mole occurs when melanocytes grow in a cluster instead of spreading throughout the epidermis. Melanocytes produce melanin pigment and give the skin color. Melanocytes could also transform into melanoma cancer cells after accumulated genetic mutations.[7] The cancer at early progression stages often resembles skin moles in physical appearance, as in both cases the topical accumulation of melanin makes the skin brown-black in color. It is thus often a challenge to differentiate between the two skin conditions *via* visual examinations. With the proposed method, it is, nevertheless, possible to solve this problem, as the cellular composition of the cancer cells is different from that of normal melanocytes due to the accumulated genetic mutations. As shown in **Figure S23**, mass fingerprints of the skin moles and normal skins are quite different from the mimic melanoma samples at either the non-tumorigenic primary stage (**Figure S23E**), vertical growth phase (**Figure S23F**) or the metastatic stage (**Figure S23G**), sharing only few common peaks with cosine similarities lower than 0.160, *i.e.* 0.083±0.038 generally, and 0.066±0.028 between the skin moles and early non-tumorigenic primary melanoma-mimic samples. While, mass fingerprints from the melanoma-mimic samples with different stages of melanoma cells shared mutual similarities higher than 0.540 (0.723±0.181). In the melanoma-mimic samples, the cancer cells were *in vitro* grown and then deposited on the sampling discs with already the collected skin surface cells from a normal skin region on the forearm of volunteer *B*. The cancer cells were deposited on the human skin samples with surface density of ~60 cells·mm^{-2}. The above results indicate that the proposed methodology could be used for the differentiation between skin nevi and melanoma lesions at early stages.

Table S1. Human skin sample information

Sample ID	Description	Volunteer	Volunteer District	Volunteer Age	Volunteer Gender	Skin Site
D1	skin dehydration 01	A	Mainland China	30	male	front waist_left
D2	skin dehydration 02	A	Mainland China	30	male	front waist_left
D3	skin dehydration 03	A	Mainland China	30	male	front waist_left
D4	skin dehydration 04	A	Mainland China	30	male	front chest_left
D5	skin dehydration 05	A	Mainland China	30	male	front chest_left
D6	skin dehydration 06	A	Mainland China	30	male	front chest_left
D7	skin dehydration 07	A	Mainland China	30	male	leg_left
D8	skin dehydration 08	A	Mainland China	30	male	leg_left
D9	skin dehydration 09	A	Mainland China	30	male	leg_left
D10	skin dehydration 10	A	Mainland China	30	male	back waist_right
D11	skin dehydration 11	A	Mainland China	30	male	back waist_right
D12	skin dehydration 12	A	Mainland China	30	male	back waist_right
M1	skin mole 01	B	France	63	male	uparm_right
M2	skin mole 02	B	France	63	male	uparm_right
M3	skin mole 03	B	France	63	male	hand back_right
M4	skin mole 04	B	France	63	male	hand back_right
M5	skin mole 05	B	France	63	male	hand back_right
M6	skin mole 06	C	Brazil	29	male	neck
M7	skin mole 07	C	Brazil	29	male	neck
M8	skin mole 08	C	Brazil	29	male	neck
M9	skin mole 09	B	France	63	male	hand back_right
M10	skin mole 10	D	Mainland China	30	female	forearm_right
M11	skin mole 11	D	Mainland China	30	female	forearm_right
M12	skin mole 12	D	Mainland China	30	female	forearm_right
M13	skin mole 13	E	Serbia	31	female	forearm_right
M14	skin mole 14	E	Serbia	31	female	forearm_right
M15	skin mole 15	E	Serbia	31	female	forearm_right
M16	skin mole 16	C	Brazil	29	male	uparm_right
M17	skin mole 17	C	Brazil	29	male	uparm_right
M18	skin mole 18	C	Brazil	29	male	uparm_right
M19	skin mole 19	F	Switzerland	28	male	neck
M20	skin mole 20	F	Switzerland	28	male	neck
M21	skin mole 21	F	Switzerland	28	male	neck
M22	skin mole 22	G	Germany	35	male	forearm_right
M23	skin mole 23	G	Germany	35	male	forearm_right
M24	skin mole 24	G	Germany	35	male	forearm_right
N1	normal skin 01	G	Germany	35	male	forearm_right
N2	normal skin 02	H	Taiwan	33	female	forearm_right
N3	normal skin 03	B	France	63	male	hand back_right
N4	normal skin 04	E	Serbia	31	female	forearm_right
N5	normal skin 05	D	Mainland China	30	female	forearm_right
N6	normal skin 06	A	Mainland China	30	male	back waist_right
N7	normal skin 07	A	Mainland China	30	male	back waist_right
N8	normal skin 08	H	Taiwan	33	female	forearm_right
N9	normal skin 09	H	Taiwan	33	female	forearm_right
N10	normal skin 10	I	India	25	male	uparm_right
N11	normal skin 11	I	India	25	male	uparm_right
N12	normal skin 12	C	Brazil	29	male	uparm_right
N13	normal skin 13	C	Brazil	29	male	uparm_right
N14	normal skin 14	C	Brazil	29	male	uparm_right
N15	normal skin 15	G	Germany	35	male	forearm_right
N16	normal skin 16	B	France	63	male	hand back_right
N17	normal skin 17	B	France	63	male	hand back_right
N18	normal skin 18	E	Serbia	31	female	forearm_right
N19	normal skin 19	E	Serbia	31	female	forearm_right
N20	normal skin 20	D	Mainland China	30	female	forearm_right
N21	normal skin 21	D	Mainland China	30	female	forearm_right
N22	normal skin 22	G	Germany	35	male	forearm_right
N23	normal skin 23	I	India	25	male	uparm_right
N24	normal skin 24	F	Switzerland	28	male	neck
N25	normal skin 25	F	Switzerland	28	male	neck
N26	normal skin 26	F	Switzerland	28	male	neck
N27	normal skin 27	A	Mainland China	30	male	back waist_right
N28	normal skin 28	A	Mainland China	30	male	back waist_right
N29	normal skin 29	A	Mainland China	30	male	back waist_right
N30	normal skin 30	A	Mainland China	30	male	back waist_right

Table S2. Human skin surface mass fingerprint peak information

Altogether 179 well-resolved peaks were detected from the investigated human skins, including dehydrated skins (D1-D12), skin moles (M1-M24) and healthy normal skins (N1-N30). The table below lists the normalized relative intensity of each peak (%) detected from each of the investigated skin samples.

Part I (skin sample #D1-D12, M1-M21)

m/z	D 1	D 2	D 3	D 4	D 5	D 6	D 7	D 8	D 9	D 10	D 11	D 12	M 1	M 2	M 3	M 4	M 5	M 6	M 7	M 8	M 9	M 10	M 11	M 12	M 13	M 14	M 15	M 16	M 17	M 18	M 19	M 20	M 21
5475	0	0	0	0	0	0	5	5	5	0	4	6	5	4	4	0	4	0	0	0	6	0	0	0	0	0	0	0	3	3	0	0	0
11339	0	0	0	0	0	0	0	0	0	5	9	11	0	0	0	0	0	0	0	0	0	0	0	0	0	0	0	0	0	0	0	0	6
15890	0	0	0	0	0	0	0	0	0	0	8	12	0	0	0	0	0	0	0	0	0	0	0	0	0	0	0	0	0	0	0	0	0
9990	0	0	0	0	0	0	0	0	0	0	3	6	0	0	0	0	0	0	0	0	0	0	0	0	0	0	0	0	0	0	0	0	0
10065	0	0	0	0	0	0	0	0	0	0	6	8	0	0	0	0	0	0	0	0	0	0	0	0	0	0	0	0	0	0	0	0	0
7875	7	7	7	21	21	19	29	27	28	14	11	14	8	14	3	0	0	14	10	12	10	7	6	7	3	0	3	7	6	4	5	3	3
7739	4	4	4	7	7	6	9	7	7	4	4	4	0	0	0	0	0	4	0	3	0	0	0	0	0	0	0	0	0	0	7	6	4
7490	6	7	7	11	10	10	6	6	5	7	8	7	0	0	0	0	0	3	0	3	0	0	0	0	0	0	0	0	0	0	12	6	0
7592	8	8	8	8	8	6	7	5	5	6	6	4	0	0	0	0	0	0	0	0	0	0	0	0	0	0	0	0	0	0	3	0	0
8522	0	0	0	0	0	0	6	6	4	0	0	0	0	0	0	0	0	0	0	0	0	0	0	0	3	3	3	0	0	0	4	0	4
3934	0	0	0	0	4	3	5	6	6	4	0	0	0	0	0	4	0	0	0	0	0	0	0	0	0	0	0	0	0	0	0	0	0
11105	0	0	0	0	0	0	9	10	7	0	0	0	0	0	0	0	0	0	0	0	0	0	0	0	0	0	0	0	0	0	0	0	0
12396	0	0	0	0	0	0	5	6	6	0	0	0	0	0	0	0	0	0	0	0	0	0	0	0	0	0	0	0	0	0	0	0	0
7551	6	0	0	4	3	0	0	0	0	0	0	0	0	0	0	0	0	0	0	0	0	0	0	0	0	0	0	0	0	0	0	0	0
11007	5	0	0	0	0	0	0	0	0	0	0	0	0	0	0	0	0	0	0	0	0	0	0	0	0	0	0	0	0	0	0	0	3
5372	8	8	8	4	4	3	5	5	4	4	5	6	4	0	4	5	4	0	0	0	4	0	0	0	0	0	0	0	0	0	8	0	4
7540	0	7	7	0	0	3	5	4	0	3	4	0	0	0	0	0	0	4	3	4	0	0	0	0	0	0	0	0	0	0	0	3	0
10758	18	21	19	13	10	13	7	6	4	5	0	0	3	4	0	0	0	0	0	0	5	4	4	5	5	3	4	0	0	0	7	4	4
12752	4	5	5	4	0	4	0	0	0	0	0	0	0	0	0	0	0	0	0	0	0	0	0	0	0	0	0	0	0	0	0	0	0
12848	4	4	4	0	0	0	0	0	0	0	0	0	0	0	0	0	0	0	0	0	0	0	0	0	0	0	0	0	0	0	0	0	0
13245	4	5	4	0	0	0	0	0	0	0	0	0	0	0	0	0	0	0	0	0	0	0	0	0	0	0	0	0	0	0	0	0	0
13337	4	4	4	0	0	0	0	0	0	0	0	0	0	0	0	0	0	0	0	0	0	0	0	0	0	0	0	0	0	0	0	0	0
13464	3	4	4	0	0	0	0	0	0	0	0	0	0	0	0	0	0	0	0	0	0	0	0	0	0	0	0	0	0	0	0	0	0
4472	4	4	4	0	0	0	3	0	0	0	4	0	0	0	0	0	0	0	0	0	0	0	0	0	0	0	0	0	0	0	0	0	0
12906	5	5	5	0	0	0	4	3	0	0	0	0	0	0	0	0	0	0	0	0	0	0	0	0	0	0	0	0	0	0	0	0	0
6146	0	0	0	0	0	0	0	0	0	0	0	0	0	0	0	0	0	0	0	0	6	7	6	0	0	0	0	0	0	0	0	0	0
6708	0	0	0	0	0	0	0	0	0	0	0	0	0	0	0	0	0	0	0	0	0	4	4	0	0	0	0	0	0	0	0	0	0
4114	11	10	11	7	9	8	34	41	40	27	16	17	0	0	0	0	0	35	32	35	0	20	19	17	19	15	20	0	19	29	4	0	6
8358	4	4	4	3	0	0	5	6	5	5	7	6	4	0	0	0	0	9	7	9	4	6	5	6	8	7	7	8	6	0	4	0	0
8107	10	10	10	11	11	10	9	10	9	6	8	8	23	32	9	7	8	27	38	33	28	50	49	50	61	52	59	33	36	27	3	0	0
8315	6	6	6	7	7	7	4	5	4	5	5	4	10	10	11	11	11	13	13	13	11	14	14	15	16	14	16	12	12	10	0	0	0
8235	100	100	100	100	100	100	100	100	100	100	100	100	100	100	100	100	100	100	100	100	100	100	100	100	100	100	100	100	100	100	8	6	7
8451	10	12	11	5	6	5	11	12	11	10	10	9	7	8	13	10	11	12	11	12	8	12	12	14	14	14	13	12	12	9	0	0	0
3869	0	0	0	0	0	0	0	0	0	0	0	0	0	6	0	0	5	0	0	0	0	0	0	0	11	0	0	9	0	0	0	0	0
4710	0	0	0	0	0	0	0	0	0	0	0	0	0	0	0	0	0	0	0	0	21	0	0	0	4	0	5	0	0	0	0	0	0
4619	0	0	0	3	5	3	0	0	0	0	0	0	12	9	0	0	0	0	0	0	14	0	0	0	3	3	0	0	0	0	5	3	7
4860	0	0	0	0	0	0	0	0	0	0	0	0	5	5	0	0	0	0	0	0	5	0	0	0	0	0	0	0	0	0	0	0	0
11287	0	0	0	0	0	0	0	0	0	0	0	0	3	5	0	0	0	0	0	0	0	0	0	0	0	0	0	0	0	0	0	0	0
3511	0	0	0	0	0	0	0	0	0	0	0	0	0	3	0	0	0	0	0	0	4	0	0	0	0	0	0	4	3	0	0	0	0
3724	0	0	0	0	0	0	0	0	0	0	0	0	4	6	0	0	0	5	4	4	6	0	0	0	0	0	0	6	5	0	0	0	0
8470	0	0	0	0	0	0	0	0	0	0	9	8	7	0	12	12	12	0	10	11	9	0	0	0	0	11	0	11	14	12	0	0	0
4415	7	8	8	0	0	0	0	0	0	32	23	21	4	4	26	15	20	8	8	8	6	0	0	0	0	0	0	13	26	18	0	0	0
6953	0	0	0	0	0	0	0	0	0	3	3	3	0	4	4	3	4	0	4	3	3	0	0	0	0	0	0	5	5	4	0	0	0
4650	0	0	0	0	0	0	0	0	0	0	0	0	0	0	0	4	3	0	0	0	0	0	0	0	0	0	0	6	4	5	0	0	0
4346	0	0	0	0	0	0	0	0	0	4	4	3	0	0	0	0	0	0	0	0	0	0	0	0	0	0	0	7	9	6	0	0	0
4909	0	0	0	0	0	0	0	0	0	0	0	3	0	0	0	0	0	0	0	0	0	0	0	0	0	0	0	4	3	0	0	0	0
4965	0	0	0	0	0	0	0	0	0	0	0	0	0	0	0	0	0	0	0	0	0	0	0	0	0	0	0	7	6	0	0	0	0
3747	0	0	0	0	0	0	0	0	0	0	0	0	3	5	0	0	0	3	5	4	5	0	0	0	4	0	0	7	6	7	7	5	8
6348	3	3	3	0	0	0	0	0	0	0	0	0	3	0	4	3	4	5	6	6	4	0	0	0	0	0	0	4	4	4	4	3	8
3855	0	0	0	0	0	0	0	0	0	0	0	0	0	5	0	8	5	12	0	0	4	0	0	0	0	0	0	6	3	8	0	0	0
3790	0	0	0	0	0	0	0	0	0	0	0	0	0	0	0	0	0	3	0	0	0	0	0	0	0	0	0	3	0	3	4	3	3
6408	0	0	0	0	0	0	0	0	0	0	0	0	0	0	0	0	0	4	0	4	0	0	0	0	3	0	3	5	0	5	5	0	5
6189	0	0	0	0	0	0	0	4	4	0	0	0	5	5	6	5	5	15	10	13	4	6	4	5	9	10	10	30	17	31	12	4	20
6245	0	0	0	0	0	0	0	0	0	0	0	0	0	0	0	0	0	4	0	4	0	0	0	0	0	0	0	4	3	5	0	0	3
6541	0	0	0	0	0	0	0	0	0	0	0	0	0	0	0	0	0	0	0	0	0	0	0	0	0	0	0	4	0	4	4	0	0
4979	0	0	0	0	0	0	0	0	0	0	0	4	0	0	0	0	0	0	0	0	0	0	0	0	0	0	0	0	0	7	3	0	3
4053	0	0	0	0	0	0	0	0	0	0	0	14	0	0	0	0	0	0	0	0	0	0	0	0	0	0	5	0	0	20	0	0	0
4921	0	0	0	0	0	0	0	0	0	0	0	0	0	0	0	0	0	0	0	0	0	0	0	0	0	0	0	0	0	5	0	0	0
3706	0	0	0	0	0	0	0	0	0	0	0	0	0	0	0	0	0	0	0	0	5	0	0	0	0	0	0	6	6	8	0	0	0
4750	0	0	0	0	0	0	0	0	0	0	0	0	5	3	0	0	0	0	0	0	5	0	0	0	0	0	0	10	9	10	7	7	5
3572	0	0	0	5	5	6	0	0	0	6	4	6	6	6	0	0	0	18	16	18	7	4	4	0	4	6	4	14	11	15	0	0	0
3689	0	0	0	0	0	0	0	0	0	0	0	0	0	5	0	0	0	12	13	12	4	0	0	0	0	0	0	9	0	0	0	0	0
3634	0	0	0	0	0	0	0	0	0	4	0	0	4	7	5	0	4	7	11	9	7	0	0	0	5	5	5	6	5	6	8	7	9
3917	3	0	0	4	5	4	4	0	3	4	0	5	0	3	0	4	4	12	24	19	5	0	0	0	8	9	7	0	6	6	8	5	9
3552	0	0	0	0	0	4	0	0	0	5	0	0	6	10	11	5	8	0	13	0	10	0	3	0	5	6	5	8	6	7	0	0	0
4595	0	0	0	0	0	0	0	0	0	3	0	4	0	0	0	3	0	4	6	6	0	5	4	4	0	0	0	9	10	11	5	0	6
5990	0	0	0	0	0	0	0	0	0	0	0	0	0	0	0	0	0	0	0	0	0	0	0	0	0	0	0	0	0	0	0	0	0
8112	0	0	0	0	0	0	0	0	0	0	0	0	0	0	0	0	0	0	0	0	0	0	0	0	0	0	0	0	0	0	0	0	0
3602	0	0	0	0	0	0	0	0	0	0	0	0	0	0	0	0	0	0	0	0	0	0	0	0	0	0	0	0	0	0	0	0	0
6888	0	0	0	0	0	0	0	0	0	0	0	0	0	0	0	0	0	0	0	0	0	0	0	0	0	0	0	0	0	0	0	0	0
7925	4	0	0	0	0	0	0	0	0	6	6	10	0	0	0	0	0	0	0	0	0	0	0	0	0	0	0	36	0	0	10	12	10
4321	0	0	0	0	0	0	0	0	0	0	0	0	0	0	0	0	0	0	0	0	0	0	0	0	0	0	0	0	0	0	0	0	0
3767	0	0	0	0	0	0	0	0	0	0	0	0	0	0	4	0	0	0	3	0	0	0	0	0	0	0	0	0	0	0	0	0	0
4078	0	0	0	0	0	0	0	0	0	0	0	0	0	0	0	0	0	0	0	0	0	0	0	0	5	5	0	6	7	0	0	0	0
8795	0	0	0	0	0	0	0	0	0	0	0	0	0	0	0	0	0	0	0	0	0	0	0	0	0	0	0	0	0	0	0	0	0
3825	0	0	0	0	0	0	0	0	0	0	0	0	0	0	0	0	0	0	0	0	0	0	0	0	0	0	0	0	0	0	0	0	0
5949	0	0	0	0	0	0	0	0	0	0	0	0	0	0	0	0	0	0	0	0	0	0	0	0	0	0	0	0	0	0	0	0	0
4145	0	0	0	0	0	0	0	0	0	0	0	0	3	4	5	7	6	6	5	6	4	3	4	3	0	0	0	0	0	0	0	0	0
4186	0	0	0	0	0	0	0	0	0	0	0	0	0	0	0	0	0	0	5	4	0	0	0	0	0	0	0	0	0	0	0	0	0
4097	0	0	0	0	0	0	0	0	0	0	0	0	19	17	29	27	28	0	0	0	23	0	0	0	0	0	0	21	0	0	0	0	0
8588	0	0	0	0	0	0	6	8	6	8	13	20	11	6	28	31	29	16	14	15	12	8	6	8	16	21	16	11	10	11	0	0	0
8667	0	0	0	0	0	0	0	0	0	0	0	0	0	0	5	6	5	0	0	0	0	0	0	0	0	0	3	0	0	0	0	0	0
7935	0	4	4	7	8	7	13	13	13	0	8	9	26	31	9	8	8	43	39	41	26	19	16	19	10	15	11	0	41	26	0	0	0
8409	0	0	0	0	0	0	0	0	0	0	0	0	0	0	0	4	0	7	5	6	4	7	6	0	8	8	7	6	9	5	4	0	0

8044	0	3	0	0	0	0	3	3	0	0	3	5	5	5	5	8	6	8	9	8	7	7	7	7	6	7	6	9	13	6	0	0	0
3958	0	0	0	0	4	0	0	0	0	3	0	3	6	6	7	12	9	0	21	20	7	8	8	7	5	6	4	11	11	11	8	6	14
8203	0	0	0	0	0	0	0	0	0	0	0	0	0	0	19	0	0	33	35	35	25	25	23	0	0	30	22	42	58	34	4	4	4
11069	0	0	0	3	0	0	0	0	0	0	0	13	28	0	0	0	0	0	9	8	0	21	0	0	0	0	0	0	0	6	0	0	0
4564	0	0	0	0	0	0	0	0	0	0	0	0	0	0	0	0	0	0	0	0	0	0	0	0	0	0	0	0	0	0	0	0	3
4768	0	0	0	0	0	0	0	0	0	0	0	0	0	0	0	0	0	0	0	0	0	0	0	0	0	0	0	0	0	0	0	0	0
8948	0	0	0	0	0	0	0	0	0	0	0	0	0	0	0	0	0	0	0	0	0	0	0	0	0	0	0	0	0	0	0	0	0
10897	21	23	22	12	23	21	15	15	10	19	12	23	0	0	0	0	0	33	61	50	47	51	49	49	37	35	34	16	21	14	50	40	48
11068	0	6	5	9	10	9	5	5	4	5	4	7	0	0	0	0	0	17	29	24	32	0	0	0	16	17	15	6	9	0	17	15	0
4289	0	0	0	0	0	0	0	0	0	0	0	0	0	0	8	0	7	5	8	7	0	0	0	0	0	0	0	0	4	0	0	0	0
3527	0	0	0	0	0	0	0	0	0	0	0	0	0	0	0	0	0	0	3	0	0	0	0	0	0	0	0	0	0	0	0	0	0
6378	0	0	0	0	0	0	0	0	0	0	0	0	0	0	0	4	0	3	4	3	3	0	0	0	0	0	0	0	4	0	3	0	0
8146	0	0	0	0	0	0	0	0	0	0	0	0	0	5	0	0	0	6	7	7	0	0	0	0	0	0	0	0	0	0	0	0	0
6438	3	3	3	0	0	0	3	0	0	0	0	0	0	0	0	4	3	12	12	12	0	0	0	0	0	0	0	0	0	0	0	0	0
5391	0	0	0	0	0	0	0	0	0	0	0	0	0	0	0	0	0	5	5	5	0	0	0	0	0	0	0	0	0	0	0	0	0
8629	0	0	0	0	0	0	3	3	0	4	0	0	0	0	0	0	0	13	12	13	0	0	0	0	0	0	0	0	0	0	0	0	0
3660	0	0	0	0	0	0	0	0	0	0	0	0	0	0	0	0	0	0	18	12	0	0	0	0	0	0	0	0	0	0	0	14	7
8849	0	0	0	0	0	0	0	0	0	0	0	0	7	0	0	0	0	0	22	0	0	0	0	0	0	0	0	0	0	0	0	0	0
6416	0	0	0	0	0	0	0	0	0	0	0	0	0	0	0	0	0	0	0	0	0	0	0	0	0	0	0	0	0	0	0	0	4
7466	0	0	0	0	0	0	0	0	0	0	3	0	0	0	0	0	0	0	0	0	0	0	0	0	0	0	0	0	0	0	0	0	6
4371	3	4	3	7	10	8	0	0	0	0	0	7	0	0	0	0	0	0	0	0	0	0	0	0	0	0	0	0	7	0	0	0	13
3900	0	4	0	4	5	4	0	0	0	0	0	0	0	4	0	0	0	0	0	0	0	0	0	0	0	0	0	6	0	0	0	0	16
4433	33	35	34	49	62	49	20	16	13	0	0	0	0	0	0	0	0	0	0	0	0	0	0	0	16	9	14	0	0	0	59	42	65
5204	0	0	0	0	0	0	0	0	0	0	0	4	0	0	0	0	0	0	0	0	0	0	0	0	0	0	0	0	0	0	0	8	0
5685	0	0	0	0	0	0	0	0	0	0	3	5	0	0	0	0	0	0	0	0	0	0	0	0	0	0	0	0	0	0	0	41	30
11199	0	0	0	0	0	0	0	0	0	0	0	0	0	0	0	0	0	0	0	0	0	0	0	0	0	0	0	0	0	0	0	0	0
11549	0	0	0	0	0	0	0	0	0	0	0	0	0	0	0	0	0	0	0	0	0	0	0	0	0	0	0	0	0	0	7	0	6
3671	0	0	0	0	0	0	0	0	0	0	0	0	0	3	4	0	0	9	0	0	0	0	0	0	0	0	0	0	0	0	12	0	8
5697	5	5	5	15	16	13	8	7	8	7	12	20	0	0	0	0	0	5	0	4	0	0	0	0	5	0	0	0	11	9	40	0	0
11481	0	0	0	5	6	5	0	0	0	6	4	5	0	0	0	0	0	0	0	0	0	0	0	0	0	0	0	0	4	4	10	13	10
5733	0	0	0	0	0	0	0	0	0	0	0	0	0	0	0	0	0	0	0	0	0	0	0	0	0	0	0	0	0	0	5	5	3
11765	0	0	0	0	0	0	0	0	0	0	0	0	0	0	0	0	0	0	0	0	0	0	0	0	0	0	0	0	0	0	7	6	5
11819	0	0	0	0	0	0	0	0	0	0	0	0	0	0	0	0	0	0	0	0	0	0	0	0	0	0	0	0	0	0	4	5	4
5635	3	3	3	5	5	4	5	4	4	0	4	6	5	6	6	6	6	3	4	4	7	0	0	0	3	0	0	0	5	0	17	15	13
5802	0	0	0	0	3	0	0	0	0	0	4	5	0	0	0	0	0	0	0	0	0	0	0	0	0	0	0	0	0	0	7	8	6
11283	5	5	5	14	16	14	6	6	5	7	7	10	4	5	3	0	0	5	8	7	6	3	0	4	9	4	6	0	10	8	28	36	31
11397	16	13	15	48	53	49	23	22	20	34	43	63	0	0	0	0	0	12	10	11	0	0	0	0	21	18	21	5	36	33	85	100	85
11615	0	0	0	7	9	8	3	3	0	7	7	9	0	0	0	0	0	0	0	0	0	0	0	0	0	0	0	6	5	17	21	16
6688	0	0	0	0	0	0	0	0	0	0	0	0	0	0	0	0	0	0	0	0	0	0	0	4	0	0	0	0	0	0	3	0	0
6870	0	0	0	0	0	0	0	0	0	0	0	0	0	0	0	0	0	0	0	0	0	0	0	0	0	0	0	0	0	0	3	0	0
5295	0	0	0	0	0	0	0	0	0	0	0	0	0	0	0	0	0	0	0	0	0	0	0	0	0	0	0	0	0	0	5	3	0
7372	0	0	0	0	0	0	0	0	0	0	0	0	0	0	0	0	0	0	0	0	0	0	0	0	0	0	0	0	0	0	6	3	0
12234	0	0	0	0	0	0	0	0	0	0	0	0	0	0	0	0	0	0	0	0	0	0	0	0	0	0	0	0	0	0	3	0	0
5279	0	0	0	0	0	0	0	0	0	0	0	0	0	0	0	0	0	0	0	0	0	0	0	0	0	0	0	0	0	0	3	0	0
12019	0	0	0	0	0	0	0	0	0	0	0	0	0	0	0	0	0	0	0	0	0	0	0	0	0	0	0	0	0	0	4	0	0
7140	0	0	0	12	10	10	0	0	0	0	4	6	0	0	0	0	0	0	0	0	0	0	0	0	0	0	0	0	0	0	27	13	12
11686	0	0	0	0	0	0	0	0	0	0	0	0	0	0	0	0	0	0	0	0	0	0	0	0	0	0	0	0	0	0	4	5	4
3586	0	0	0	0	0	0	0	0	0	0	0	0	0	0	0	0	0	0	0	0	0	0	0	0	0	0	0	0	0	0	10	4	5
7244	0	0	0	0	0	0	0	0	0	0	0	0	0	0	0	0	0	0	0	0	0	0	0	0	0	0	0	0	0	0	15	7	7
9901	0	0	0	0	0	0	0	0	0	4	0	0	0	0	0	0	0	0	0	0	0	0	0	0	0	0	0	0	0	0	3	0	0
4696	0	0	0	0	0	0	0	0	0	0	0	3	16	15	8	8	8	0	0	0	0	0	0	0	0	0	0	8	10	9	4	3	0
4212	16	15	16	7	8	7	13	13	11	11	13	11	4	4	6	5	5	13	15	14	6	7	8	6	9	9	9	12	9	10	6	0	9
5839	0	0	0	0	0	0	0	0	0	0	0	0	0	0	0	0	0	0	0	0	0	0	3	0	3	4	4	0	0	0	4	3	3
8867	5	5	5	12	14	15	9	12	12	11	15	23	0	5	7	9	8	13	0	18	10	12	11	12	7	7	6	13	9	6	12	12	16
10898	0	0	0	19	8	11	15	15	14	0	14	19	43	0	0	0	0	0	0	0	0	0	0	0	0	0	0	0	0	0	0	0	0
8263	0	0	0	0	0	0	0	0	0	0	0	0	0	0	0	0	0	0	0	0	0	0	0	0	0	0	0	0	0	0	0	0	0
4391	0	0	0	0	0	0	0	0	0	5	5	3	0	0	0	0	0	0	0	0	0	5	6	5	0	0	0	5	6	4	12	9	0
4175	0	0	0	0	0	4	3	4	4	3	4	0	0	3	3	3	3	0	0	0	0	3	4	4	0	0	0	0	0	0	7	7	12
4256	0	0	0	0	0	0	0	0	0	0	0	0	0	0	0	0	0	0	0	0	0	3	0	0	0	0	0	0	0	0	5	4	8
3809	0	0	0	0	0	0	0	0	0	0	0	0	0	0	0	0	0	0	0	0	0	0	0	0	0	0	0	0	0	0	0	0	0
3980	0	0	0	0	0	0	3	4	3	5	4	5	0	4	0	5	3	18	12	0	0	9	9	8	5	6	4	0	4	0	21	25	23
4240	0	0	0	0	0	0	0	0	0	0	0	0	0	0	0	0	0	0	7	0	0	4	5	5	3	0	0	0	0	0	6	4	9
4035	14	13	13	12	14	14	6	7	6	10	7	0	54	57	60	52	55	43	59	51	64	49	56	51	46	44	41	25	29	0	100	99	100
4286	0	0	0	0	0	0	4	4	4	6	6	9	0	0	0	8	0	0	0	0	0	18	20	18	7	11	8	0	0	4	37	40	38
3878	7	7	7	8	10	10	9	10	9	13	10	17	4	0	6	7	7	13	29	22	7	14	18	15	0	14	10	0	15	9	27	20	30
5447	8	8	8	6	7	6	6	6	5	5	4	7	4	3	14	14	14	17	27	23	8	14	13	11	10	9	9	4	8	6	25	17	25
5531	0	0	0	0	0	3	3	3	3	0	0	4	4	0	0	0	0	0	0	0	0	0	6	6	5	5	5	0	0	0	11	7	11
4493	0	0	0	0	0	0	0	0	0	0	0	0	0	0	0	0	0	0	0	0	0	0	0	0	0	0	0	0	0	0	0	4	0
5003	0	0	0	0	0	0	0	0	0	0	0	0	0	0	0	0	0	0	0	0	0	0	0	0	0	0	0	0	0	0	0	0	0
5033	0	0	0	0	0	0	0	0	0	0	0	0	0	0	0	0	0	0	0	0	0	0	0	0	0	0	0	0	0	0	0	0	0
6106	0	0	0	0	0	0	0	0	0	0	0	0	0	0	0	0	0	0	0	0	0	0	0	0	3	0	0	0	0	0	0	0	0
4538	0	0	0	0	0	0	0	0	0	0	0	0	0	5	0	3	3	0	0	0	5	0	0	0	0	5	0	0	0	0	0	0	0
4828	6	0	7	0	0	0	0	0	0	0	0	0	12	16	9	0	9	0	0	0	15	0	0	0	4	0	4	0	0	0	0	0	0
5538	5	5	5	0	0	0	4	4	4	0	3	5	0	0	7	6	6	7	12	10	5	7	0	0	0	0	0	0	0	0	9	0	0
5159	0	0	0	0	0	0	0	0	0	0	0	3	0	0	0	0	0	0	0	0	0	5	5	4	8	7	7	0	0	0	8	4	4
7291	0	0	0	0	0	0	0	0	0	0	0	0	0	0	0	0	0	0	0	0	0	0	0	0	3	3	3	0	0	0	0	0	0
14589	0	0	0	0	0	0	0	0	0	0	0	0	0	0	0	0	0	0	0	0	0	0	0	0	7	4	6	0	0	0	0	0	0
10907	0	0	0	0	0	0	0	0	0	0	0	0	0	42	36	36	36	0	0	0	0	0	0	0	0	0	0	0	0	0	0	0	0
11084	11	12	12	0	0	0	9	9	8	12	8	0	0	30	18	17	17	0	0	0	0	0	20	21	0	0	0	0	0	0	0	0	19
4818	0	7	0	10	14	14	0	0	0	0	0	0	0	0	0	9	0	10	13	12	0	0	0	0	0	0	0	9	10	8	4	5	6
17062	0	0	0	0	0	0	0	0	0	0	0	0	0	0	0	0	0	0	0	0	0	0	0	0	0	0	0	0	0	0	0	0	0
16904	0	0	0	0	0	0	0	0	0	0	0	0	0	0	0	0	0	0	0	0	0	0	0	0	0	0	0	0	0	0	0	0	0
9360	0	0	0	0	0	0	0	0	0	0	0	0	0	0	0	0	0	0	0	0	0	0	0	0	0	0	0	0	0	0	0	0	0
14796	0	0	0	0	0	0	0	0	0	0	0	0	0	0	0	0	0	0	0	0	0	0	0	0	0	0	0	0	0	0	0	0	0
6002	0	0	0	0	0	0	0	0	0	0	0	0	0	0	3	0	0	0	0	0	0	0	0	0	0	0	0	0	0	0	0	0	0
4524	0	0	0	0	0	0	0	0	0	0	0	0	0	0	0	0	0	0	3	0	0	0	0	0	0	0	0	0	0	0	5	0	0
16980	0	0	0	0	0	0	0	0	0	0	0	0	0	0	0	0	0	0	0	0	0	0	0	0	0	0	0	0	0	0	0	0	0
17014	0	0	0	0	0	0	0	0	0	0	0	0	0	0	0	0	0	0	0	0	0	0	0	0	0	0	0	0	0	0	0	0	0
10594	7	8	8	4	4	3	0	0	0	3	0	0	0	0	0	0	0	0	0	0	0	6	5	6	0	0	0	0	0	0	5	4	3
10693	0	0	0	0	0	0	0	0	0	0	0	0	0	0	0	0	0	0	0	0	0	0	0	0	0	0	0	0	0	0	0	0	0
16718	0	0	0	0	0	0	0	0	0	0	0	0	0	0	0	0	0	0	0	0	0	0	0	0	0	0	0	0	0	0	5	0	0
16845	0	0	0	0	0	0	0	0	0	0	0	0	0	0	0	0	0	0	0	0	0	0	0	0	0	0	0	0	0	0	4	0	0
5226	4	4	4	0	0	0	4	4	4	4	5	4	0	0	0	0	0	0	4	3	0	5	4	4	0	0	0	0	0	0	9	0	5
10325	0	0	0	0	0	0	0	3	0	3	5	5	0	0	0	0	0	0	0	0	0	12	12	12	0	0	0	0	0	0	13	11	6
10456	8	8	8	4	5	4	10	10	8	16	13	12	0	0	0	0	0	0	0	0	0	14	13	14	4	0	0	0	0	0	19	17	10

Part II (skin sample #M22-M24, N1-N30)

m/z	M 22	M 23	M 24	N 1	N 2	N 3	N 4	N 5	N 6	N 7	N 8	N 9	N 10	N 11	N 12	N 13	N 14	N 15	N 16	N 17	N 18	N 19	N 20	N 21	N 22	N 23	N 24	N 25	N 26	N 27	N 28	N 29	N 30
5475	0	0	0	0	0	0	0	0	0	0	0	0	0	0	0	0	0	0	0	0	0	0	0	0	0	0	0	0	0	0	0	0	0
11339	0	0	0	0	0	0	0	0	0	0	0	0	0	0	0	0	0	0	0	0	0	0	0	0	0	0	0	0	0	0	0	0	0
15890	0	0	0	4	0	0	0	0	0	0	0	0	0	0	0	0	0	3	3	0	0	0	0	0	3	0	0	0	0	0	0	0	0
9990	0	0	0	0	0	0	0	0	0	0	0	0	0	0	0	0	0	0	0	0	0	0	0	0	0	0	0	0	0	0	0	0	0
10065	0	0	0	0	0	0	0	0	0	0	0	0	0	0	0	0	0	0	0	0	0	0	0	0	0	0	0	0	0	0	0	0	0
7875	5	0	3	0	0	0	0	0	3	5	0	0	0	0	0	0	0	0	0	0	0	0	0	0	0	0	0	0	0	4	5	3	5
7739	0	0	0	0	3	0	0	0	0	4	0	4	4	4	0	0	0	0	0	0	0	0	0	0	0	0	0	0	0	3	4	3	4
7490	0	0	0	0	0	0	0	0	0	0	0	0	0	0	0	0	0	0	0	0	0	0	0	0	0	0	0	0	0	0	0	0	0
7592	0	0	0	0	0	0	0	0	0	0	0	0	0	0	0	0	0	0	0	0	0	0	0	0	0	0	0	0	0	0	0	0	0
8522	0	0	0	0	0	0	0	0	0	0	0	0	0	0	0	0	0	0	0	0	0	0	0	0	0	0	0	0	0	0	0	0	0
3934	0	0	0	0	0	0	0	0	0	0	0	0	0	0	0	0	0	0	0	0	0	0	0	0	0	0	0	0	0	0	0	0	0
11105	0	0	0	0	0	0	0	0	0	0	0	0	0	0	0	0	0	0	0	0	0	0	0	0	0	0	0	0	0	0	0	0	0
12396	0	0	0	0	0	0	0	0	0	0	0	0	0	0	0	0	0	0	0	0	0	0	0	0	0	0	0	0	0	4	0	0	3
7551	0	0	0	0	0	0	0	0	0	0	0	0	0	0	0	0	0	0	0	0	0	0	0	0	0	0	0	0	0	0	0	0	0
11007	0	0	0	0	0	0	0	0	0	0	0	0	0	0	0	0	0	0	0	0	0	0	0	0	0	0	0	0	0	0	0	0	0
5372	0	0	0	0	7	0	3	0	4	3	5	5	3	4	0	6	4	0	0	0	3	4	3	4	0	0	3	3	3	0	0	0	4
7540	0	0	0	0	0	0	0	0	0	0	0	0	0	0	0	0	0	0	0	0	0	0	0	0	0	0	0	0	0	0	0	0	0
10758	4	4	3	0	4	3	5	9	4	4	5	3	5	7	4	4	5	0	7	5	7	6	9	8	3	4	0	3	3	6	4	4	5
12752	0	0	0	0	0	0	0	0	0	0	0	0	0	0	0	0	0	0	0	0	0	0	0	0	0	0	0	0	0	0	0	0	0
12848	0	3	0	0	0	0	0	0	0	0	0	0	0	0	0	0	0	0	0	0	0	0	0	0	0	0	0	0	0	0	0	0	0
13245	0	0	0	0	0	0	0	0	0	0	0	0	0	0	0	0	0	0	0	0	0	0	0	0	0	0	0	0	0	0	0	0	0
13337	0	0	0	0	0	0	0	0	0	0	0	0	0	0	0	0	0	0	0	0	0	0	0	0	0	0	0	0	0	0	0	0	0
13464	0	0	0	0	0	0	0	0	0	0	0	0	0	0	0	0	0	0	0	0	0	0	0	0	0	0	0	0	0	0	0	0	0
4472	0	0	0	0	0	0	0	0	0	0	0	0	0	0	0	0	0	0	0	0	0	0	0	0	0	0	0	0	0	0	0	0	0
12906	0	0	0	0	0	0	0	0	0	0	0	0	0	0	0	0	0	0	0	0	0	0	0	0	0	0	0	0	0	0	0	0	0
6146	0	0	0	4	0	0	0	0	0	0	0	4	0	0	0	0	0	0	0	0	0	0	0	0	0	0	0	0	0	0	0	0	0
6708	0	0	0	0	0	0	0	0	0	0	0	0	0	0	0	0	0	0	0	0	0	0	3	0	0	0	0	0	0	0	0	0	0
4114	9	6	5	4	9	0	13	9	3	5	0	0	7	8	0	10	0	0	0	10	16	26	12	13	0	7	4	0	0	0	0	0	6
8358	8	6	4	0	0	0	5	4	0	0	0	0	0	0	0	0	0	0	5	0	4	5	5	5	0	0	0	0	0	0	0	0	0
8107	12	14	5	0	0	4	18	8	0	0	0	0	0	0	0	4	4	0	4	0	20	21	8	6	0	0	0	0	0	0	0	0	0
8315	5	6	0	0	0	4	8	5	0	0	0	0	0	0	0	0	0	0	5	3	8	8	6	5	0	0	0	0	0	0	0	0	0
8235	57	56	23	0	10	27	52	41	7	9	8	8	5	7	0	10	0	0	25	21	56	58	36	41	0	4	4	5	0	7	9	7	9
8451	9	9	4	4	3	5	8	6	0	0	3	3	0	4	7	7	8	4	9	5	8	8	7	5	4	0	0	0	0	0	0	0	0
3869	0	0	0	0	0	18	0	0	0	0	0	0	0	0	0	0	0	0	0	0	0	0	0	0	0	0	0	0	0	0	0	0	0
4710	0	0	0	0	0	0	0	0	0	0	0	0	0	0	0	0	0	0	0	4	0	0	0	0	0	0	0	0	0	0	0	0	0
4619	0	0	0	0	0	3	0	0	0	0	0	0	0	0	0	0	0	0	0	6	0	0	0	0	0	0	0	4	4	0	0	0	0
4860	0	0	0	0	0	0	0	0	0	0	0	0	0	0	0	0	0	0	0	0	0	0	0	0	0	0	0	0	0	0	0	0	0
11287	0	0	0	0	0	0	0	0	0	0	0	0	0	0	0	0	0	0	0	0	0	0	0	0	0	0	0	0	0	0	0	0	0
3511	0	0	0	0	0	0	0	0	0	0	0	0	0	0	0	3	0	0	0	0	0	0	0	0	3	0	0	0	0	0	0	0	0
3724	0	0	0	0	0	0	0	0	0	0	0	0	0	0	0	0	0	0	0	0	0	0	0	0	0	0	0	0	0	0	0	0	0
8470	0	8	4	0	0	6	9	6	0	0	0	0	0	0	0	0	0	0	0	0	8	8	0	6	0	0	0	0	0	0	0	0	0
4415	0	0	0	0	0	0	0	0	0	0	0	0	0	0	0	6	0	0	3	6	4	4	0	0	3	0	0	0	0	0	0	0	0
6953	0	3	4	0	0	0	0	0	0	0	0	0	0	0	0	0	0	0	0	0	0	0	0	0	0	0	0	0	0	0	0	0	0
4650	0	0	0	0	0	0	0	0	0	0	0	0	0	0	0	0	0	0	0	0	0	0	0	0	0	0	0	0	0	0	0	0	0
4346	0	0	0	0	0	0	0	0	0	0	0	0	0	0	0	4	4	0	0	0	0	0	0	0	0	0	0	0	0	0	0	0	0
4909	0	0	0	0	0	0	0	0	0	0	0	0	0	0	0	0	0	0	0	0	0	0	0	0	0	0	0	0	0	0	0	0	0
4965	0	0	0	0	0	0	0	0	0	0	0	0	0	0	0	0	4	0	0	0	0	0	0	0	3	0	0	0	0	0	0	0	0
3747	0	0	0	5	0	0	0	0	4	0	3	4	0	0	0	0	0	4	0	0	3	3	0	0	3	0	0	5	7	0	0	4	0
6348	0	0	0	0	0	0	0	0	4	3	0	0	0	0	0	0	0	0	0	0	7	5	0	0	0	0	0	0	4	0	0	3	3
3855	0	0	0	0	0	0	0	0	0	0	0	0	0	0	4	6	7	0	0	0	0	0	0	0	0	0	0	0	0	0	0	0	0
3790	0	0	0	0	0	0	0	0	0	0	0	0	0	0	0	3	3	0	0	0	0	0	0	0	0	0	0	0	0	0	0	0	0
6408	3	3	3	0	0	0	0	0	3	0	0	0	0	0	0	3	3	0	0	0	0	0	0	0	0	0	0	0	4	0	0	0	0
6189	0	0	0	0	0	0	5	5	10	9	0	0	3	0	10	17	18	0	0	0	10	7	6	4	0	3	5	11	18	7	8	9	6
6245	0	0	0	0	0	0	0	0	0	0	0	0	0	0	0	3	3	0	0	0	0	0	0	0	0	0	0	0	3	0	0	0	0
6541	0	0	0	0	0	0	0	0	0	0	0	0	0	0	0	0	0	0	0	0	0	0	0	0	0	0	0	0	0	0	0	0	0
4979	0	0	0	0	0	3	0	0	0	0	0	0	0	0	0	0	0	0	3	0	0	0	0	0	4	0	0	0	0	0	0	0	0
4053	0	0	0	0	0	0	0	0	0	0	0	0	0	0	0	0	0	0	0	0	0	0	0	0	0	0	0	0	0	0	0	0	0
4921	0	0	0	0	0	0	0	0	0	0	0	0	0	0	0	0	0	0	0	0	0	0	0	0	0	0	0	0	0	0	0	0	0
3706	4	0	3	3	0	0	0	0	3	0	3	5	0	0	0	0	0	0	0	0	0	0	3	0	6	0	0	0	0	0	4	0	0
4750	8	5	8	5	5	6	6	0	6	5	4	6	5	5	9	10	12	5	5	5	5	7	0	3	6	4	3	4	0	0	4	4	5
3572	0	0	0	0	8	4	3	4	10	10	7	9	7	6	9	10	18	0	0	4	4	4	6	5	10	7	0	5	5	7	11	7	9
3689	0	0	0	7	0	5	0	0	4	4	0	0	3	0	8	13	14	9	4	5	0	0	3	4	11	3	0	0	4	3	4	0	4
3634	0	0	0	9	9	5	4	4	12	12	6	5	8	8	11	17	15	9	6	4	7	7	3	4	10	8	6	10	10	8	11	9	11
3917	3	0	4	9	7	8	6	7	11	11	5	7	12	12	21	33	29	10	8	12	6	8	9	8	11	12	9	13	13	9	11	8	10
3552	0	0	4	8	4	5	0	5	9	10	4	4	7	6	9	8	12	11	0	0	0	0	6	6	14	7	0	5	5	7	9	5	8
4595	0	0	0	10	6	0	0	5	7	7	6	8	5	5	4	6	4	12	0	0	0	0	7	5	14	4	0	6	6	7	8	6	7
5990	0	3	0	0	0	0	0	0	0	0	0	0	0	0	0	0	4	0	0	0	0	0	0	0	5	0	0	0	0	0	0	0	0
8112	0	0	0	0	0	3	0	0	0	0	0	0	0	0	0	0	6	0	0	0	0	0	0	0	0	0	0	0	0	0	0	0	0
3602	0	0	0	0	0	0	0	0	0	0	0	0	0	0	0	0	5	0	0	0	0	0	0	0	0	0	0	0	0	0	0	0	0
6888	0	0	0	0	0	0	0	0	0	0	0	0	0	0	0	0	4	0	0	0	0	0	0	0	0	0	0	0	0	0	0	0	0
7925	0	0	0	0	0	0	0	0	0	0	0	0	0	0	0	41	42	0	0	0	0	0	0	0	19	0	10	10	11	0	0	0	0
4321	3	0	0	0	0	0	0	0	0	0	0	0	0	0	0	5	3	0	0	0	0	0	0	0	3	0	0	0	0	0	0	0	0
3767	0	0	0	4	0	0	0	0	0	0	0	0	0	0	9	17	11	5	0	0	0	0	0	0	7	0	0	0	0	0	0	0	0
4078	0	0	0	0	0	0	0	0	0	0	0	0	0	0	0	17	13	0	0	0	0	0	0	0	0	0	0	0	5	0	0	0	4
8795	0	0	0	0	0	0	0	0	0	0	0	0	0	0	0	3	4	0	0	0	0	0	0	0	0	0	0	0	0	0	0	0	0
3825	0	0	0	0	0	0	0	0	0	0	0	0	0	0	0	4	4	0	0	0	0	0	0	0	0	0	0	0	0	0	0	0	0
5949	0	0	0	0	0	0	0	0	0	0	0	0	0	0	0	3	3	0	0	0	0	0	0	0	0	0	0	0	0	0	0	0	0
4145	0	0	0	0	0	0	0	0	0	4	0	0	0	0	7	17	11	0	0	0	0	0	3	3	0	0	0	0	0	3	0	0	0
4186	3	0	0	0	0	0	0	0	0	0	0	0	0	0	0	4	5	0	0	0	0	0	0	0	0	0	0	0	0	0	0	0	0
4097	0	0	0	6	11	17	13	0	0	0	11	10	7	7	13	17	15	4	13	11	16	27	0	0	0	6	3	4	0	0	0	0	0
8588	0	4	0	28	11	21	13	23	4	5	17	10	11	14	34	38	40	25	23	25	11	12	26	22	25	7	0	0	0	6	4	4	4
8667	0	0	0	3	0	4	0	0	0	0	0	0	0	0	4	4	4	0	4	4	0	0	0	0	0	0	0	0	0	0	0	0	0
7935	9	13	11	20	25	12	27	8	12	11	25	22	13	17	33	0	0	18	16	16	33	33	12	7	0	10	0	0	0	11	9	11	10
8409	3	0	0	0	0	0	9	0	0	0	0	0	0	3	0	3	3	3	7	0	9	9	5	0	3	0	0	0	0	0	0	0	0
8044	0	4	0	8	5	4	7	6	6	7	5	4	5	7	11	11	13	8	4	5	8	8	7	5	8	4	0	0	0	7	7	6	8
3958	0	0	0	10	14	6	19	9	0	0	14	14	10	10	16	19	18	9	6	5	23	18	13	9	10	9	7	10	10	0	0	0	0
8203	0	0	0	20	20	19	55	17	10	5	23	19	12	17	32	37	40	18	0	17	61	62	21	15	18	8	0	0	0	5	5	4	5
11069	0	0	0	0	0	0	0	0	0	0	36	0	0	0	23	0	0	0	0	0	0	0	0	22	42	0	0	0	0	0	25	0	0
4564	0	0	0	0	0	0	0	0	0	0	0	0	0	0	4	5	0	0	0	0	0	0	0	0	0	0	0	0	0	0	0	0	0
4768	0	0	0	0	0	0	0	0	0	0	0	0	0	0	8	0	0	0	0	0	0	0	0	0	0	0	0	0	0	0	0	0	0
8948	0	0	0	0	0	0	0	0	0	0	0	0	0	0	0	0	0	0	0	0	4	0	0	0	0	0	0	0	0	0	0	0	0
10897	0	39	30	0	0	0	0	0	0	0	0	0	0	0	44	42	47	80	68	51	73	69	58	64	85	44	63	54	54	66	49	51	57
11068	0	22	17	0	0	42	0	0	0	0	0	0	0	0	0	20	22	0	0	0	32	31	23	0	0	21	25	0	22	0	0	26	28
4289	0	0	0	0	0	6	0	10	0	21	0	0	0	0	0	0	0	0	0	0	0	0	0	0	0	35	0	0	0	0	0	0	0
3527	0	0	0	0	0	0	0	0	0	0	0	0	0	0	0	0	0	0	0	0	0	0	0	0	0	0	0	5	5	0	0	0	0
6378	0	0	0	0	0	0	0	0	0	0	0	0	0	0	0	4	0	0	0	0	0	0	0	0	0	0	0	0	0	0	0	0	0

8146	0	0	0	0	3	0	0	0	0	0	0	3	0	0	5	5	0	0	0	0	0	0	0	0	0	0	0	0	0	0	0	0	0
6438	0	0	0	4	0	0	0	0	0	0	0	0	0	0	0	0	0	4	0	0	0	0	0	0	5	0	0	0	0	0	0	0	0
5391	0	0	0	0	0	0	0	0	0	0	0	0	0	0	0	0	0	0	0	0	0	0	0	0	0	0	0	0	0	0	0	0	0
8629	0	0	0	0	0	0	0	0	0	0	0	0	0	0	0	0	0	0	0	0	0	0	0	0	0	0	0	0	0	0	0	3	0
3660	0	9	13	5	0	0	0	0	7	0	0	0	0	0	0	0	0	0	3	0	0	0	0	0	0	5	6	0	4	7	5	6	
8849	0	0	0	0	0	0	0	0	0	0	0	0	0	0	0	0	3	0	0	0	0	0	0	0	0	0	0	0	0	0	0	0	0
6416	0	0	0	0	0	0	0	0	0	0	0	0	0	0	0	0	3	0	0	0	0	0	0	0	0	0	0	0	0	0	0	0	0
7466	0	0	0	0	0	0	0	0	0	0	0	0	0	0	0	0	0	0	0	0	0	0	0	0	0	0	0	0	0	0	0	0	0
4371	0	0	0	0	0	0	0	0	5	4	0	0	0	0	0	0	0	0	0	0	0	0	0	0	0	0	0	0	4	5	4	3	
3900	0	0	0	0	0	0	0	0	0	0	0	0	0	0	0	0	0	0	0	0	0	0	0	0	8	14	14	0	0	0	0	0	
4433	9	8	9	5	5	0	7	4	13	8	5	5	6	7	10	9	10	7	0	0	10	11	5	5	9	5	26	41	45	11	14	10	8
5204	0	0	0	0	0	0	0	0	0	0	0	0	0	0	0	0	0	0	0	0	0	0	0	0	0	0	0	0	0	0	0	0	0
5685	0	0	0	0	0	0	0	0	0	0	0	0	0	0	0	0	0	0	0	0	0	0	0	0	0	4	4	4	0	0	0	0	0
11199	6	8	0	0	0	0	0	0	0	0	0	0	0	0	0	0	0	0	0	0	0	0	0	0	0	0	0	0	0	0	0	0	0
11549	0	11	0	0	0	0	0	0	0	0	0	0	0	0	0	0	0	0	0	0	0	0	0	0	0	0	0	0	0	0	0	0	0
3671	17	0	0	0	0	5	0	0	0	6	0	0	0	0	5	8	4	6	0	0	0	0	0	3	7	3	5	0	0	0	0	0	0
5697	35	25	21	0	0	0	0	0	0	0	0	0	0	0	0	0	0	0	0	0	0	0	0	0	0	0	0	0	0	0	0	0	0
11481	16	0	0	0	0	0	0	0	0	0	0	0	0	0	0	0	0	0	0	0	0	0	0	0	0	0	0	0	0	0	0	0	0
5733	6	0	0	0	0	0	0	0	0	0	0	0	0	0	0	0	0	0	0	0	0	0	0	0	0	0	0	0	0	0	0	0	0
11765	5	0	0	0	0	0	0	0	0	0	0	0	0	0	0	0	0	0	0	0	0	0	0	0	0	0	0	0	0	0	0	0	0
11819	4	0	0	0	0	0	0	0	0	0	0	0	0	0	0	0	0	0	0	0	0	0	0	0	0	0	0	0	0	0	0	0	0
5635	13	13	12	5	8	6	3	0	6	5	6	6	5	6	4	3	3	5	5	3	3	4	4	4	6	4	5	5	4	4	5	5	5
5802	9	7	5	0	0	0	0	0	0	0	0	0	0	0	0	0	0	0	0	0	0	0	0	0	0	0	0	0	0	0	0	0	0
11283	33	47	49	9	7	11	7	4	7	6	5	5	5	7	4	0	3	9	10	8	7	7	5	0	9	4	6	5	5	8	6	7	6
11397	100	100	100	5	0	0	9	3	10	6	0	0	0	0	0	0	0	5	0	0	6	6	12	0	5	0	9	9	10	6	5	13	6
11615	24	23	22	6	0	0	0	0	0	0	0	0	0	0	0	0	0	4	0	0	0	0	0	0	0	0	0	0	0	0	0	0	0
6688	0	0	0	0	0	0	0	0	0	0	0	0	0	0	0	0	0	0	0	0	0	0	0	0	0	0	0	0	0	0	0	0	0
6870	0	0	0	0	0	0	0	0	0	0	0	0	0	0	0	3	0	0	0	0	0	0	0	0	0	0	0	0	0	0	0	0	0
5295	0	0	0	0	0	0	0	0	0	0	0	0	0	0	0	0	0	0	0	0	0	0	0	0	0	4	0	3	0	0	0	0	0
7372	0	0	0	0	0	0	0	0	0	0	0	0	0	0	0	0	0	0	0	0	0	0	0	0	0	0	0	0	0	0	0	0	0
12234	0	0	0	0	0	0	0	0	0	0	0	0	0	0	0	0	0	0	0	0	0	0	0	0	0	0	0	0	0	0	0	0	0
5279	0	0	0	0	0	0	0	0	0	0	0	0	0	0	0	0	0	0	0	0	0	0	0	0	0	0	0	0	0	0	0	0	0
12019	0	0	0	0	0	0	0	0	0	0	0	0	0	0	0	0	0	0	0	0	0	0	0	0	0	0	0	0	0	0	0	0	0
7140	3	0	4	0	0	0	0	0	0	0	0	0	0	0	0	0	0	0	0	0	0	0	0	0	0	0	3	0	0	0	0	0	0
11686	0	0	0	0	0	0	0	0	0	0	0	0	0	0	0	0	0	0	0	0	0	0	0	0	0	0	0	0	0	0	0	0	0
3586	0	0	0	0	0	0	0	0	0	0	0	0	0	0	0	0	0	0	0	0	0	0	0	0	0	0	0	0	0	0	0	0	0
7244	0	0	0	0	0	0	0	0	0	0	0	0	0	0	0	0	0	0	0	0	0	0	0	0	0	3	0	3	0	0	0	0	0
9901	0	0	0	0	0	0	0	0	0	3	0	0	0	0	0	0	0	0	0	0	0	0	0	0	0	0	0	0	0	0	0	0	3
4696	0	0	0	0	0	0	0	0	12	10	0	0	0	0	4	5	5	0	0	0	0	0	4	0	0	0	0	0	0	8	10	7	10
4212	0	0	0	5	11	4	4	7	26	18	11	13	9	9	8	7	15	5	4	5	7	8	8	7	7	9	5	10	12	16	17	19	13
5839	0	0	0	0	0	0	0	3	18	12	3	4	4	4	3	5	9	0	0	0	3	0	3	0	0	4	4	7	7	11	14	15	10
8867	0	3	3	15	6	0	10	11	25	31	6	7	14	17	10	11	14	13	4	6	17	15	13	10	12	11	13	17	17	29	30	25	35
10898	0	0	0	0	0	66	63	60	56	53	81	63	58	72	0	0	0	0	0	0	0	0	0	0	0	0	0	0	0	0	0	0	0
8263	0	0	0	0	0	0	0	0	0	0	0	4	4	5	0	0	0	0	0	0	0	0	0	0	0	3	0	0	0	0	0	0	0
4391	0	0	0	0	7	0	0	0	4	0	7	7	12	13	6	8	9	0	0	0	0	0	0	0	0	10	5	8	10	0	0	0	0
4175	0	0	0	0	4	0	0	0	5	0	4	5	11	11	0	0	0	3	0	0	0	3	0	0	4	11	0	6	4	0	0	4	0
4256	0	0	0	0	0	0	0	0	5	3	4	0	8	7	0	4	0	0	4	0	0	4	0	5	0	8	0	7	5	4	3	4	0
3809	4	0	0	0	4	0	0	0	4	0	0	3	0	0	0	0	0	0	0	0	0	0	0	0	0	0	0	0	0	0	3	0	3
3980	26	20	29	8	21	0	17	4	27	24	16	21	12	12	7	8	7	9	7	0	0	12	4	0	11	12	16	19	18	20	25	19	26
4240	0	0	0	4	7	5	3	6	0	0	6	5	6	6	7	8	4	5	5	6	4	5	6	0	6	0	3	6	5	0	0	0	0
4035	30	31	30	100	100	100	100	100	100	100	100	100	100	100	100	100	100	100	100	100	100	100	100	100	100	100	100	100	100	100	100	100	100
4286	25	19	28	30	52	5	16	0	24	0	43	54	37	40	16	12	17	34	16	6	14	15	9	10	38	0	26	28	27	18	19	16	22
3878	17	14	16	19	33	0	22	20	24	21	27	29	26	26	17	13	17	23	21	17	22	22	21	19	28	26	22	31	30	19	19	18	21
5447	12	14	19	24	50	20	20	12	23	19	41	36	28	33	18	14	13	26	17	9	27	29	19	24	30	23	31	26	21	23	23	24	23
5531	0	8	12	0	27	14	0	6	0	15	20	19	0	0	0	8	7	0	0	5	0	14	0	0	0	0	0	13	10	0	0	15	0
4493	0	0	3	3	5	0	0	0	0	0	5	7	4	4	0	0	0	0	0	0	0	0	0	0	0	3	0	0	0	0	0	0	0
5003	0	0	0	0	3	0	0	0	0	0	0	3	0	0	0	0	0	0	0	0	0	0	0	0	0	0	0	0	0	0	0	0	0
5033	0	0	0	0	0	0	0	0	6	0	0	0	0	0	0	0	0	0	0	3	0	0	0	0	4	0	0	0	0	0	0	0	0
6106	0	0	0	0	0	0	0	0	4	0	0	0	0	0	0	0	0	3	0	0	0	0	0	0	4	0	0	0	0	0	0	4	0
4538	0	0	0	0	0	4	0	0	0	0	0	0	0	0	0	0	0	0	0	7	0	0	0	0	7	0	0	0	0	0	0	0	0
4828	0	0	0	0	0	6	0	0	0	0	0	0	6	6	0	0	0	33	0	4	0	0	0	0	39	6	0	3	5	8	0	7	0
5538	7	0	0	13	0	0	9	0	14	0	0	0	14	16	8	0	0	14	10	0	12	0	8	10	15	11	14	0	0	14	14	0	14
5159	0	0	0	4	6	0	0	0	4	6	6	8	5	5	0	0	0	4	4	0	0	0	0	0	5	4	0	0	0	3	0	4	6
7291	0	0	0	4	0	0	0	0	6	0	0	3	4	5	0	0	0	3	0	0	5	5	0	0	3	4	0	0	0	0	0	3	0
14589	0	0	0	8	0	4	4	0	5	5	0	0	3	4	0	0	0	6	0	0	5	5	0	0	6	0	0	0	0	6	5	4	5
10907	34	0	0	81	91	0	0	0	0	0	0	0	0	0	0	0	0	0	0	0	0	0	0	0	0	0	0	0	0	0	0	0	0
11084	21	0	0	42	45	0	28	24	27	26	0	32	28	35	0	0	0	41	41	30	0	0	0	0	0	0	0	23	0	32	0	0	0
4818	0	0	0	27	0	0	0	0	8	9	0	0	0	0	0	3	4	0	6	0	0	0	0	0	0	0	0	0	0	0	6	0	8
17062	0	0	0	4	0	0	0	0	0	0	0	0	0	0	0	0	0	0	0	0	0	0	0	0	0	0	0	0	0	0	0	0	0
16904	0	0	0	4	0	0	0	0	0	0	0	0	0	0	0	0	0	0	0	0	0	0	0	0	0	0	0	0	0	0	0	0	0
9360	0	0	0	4	0	0	0	0	0	0	0	0	0	0	0	0	0	0	0	0	0	0	0	0	0	0	0	0	0	0	0	0	0
14796	0	0	0	4	0	0	0	0	0	0	0	0	0	0	0	0	0	0	0	0	0	0	0	0	0	0	0	0	0	0	0	0	0
6002	0	0	0	4	0	0	0	0	0	0	0	3	0	0	0	0	0	4	0	0	0	0	0	0	0	0	0	0	0	0	0	0	0
4524	0	0	0	6	0	0	0	0	0	0	0	0	0	0	0	0	0	6	0	0	0	0	0	0	0	0	0	0	0	0	0	0	0
16980	0	0	0	4	0	0	0	0	0	0	0	0	0	0	0	0	0	3	0	0	0	0	0	0	0	0	0	0	0	0	0	0	0
17014	0	0	0	4	0	0	0	0	0	0	0	0	0	0	0	0	0	3	0	0	0	0	0	0	0	0	0	0	0	0	0	0	0
10594	0	0	0	0	0	0	0	8	4	4	0	0	3	4	0	0	0	0	5	0	0	0	7	7	0	0	4	4	4	5	4	0	4
10693	0	0	0	0	0	0	0	5	0	0	0	0	0	4	0	0	0	0	4	0	0	0	4	4	0	0	0	0	0	3	0	0	0
16718	0	0	0	4	0	0	0	4	0	0	0	0	0	0	0	0	0	3	4	0	0	0	4	0	3	0	0	0	0	0	0	0	0
16845	0	0	0	5	0	0	0	4	0	0	0	0	0	0	0	0	0	5	4	0	0	0	3	0	4	0	0	0	0	0	0	0	0
5226	0	0	0	5	6	0	4	5	0	3	6	7	8	10	4	3	4	6	4	0	0	0	6	6	6	7	0	0	0	0	0	0	3
10325	0	3	4	12	8	0	6	12	7	10	7	9	8	10	0	0	0	12	16	0	5	0	7	6	12	7	0	0	3	9	11	8	12
10456	3	4	4	11	5	0	7	18	0	4	5	6	11	13	0	0	0	12	15	0	6	4	12	11	12	9	0	0	3	5	5	0	5

Table S3. Cosine similarities of mouse skin surface mass fingerprints

	H2_3	H2_2	H2_1	H1_2	H1_1	H1_3	H3_3	H3_2	H3_1	B_F_1	B_F_3	B_F_2	B_M_3	B_M_1	B_M_2	T10_2	T10_3	T10_1	T15_2	T15_3	T15_1
H2_3	1	0.996	0.996	0.988	0.985	0.984	0.984	0.984	0.986	0.87	0.877	0.868	0.872	0.863	0.856	0.286	0.29	0.272	0.217	0.178	0.126
H2_2	0.996	1	0.996	0.986	0.985	0.984	0.986	0.987	0.987	0.868	0.876	0.866	0.873	0.863	0.858	0.295	0.299	0.28	0.227	0.187	0.137
H2_1	0.996	0.996	1	0.984	0.985	0.987	0.983	0.984	0.984	0.871	0.877	0.869	0.871	0.861	0.853	0.288	0.292	0.273	0.221	0.182	0.13
H1_2	0.988	0.986	0.984	1	0.98	0.978	0.974	0.974	0.977	0.872	0.877	0.87	0.863	0.854	0.849	0.297	0.3	0.284	0.218	0.178	0.127
H1_1	0.985	0.985	0.985	0.98	1	0.995	0.973	0.976	0.979	0.871	0.877	0.87	0.865	0.855	0.849	0.294	0.296	0.279	0.215	0.175	0.125
H1_3	0.984	0.984	0.987	0.978	0.995	1	0.97	0.972	0.975	0.876	0.88	0.874	0.867	0.858	0.849	0.295	0.297	0.28	0.213	0.174	0.124
H3_3	0.984	0.986	0.983	0.974	0.973	0.97	1	0.998	0.996	0.837	0.849	0.837	0.851	0.84	0.831	0.273	0.277	0.258	0.219	0.177	0.125
H3_2	0.984	0.987	0.984	0.974	0.976	0.972	0.998	1	0.996	0.838	0.849	0.837	0.851	0.84	0.832	0.276	0.28	0.262	0.22	0.178	0.127
H3_1	0.986	0.987	0.984	0.977	0.979	0.975	0.996	0.996	1	0.847	0.857	0.847	0.854	0.844	0.835	0.279	0.283	0.265	0.218	0.177	0.125
B_F_1	0.87	0.868	0.871	0.872	0.871	0.876	0.837	0.838	0.847	1	0.997	0.996	0.835	0.832	0.846	0.458	0.455	0.446	0.276	0.234	0.19
B_F_3	0.877	0.876	0.877	0.877	0.877	0.88	0.849	0.849	0.857	0.997	1	0.996	0.841	0.838	0.852	0.457	0.455	0.445	0.279	0.236	0.194
B_F_2	0.868	0.866	0.869	0.87	0.87	0.874	0.837	0.837	0.847	0.996	0.996	1	0.832	0.829	0.841	0.453	0.45	0.44	0.273	0.23	0.187
B_M_3	0.872	0.873	0.871	0.863	0.865	0.867	0.851	0.851	0.854	0.835	0.841	0.832	1	0.996	0.99	0.621	0.623	0.612	0.526	0.49	0.451
B_M_1	0.863	0.863	0.861	0.854	0.855	0.858	0.84	0.84	0.844	0.832	0.838	0.829	0.996	1	0.992	0.634	0.637	0.627	0.534	0.498	0.46
B_M_2	0.856	0.858	0.853	0.849	0.849	0.849	0.831	0.832	0.835	0.846	0.852	0.841	0.99	0.992	1	0.652	0.654	0.642	0.539	0.504	0.467
T10_2	0.286	0.295	0.288	0.297	0.294	0.295	0.273	0.276	0.279	0.458	0.457	0.453	0.621	0.634	0.652	1	0.997	0.994	0.905	0.895	0.899
T10_3	0.29	0.299	0.292	0.3	0.296	0.297	0.277	0.28	0.283	0.455	0.455	0.45	0.623	0.637	0.654	0.997	1	0.995	0.909	0.899	0.893
T10_1	0.272	0.28	0.273	0.284	0.279	0.28	0.258	0.262	0.265	0.446	0.445	0.44	0.612	0.627	0.642	0.994	0.995	1	0.901	0.891	0.887
T15_2	0.217	0.227	0.221	0.218	0.215	0.213	0.219	0.22	0.218	0.276	0.279	0.273	0.526	0.534	0.539	0.905	0.909	0.901	1	0.992	0.989
T15_3	0.178	0.187	0.182	0.178	0.175	0.174	0.177	0.178	0.177	0.234	0.236	0.23	0.49	0.498	0.504	0.895	0.899	0.891	0.992	1	0.991
T15_1	0.126	0.137	0.13	0.127	0.125	0.124	0.125	0.127	0.125	0.19	0.194	0.187	0.451	0.46	0.467	0.899	0.893	0.887	0.989	0.991	1
T24_3	0.121	0.13	0.123	0.116	0.118	0.117	0.122	0.125	0.12	0.145	0.151	0.141	0.468	0.477	0.48	0.882	0.888	0.883	0.962	0.962	0.971
T24_2	0.113	0.122	0.115	0.109	0.111	0.11	0.112	0.114	0.11	0.146	0.151	0.143	0.459	0.467	0.471	0.878	0.88	0.876	0.961	0.969	0.971
T24_1	0.125	0.135	0.128	0.12	0.122	0.12	0.128	0.13	0.125	0.149	0.154	0.144	0.466	0.474	0.477	0.871	0.874	0.871	0.961	0.965	0.97
T50_3	0.117	0.129	0.124	0.108	0.118	0.117	0.115	0.119	0.115	0.14	0.145	0.137	0.428	0.426	0.427	0.764	0.762	0.761	0.867	0.867	0.888
T50_1	0.109	0.121	0.117	0.101	0.109	0.108	0.107	0.11	0.106	0.128	0.133	0.128	0.415	0.415	0.418	0.773	0.773	0.768	0.884	0.886	0.904
T50_2	0.108	0.118	0.115	0.1	0.107	0.107	0.105	0.108	0.105	0.128	0.132	0.126	0.414	0.414	0.414	0.783	0.782	0.779	0.889	0.892	0.909
T70_3	0.104	0.114	0.108	0.096	0.103	0.1	0.1	0.105	0.1	0.127	0.133	0.123	0.419	0.42	0.422	0.785	0.785	0.789	0.888	0.886	0.908
T70_2	0.092	0.102	0.097	0.087	0.092	0.088	0.09	0.093	0.09	0.116	0.122	0.112	0.416	0.418	0.419	0.792	0.791	0.786	0.894	0.893	0.914
T70_1	0.099	0.11	0.104	0.092	0.099	0.096	0.097	0.101	0.097	0.122	0.127	0.117	0.415	0.417	0.417	0.785	0.782	0.778	0.886	0.887	0.906
T130_1	0.131	0.139	0.14	0.12	0.124	0.126	0.126	0.131	0.123	0.124	0.129	0.124	0.371	0.37	0.361	0.641	0.646	0.638	0.756	0.76	0.778
T130_2	0.124	0.131	0.133	0.111	0.115	0.118	0.116	0.121	0.112	0.115	0.119	0.115	0.355	0.354	0.345	0.607	0.611	0.604	0.721	0.725	0.745
T130_3	0.12	0.127	0.13	0.107	0.111	0.114	0.115	0.119	0.11	0.113	0.117	0.113	0.351	0.349	0.341	0.606	0.612	0.605	0.728	0.732	0.752
T140_2	0.129	0.137	0.14	0.117	0.123	0.126	0.122	0.128	0.118	0.137	0.14	0.137	0.38	0.381	0.376	0.674	0.677	0.669	0.788	0.798	0.809
T140_1	0.133	0.141	0.146	0.121	0.126	0.129	0.124	0.131	0.12	0.139	0.142	0.139	0.383	0.386	0.378	0.673	0.681	0.672	0.789	0.789	0.808
T140_3	0.131	0.139	0.144	0.118	0.124	0.127	0.124	0.13	0.119	0.135	0.139	0.135	0.384	0.387	0.378	0.67	0.678	0.668	0.786	0.784	0.804
T168_1	0.146	0.155	0.159	0.133	0.141	0.142	0.137	0.146	0.131	0.147	0.152	0.147	0.34	0.345	0.328	0.471	0.486	0.47	0.544	0.535	0.556
T168_2	0.144	0.153	0.157	0.13	0.138	0.139	0.133	0.142	0.127	0.146	0.151	0.147	0.339	0.344	0.327	0.469	0.484	0.468	0.541	0.532	0.552
T168_3	0.154	0.164	0.168	0.14	0.148	0.15	0.146	0.155	0.139	0.142	0.147	0.142	0.321	0.326	0.307	0.394	0.408	0.392	0.464	0.456	0.474
T182_1	0.151	0.138	0.144	0.117	0.125	0.128	0.123	0.131	0.116	0.129	0.133	0.13	0.301	0.307	0.287	0.399	0.415	0.398	0.465	0.458	0.478
T182_3	0.135	0.142	0.149	0.119	0.129	0.132	0.126	0.135	0.119	0.128	0.131	0.129	0.298	0.304	0.281	0.388	0.403	0.388	0.455	0.448	0.468
T182_2	0.13	0.137	0.144	0.115	0.123	0.126	0.122	0.131	0.115	0.126	0.129	0.127	0.292	0.299	0.278	0.376	0.392	0.376	0.438	0.429	0.449

(To be continued on next page)

(Continued from the last page)

	T24_3	T24_2	T24_1	T50_3	T50_1	T50_2	T70_3	T70_2	T70_1	T130_1	T130_2	T130_3	T140_2	T140_1	T140_3	T168_1	T168_2	T168_3	T182_1	T182_3	T182_2
H2_3	0.121	0.113	0.125	0.117	0.109	0.108	0.104	0.092	0.099	0.131	0.124	0.12	0.129	0.133	0.131	0.146	0.144	0.154	0.151	0.135	0.13
H2_2	0.13	0.122	0.135	0.129	0.121	0.118	0.114	0.102	0.11	0.139	0.131	0.127	0.137	0.141	0.139	0.155	0.153	0.164	0.138	0.142	0.137
H2_1	0.123	0.115	0.128	0.124	0.117	0.115	0.108	0.097	0.104	0.14	0.133	0.13	0.14	0.146	0.144	0.159	0.157	0.168	0.144	0.149	0.144
H1_2	0.116	0.109	0.12	0.108	0.101	0.1	0.096	0.087	0.092	0.12	0.111	0.107	0.117	0.121	0.118	0.133	0.13	0.14	0.117	0.119	0.115
H1_1	0.118	0.111	0.122	0.118	0.109	0.107	0.103	0.092	0.099	0.124	0.115	0.111	0.123	0.126	0.124	0.141	0.138	0.148	0.125	0.129	0.123
H1_3	0.117	0.11	0.12	0.117	0.108	0.107	0.1	0.088	0.096	0.126	0.118	0.114	0.126	0.129	0.127	0.142	0.139	0.15	0.128	0.132	0.126
H3_3	0.122	0.112	0.128	0.115	0.107	0.105	0.1	0.09	0.097	0.126	0.116	0.115	0.122	0.124	0.124	0.137	0.133	0.146	0.123	0.126	0.122
H3_2	0.125	0.114	0.13	0.119	0.11	0.108	0.105	0.093	0.101	0.131	0.121	0.119	0.128	0.131	0.13	0.146	0.142	0.155	0.131	0.135	0.131
H3_1	0.12	0.11	0.125	0.115	0.106	0.105	0.1	0.09	0.097	0.123	0.112	0.11	0.118	0.12	0.119	0.131	0.127	0.139	0.116	0.119	0.115
B_F_1	0.145	0.146	0.149	0.14	0.128	0.128	0.127	0.116	0.122	0.124	0.115	0.113	0.137	0.139	0.135	0.147	0.146	0.142	0.129	0.128	0.126
B_F_3	0.151	0.151	0.154	0.145	0.133	0.132	0.133	0.122	0.127	0.129	0.119	0.117	0.14	0.142	0.139	0.152	0.151	0.147	0.133	0.131	0.129
B_F_2	0.141	0.143	0.144	0.137	0.128	0.126	0.123	0.112	0.117	0.124	0.115	0.113	0.137	0.139	0.135	0.147	0.147	0.142	0.13	0.129	0.127
B_M_3	0.468	0.459	0.466	0.428	0.415	0.414	0.419	0.416	0.415	0.371	0.355	0.351	0.38	0.383	0.384	0.34	0.339	0.321	0.301	0.298	0.292
B_M_1	0.477	0.467	0.474	0.426	0.415	0.414	0.42	0.418	0.417	0.37	0.354	0.349	0.381	0.386	0.387	0.345	0.344	0.326	0.307	0.304	0.299
B_M_2	0.48	0.471	0.477	0.427	0.418	0.414	0.422	0.419	0.417	0.361	0.345	0.341	0.376	0.378	0.378	0.328	0.327	0.307	0.287	0.281	0.278
T10_2	0.882	0.878	0.871	0.764	0.773	0.783	0.785	0.792	0.785	0.641	0.607	0.606	0.674	0.673	0.67	0.471	0.469	0.394	0.399	0.388	0.376
T10_3	0.888	0.88	0.874	0.762	0.773	0.782	0.785	0.791	0.782	0.646	0.611	0.612	0.677	0.681	0.678	0.486	0.484	0.408	0.415	0.403	0.392
T10_1	0.883	0.876	0.871	0.761	0.768	0.779	0.789	0.786	0.778	0.638	0.604	0.605	0.669	0.672	0.668	0.47	0.468	0.392	0.398	0.388	0.376
T15_2	0.962	0.961	0.961	0.867	0.884	0.889	0.888	0.894	0.886	0.756	0.721	0.728	0.788	0.789	0.786	0.544	0.541	0.464	0.465	0.455	0.438
T15_3	0.962	0.969	0.965	0.867	0.886	0.892	0.886	0.893	0.887	0.76	0.725	0.732	0.798	0.789	0.784	0.535	0.532	0.456	0.458	0.448	0.429
T15_1	0.971	0.971	0.97	0.888	0.904	0.909	0.908	0.914	0.906	0.778	0.745	0.752	0.809	0.808	0.804	0.556	0.552	0.474	0.478	0.468	0.449
T24_3	1	0.989	0.987	0.896	0.919	0.914	0.918	0.924	0.913	0.774	0.741	0.747	0.802	0.803	0.8	0.554	0.551	0.473	0.474	0.462	0.445
T24_2	0.989	1	0.99	0.898	0.911	0.916	0.915	0.924	0.914	0.774	0.741	0.746	0.812	0.797	0.793	0.537	0.534	0.459	0.458	0.447	0.427
T24_1	0.987	0.99	1	0.91	0.924	0.929	0.924	0.932	0.922	0.797	0.769	0.776	0.836	0.823	0.82	0.566	0.562	0.491	0.492	0.481	0.459
T50_3	0.896	0.898	0.91	1	0.99	0.988	0.98	0.978	0.982	0.894	0.876	0.876	0.896	0.877	0.875	0.635	0.631	0.561	0.553	0.537	0.512
T50_1	0.919	0.911	0.924	0.99	1	0.993	0.978	0.974	0.976	0.901	0.88	0.884	0.909	0.893	0.889	0.646	0.642	0.569	0.567	0.55	0.528
T50_2	0.914	0.916	0.929	0.988	0.993	1	0.978	0.974	0.977	0.911	0.891	0.892	0.919	0.903	0.898	0.64	0.636	0.564	0.563	0.548	0.521
T70_3	0.918	0.915	0.924	0.98	0.978	0.978	1	0.994	0.993	0.88	0.857	0.851	0.883	0.873	0.87	0.635	0.63	0.558	0.555	0.536	0.514
T70_2	0.924	0.924	0.932	0.978	0.974	0.974	0.994	1	0.993	0.865	0.842	0.836	0.869	0.857	0.853	0.617	0.611	0.537	0.534	0.515	0.494
T70_1	0.913	0.914	0.922	0.982	0.976	0.977	0.993	0.993	1	0.875	0.851	0.845	0.876	0.859	0.856	0.618	0.612	0.54	0.533	0.517	0.494
T130_1	0.774	0.774	0.797	0.894	0.901	0.911	0.88	0.865	0.875	1	0.993	0.986	0.97	0.967	0.965	0.814	0.812	0.768	0.765	0.755	0.73
T130_2	0.741	0.741	0.769	0.876	0.88	0.891	0.857	0.842	0.851	0.993	1	0.989	0.967	0.964	0.961	0.818	0.816	0.779	0.772	0.764	0.74
T130_3	0.747	0.746	0.776	0.876	0.884	0.892	0.851	0.836	0.845	0.986	0.989	1	0.969	0.967	0.965	0.822	0.818	0.782	0.775	0.766	0.742
T140_2	0.802	0.812	0.836	0.896	0.909	0.919	0.883	0.869	0.876	0.97	0.967	0.969	1	0.985	0.984	0.812	0.81	0.77	0.771	0.763	0.738
T140_1	0.803	0.797	0.823	0.877	0.893	0.903	0.873	0.857	0.859	0.967	0.964	0.967	0.985	1	0.997	0.856	0.848	0.807	0.812	0.805	0.783
T140_3	0.8	0.793	0.82	0.875	0.889	0.898	0.87	0.853	0.856	0.965	0.961	0.965	0.984	0.997	1	0.863	0.861	0.821	0.824	0.817	0.796
T168_1	0.554	0.537	0.566	0.635	0.646	0.64	0.635	0.617	0.618	0.814	0.818	0.822	0.812	0.856	0.863	1	0.997	0.989	0.975	0.971	0.969
T168_2	0.551	0.534	0.562	0.631	0.642	0.636	0.63	0.611	0.612	0.812	0.816	0.818	0.81	0.848	0.861	0.997	1	0.986	0.974	0.971	0.975
T168_3	0.473	0.459	0.491	0.561	0.569	0.564	0.558	0.537	0.54	0.768	0.779	0.782	0.77	0.807	0.821	0.989	0.986	1	0.981	0.989	0.978
T182_1	0.474	0.458	0.492	0.553	0.567	0.563	0.555	0.534	0.533	0.765	0.772	0.775	0.771	0.812	0.824	0.975	0.974	0.981	1	0.996	0.995
T182_3	0.462	0.447	0.481	0.537	0.55	0.548	0.536	0.515	0.517	0.755	0.764	0.766	0.763	0.805	0.817	0.971	0.971	0.989	0.996	1	0.995
T182_2	0.445	0.427	0.459	0.512	0.528	0.521	0.514	0.494	0.494	0.73	0.74	0.742	0.738	0.783	0.796	0.969	0.975	0.978	0.995	0.995	1

Table S4. Comparison of peak intensities between healthy and speckle skins from mice

Peak Mass (*m/z*)	log2 FC*	P-value*	Figure 3 Presence	Peak Mass (*m/z*)	log2 FC	P-value	Figure 3 Presence	Peak Mass (*m/z*)	log2 FC	P-value	Figure 3 Presence
2018.1	2.474	9.19E-2		5443.6	0.553	3.42E-2		9837.3	1.319	3.83E-2	
2032.3	1.889	7.62E-2		5476.8	-2.999	5.16E-5		9929.3	-0.650	2.29E-1	
2111.1	2.412	9.05E-2		5494.0	3.156	5.04E-4		9978.9	0.000	--	*Peak 6*
2167.8	0.037	3.63E-1		5528.4	-2.676	4.13E-3		10165.2	-0.155	8.82E-2	*Peak 7*
2351.0	-2.683	1.42E-4		5546.5	1.613	7.56E-2		10294.8	0.421	1.56E-1	
3094.9	0.126	3.63E-1		5656.9	-2.117	1.38E-2		10406.3	0.660	1.66E-1	
3415.5	4.170	6.79E-4		5673.7	-1.809	2.29E-2		10870.7	1.360	1.79E-1	*Peak 9*
3531.8	3.476	6.23E-4		5693.8	3.766	7.91E-5		10970.6	0.391	4.11E-1	
3661.0	3.284	7.95E-2		5709.7	-0.218	4.21E-1		11075.9	-0.165	3.67E-1	
3726.7	0.152	3.63E-1		5837.1	1.994	4.47E-6		11102.8	-0.207	5.15E-1	
3802.5	4.175	2.48E-2		5910.2	1.775	1.58E-1		11304.5	-0.235	6.76E-1	
3820.3	3.624	7.13E-3		6190.3	-1.934	3.63E-1		11345.2	-0.030	3.17E-1	
3891.1	2.299	1.68E-2		6579.9	-1.349	4.86E-1		11515.0	-2.924	8.26E-4	
3901.0	2.669	3.62E-2		6706.4	-0.051	8.91E-1		11545.8	0.606	5.40E-2	*Peak 10*
3949.1	4.747	3.90E-3		6909.5	-0.629	1.50E-1		11634.0	0.633	3.41E-1	
3991.4	0.991	4.36E-1		7010.3	-0.773	1.37E-1		12370.8	0.615	1.81E-1	
4109.4	2.218	4.13E-2		7030.7	-0.739	1.02E-1		12721.8	3.794	1.22E-2	
4193.9	2.700	3.44E-2		7492.7	4.405	2.66E-3	*Peak 2*	13799.8	0.121	2.73E-1	
4244.4	1.854	6.26E-3		7552.5	-1.120	8.05E-3		14003.5	-0.487	3.56E-1	
4334.0	4.278	3.80E-3		7658.3	-0.758	8.63E-3		14043.0	-0.155	6.53E-1	
4374.4	2.175	2.52E-1		7810.6	3.941	4.12E-4	*Peak 3*	14877.6	2.220	2.87E-2	
4453.8	-0.264	1.39E-1		8185.1	2.452	4.52E-3		15098.8	0.149	2.51E-1	
4463.4	3.175	3.84E-2		8419.1	0.486	8.93E-1		15311.5	-0.135	9.55E-1	
4621.2	3.621	2.90E-2		8560.5	4.518	3.78E-5		16669.4	2.611	2.93E-4	
4690.3	5.516	1.77E-2	*Peak 1*	8627.4	0.329	3.63E-1		16782.1	2.209	6.61E-2	
4752.2	1.972	5.91E-2		8712.0	3.687	1.93E-2	*Peak 4*				
4836.8	2.641	7.71E-2		8825.9	2.051	8.61E-2					
4865.7	4.711	1.53E-2		8947.9	3.359	3.56E-2					
4909.8	2.368	5.52E-3		9235.2	2.648	2.29E-2					
4957.7	-1.148	4.09E-1		9272.0	3.578	1.72E-2					
4981.5	-0.048	8.73E-1		9365.9	3.963	5.39E-2	*Peak 5*				
5086.0	-0.394	1.07E-2		9663.4	0.742	2.59E-1					
5139.2	-2.934	8.57E-6		9721.4	2.872	4.44E-5					

*log2 FC: log2 fold change. For each peak, the value is calculated as $\log_2$ ((mean value of the relative peak intensity in black speckle skins) divided by (mean value of the relative peak intensity in healthy skins)).

* P-value: the value of probability, *i.e.* the level of statistical significance generated from paired t-test.

Table S5. A list of all investigated machine learning classification algorithms

Altogether 84 classifiers on the Weka (Waikato environment for knowledge analysis) machine learning workbench have been investigated for the skin lesion classification. These classifiers come from the common learning models like Bayes, Functions, Lazy, Meta and Trees.

Model	Subtype Algorithm
Bayes	AODE
	AODEsr
	BayesianLogisticRegression
	BayesNet
	ComplementNaiveBayes
	DMNBtext
	HNB
	NaiveBayes
	NaiveBayesMultinomial
	NaiveBayesMultinomialUpdateable
	NaiveBayesSimple
	NaiveBayesUpdateable
	WAODE
Meta	AdoBoostM1
	AdditiveRegression
	AltributedSelectedClassifier
	Bagging
	ClassificationViaClustering
	ClassificationViaRegression
	CostSensitiveClassifier
	CVParameterSelection
	Dagging
	Decorate
	END
	EnsembleSelection
	FilteredClassifier
	Grading
	GridSearch
	LogitBoost
	MetaBoost
	MultiBoostAB
	MultiClassClassifier(MCC)
	OneClassClassifier
	OrdinalClassClassifier
	RacedIncrementalLogitBoost
	RandomCommittee
	RandomSubSpace
	RealAdaBoost
	RegressionByDiscretization
	RotationForest
	Stacking
	StackingC
	ThresholdSelector
	Vote
Functions	GaussianProcesses
	IsotonicRegression
	LeastMedSq
	LibLINEAR
	LibSVM
	LinearRegression
	Logistic
	MultilayerPerceptron
	MultilayerPerceptronCS
	PaceRegression
	PLSClassififier
	RBFNetwork
	SimpleLinearRegression
	SimpleLogstic
	SMO
	SMOreg
	SPegasos
	VotedPerceptron
	Winnow
Lazy	IB1
	IBk
	KStar
	LBR
	LWL
Trees	ADTree
	BFTree
	DecisionStump
	FT
	Id3
	J48
	J48graft
	LADTree
	LMT
	M5P
	NBTree
	RandomForest
	RandomTree
	REPTree
	SimpleCart
	UserClassifier

Table S6. PCA scores of mouse skin surface mass fingerprints

ID	PC0 score	PC1 score	PC2 score
Eigenvalue	49.6885	25.2124	14.7624
Variance	0.246	0.1248	0.0731
Cumulative	0.246	0.3708	0.4439
Healthy#0	2.0453	-0.6454	0.4114
Healthy#1	2.1018	-0.3138	0.9412
Healthy#2	2.1424	-0.6484	0.4888
Healthy#3	2.232	-0.4812	0.4576
Healthy#4	2.1454	-0.2578	0.8263
Healthy#5	2.2527	-0.6591	0.4995
Healthy#6	2.0751	-0.4181	0.3603
Healthy#7	2.2543	-0.6794	0.4103
Healthy#8	2.1857	-0.6146	0.4358
Healthy#9	2.0406	-0.3393	0.9936
Healthy#10	1.8724	-0.5457	0.5394
Healthy#11	2.1097	-0.329	0.6884
Healthy#12	2.1049	-0.5073	0.5784
Healthy#13	1.8186	-0.5133	0.3727
Healthy#14	1.9607	-0.7878	0.3836
Healthy#15	2.1262	-0.583	0.3616
Healthy#16	2.1716	-0.4233	0.2466
Healthy#17	1.7338	-0.538	0.3656
Few Black Speckles#18	1.262	1.3487	2.192
Few Black Speckles#19	1.1527	1.3845	2.2866
Few Black Speckles#20	1.1492	1.5974	2.4201
More Black Speckles#21	0.116	2.5091	2.2082
More Black Speckles#22	0.2646	2.3331	2.45
More Black Speckles#23	-0.0218	2.2542	1.719
Early Tumor#24	-0.9701	4.3615	2.4354
Early Tumor#25	-0.462	4.1278	2.7705
Early Tumor#26	-0.7647	4.1226	2.5379
Early Tumor#27	-2.1437	5.1228	1.5542
Early Tumor#28	-1.6114	4.7318	1.4558
Early Tumor#29	-1.5254	4.4835	1.5297
Early Tumor#30	-2.4641	4.5145	0.5089
Early Tumor#31	-2.2272	3.8726	0.0521
Early Tumor#32	-2.1822	4.3972	0.1422
Medium-Sized Tumor#33	-3.1863	2.0701	-2.3317
Medium-Sized Tumor#34	-3.3447	1.7315	-1.8449
Medium-Sized Tumor#35	-3.3872	1.6247	-2.1229
Medium-Sized Tumor#36	-3.3838	2.1007	-2.2309
Medium-Sized Tumor#37	-3.7176	2.421	-2.214
Medium-Sized Tumor#38	-3.7337	2.5372	-2.7673
Metastatic Tumor#39	-4.0701	0.0571	0.1718
Metastatic Tumor#40	-4.9189	-0.2811	0.2056
Metastatic Tumor#41	-4.6723	0.1132	0.1847
Metastatic Tumor#42	-5.1344	0.2141	0.7391
Metastatic Tumor#43	-5.4726	-0.0423	0.9852
Metastatic Tumor#44	-5.471	0.2033	1.2368
Metastatic Tumor#45	-6.3074	-0.8416	1.7319
Metastatic Tumor#46	-6.2541	-0.3785	1.7916
Metastatic Tumor#47	-6.4719	-0.8822	1.9109
Metastatic Tumor#48	-5.9317	-0.9352	2.1828
Metastatic Tumor#49	-6.1009	-0.6065	2.2472
Metastatic Tumor#50	-6.0403	-0.7367	2.3632

Table S7. One-way ANOVA test of mouse skin surface mass fingerprint PCA scores

ID*	PC0 score				PC1 score				PC2 score			
	MeanDiff*	SEM*	F-value	P-value	MeanDiff	SEM	F-value	P-value	MeanDiff	SEM	F-value	P-value
Speckles & Healthy	-1.4225	0.2475	8.2570	4.17E-05	2.4203	0.1650	53.8242	8.90E-17	1.6926	0.2929	8.3467	3.78E-05
Early T & Healthy	-3.6708	0.2144	73.3125	2.30E-19	4.9307	0.1429	297.8502	3.02E-32	0.9229	0.2537	3.3088	1.83E-02
Early T & Speckles	-2.2483	0.2767	16.5013	1.88E-08	2.5104	0.1844	46.3256	1.43E-15	-0.7697	0.3275	1.3808	2.55E-01
Medium T & Healthy	-5.5352	0.2475	125.0186	4.27E-24	2.5967	0.1650	61.9543	6.13E-18	-2.7720	0.2929	22.3873	2.60E-10
Medium T & Speckles	-4.1127	0.3032	46.0117	1.62E-15	0.1764	0.2020	0.1905	9.42E-01	-4.4646	0.3588	38.7156	3.54E-14
Medium T & Early T	-1.8644	0.2767	11.3464	1.73E-06	-2.3341	0.1844	40.0451	1.96E-14	-3.6949	0.3275	31.8208	1.01E-12
Metastatic T & Healthy	-7.6468	0.1957	381.7567	1.22E-34	0.1728	0.1304	0.4388	7.80E-01	0.7925	0.2316	2.9278	3.08E-02
Metastatic T & Speckles	-6.2243	0.2625	140.5186	3.63E-25	-2.2475	0.1750	41.2569	1.15E-14	-0.9001	0.3107	2.0981	9.64E-02
Metastatic T & Early T	-3.9759	0.2315	73.7195	2.06E-19	-4.7580	0.1543	237.7223	4.32E-30	-0.1304	0.2740	0.0566	9.94E-01
Metastatic T & Medium T	-2.1116	0.2625	16.1725	2.45E-08	-2.4239	0.1750	47.9859	7.51E-16	3.5645	0.3107	32.9049	5.77E-13

*MeanDiff: mean difference in the PCA scores.

*SEM: standard error of the mean.

*ID. Speckles: Black speckles; Early T: Early tumor; Medium T: Medium-sized tumor; Metastatic T: Metastatic tumor

Table S8. Mass spectral cosine similarities of mouse blood-circulating exosomes

	H2_1	H2_3	H2_2	H3_1	H3_2	H3_3	H1_1	H1_3	H1_2	B_F_2	B_F_1	B_F_3	B_M_2	B_M_3	B_M_1	T10_3	T10_1	T10_2	T15_2	T15_3	T15_1
H2_1	1	0.997	0.998	0.992	0.993	0.991	0.99	0.988	0.988	0.955	0.957	0.955	0.951	0.951	0.946	0.88	0.868	0.866	0.844	0.844	0.841
H2_3	0.997	1	0.996	0.991	0.991	0.99	0.985	0.986	0.985	0.954	0.955	0.952	0.949	0.948	0.944	0.881	0.866	0.865	0.845	0.842	0.847
H2_2	0.998	0.996	1	0.99	0.991	0.987	0.991	0.989	0.99	0.954	0.955	0.953	0.95	0.949	0.945	0.878	0.865	0.867	0.843	0.843	0.846
H3_1	0.992	0.991	0.99	1	0.996	0.998	0.99	0.988	0.984	0.953	0.955	0.954	0.951	0.95	0.944	0.873	0.86	0.855	0.836	0.835	0.838
H3_2	0.993	0.991	0.991	0.996	1	0.998	0.99	0.986	0.989	0.954	0.955	0.954	0.953	0.951	0.945	0.881	0.866	0.865	0.844	0.844	0.845
H3_3	0.991	0.99	0.987	0.998	0.998	1	0.985	0.985	0.987	0.948	0.95	0.947	0.944	0.943	0.937	0.87	0.857	0.854	0.834	0.832	0.836
H1_1	0.99	0.985	0.991	0.99	0.99	0.985	1	0.992	0.991	0.958	0.963	0.961	0.957	0.959	0.952	0.887	0.873	0.87	0.85	0.851	0.85
H1_3	0.988	0.986	0.989	0.988	0.986	0.985	0.992	1	0.997	0.967	0.969	0.965	0.963	0.963	0.96	0.886	0.875	0.873	0.853	0.852	0.853
H1_2	0.988	0.985	0.99	0.984	0.989	0.987	0.991	0.997	1	0.968	0.97	0.968	0.965	0.965	0.961	0.89	0.879	0.877	0.854	0.854	0.855
B_F_2	0.955	0.954	0.954	0.953	0.954	0.948	0.958	0.967	0.968	1	0.997	0.996	0.991	0.989	0.986	0.947	0.938	0.937	0.912	0.915	0.913
B_F_1	0.957	0.955	0.955	0.955	0.955	0.95	0.963	0.969	0.97	0.997	1	0.998	0.99	0.985	0.99	0.945	0.935	0.934	0.913	0.913	0.912
B_F_3	0.955	0.952	0.953	0.954	0.954	0.947	0.961	0.965	0.968	0.996	0.998	1	0.988	0.987	0.989	0.949	0.938	0.937	0.916	0.914	0.913
B_M_2	0.951	0.949	0.95	0.951	0.953	0.944	0.957	0.963	0.965	0.991	0.99	0.988	1	0.997	0.998	0.951	0.941	0.94	0.919	0.921	0.918
B_M_3	0.951	0.948	0.949	0.95	0.951	0.943	0.959	0.963	0.965	0.989	0.985	0.987	0.997	1	0.997	0.949	0.94	0.941	0.918	0.922	0.916
B_M_1	0.946	0.944	0.945	0.944	0.945	0.937	0.952	0.96	0.961	0.986	0.99	0.989	0.998	0.997	1	0.95	0.943	0.942	0.922	0.924	0.917
T10_3	0.88	0.881	0.878	0.873	0.881	0.87	0.887	0.886	0.89	0.947	0.945	0.949	0.951	0.949	0.95	1	0.997	0.996	0.981	0.983	0.98
T10_1	0.868	0.866	0.865	0.86	0.866	0.857	0.873	0.875	0.879	0.938	0.935	0.938	0.941	0.94	0.943	0.997	1	0.997	0.982	0.983	0.984
T10_2	0.866	0.865	0.867	0.855	0.865	0.854	0.87	0.873	0.877	0.937	0.934	0.937	0.94	0.941	0.942	0.996	0.997	1	0.986	0.988	0.983
T15_2	0.844	0.845	0.843	0.836	0.844	0.834	0.85	0.853	0.854	0.912	0.913	0.916	0.919	0.918	0.922	0.981	0.982	0.986	1	0.996	0.994
T15_3	0.844	0.842	0.843	0.835	0.844	0.832	0.851	0.852	0.854	0.915	0.913	0.914	0.921	0.922	0.924	0.983	0.983	0.988	0.996	1	0.993
T15_1	0.841	0.847	0.846	0.838	0.845	0.836	0.85	0.853	0.855	0.913	0.912	0.913	0.918	0.916	0.917	0.98	0.984	0.983	0.994	0.993	1
T24_2	0.839	0.838	0.84	0.833	0.84	0.829	0.848	0.85	0.852	0.902	0.9	0.906	0.91	0.909	0.911	0.975	0.975	0.977	0.986	0.985	0.984
T24_1	0.83	0.837	0.835	0.826	0.834	0.823	0.84	0.842	0.845	0.895	0.891	0.895	0.9	0.899	0.901	0.968	0.968	0.97	0.983	0.981	0.982
T24_3	0.832	0.834	0.835	0.824	0.832	0.819	0.841	0.843	0.845	0.901	0.897	0.902	0.906	0.905	0.908	0.977	0.973	0.978	0.984	0.985	0.987
T50_3	0.797	0.796	0.796	0.786	0.797	0.784	0.801	0.813	0.816	0.865	0.861	0.867	0.866	0.865	0.869	0.953	0.957	0.96	0.973	0.971	0.97
T50_1	0.789	0.789	0.788	0.775	0.789	0.777	0.791	0.805	0.808	0.855	0.85	0.856	0.856	0.855	0.86	0.951	0.954	0.955	0.969	0.97	0.968
T50_2	0.791	0.79	0.79	0.78	0.791	0.778	0.795	0.807	0.809	0.857	0.852	0.857	0.857	0.855	0.861	0.947	0.951	0.953	0.967	0.965	0.965
T70_2	0.766	0.763	0.765	0.754	0.765	0.75	0.773	0.787	0.789	0.841	0.838	0.843	0.843	0.84	0.848	0.945	0.949	0.95	0.963	0.963	0.962
T70_3	0.772	0.771	0.773	0.761	0.772	0.757	0.779	0.794	0.796	0.847	0.843	0.85	0.849	0.849	0.854	0.95	0.954	0.955	0.967	0.967	0.966
T70_1	0.775	0.772	0.774	0.763	0.772	0.759	0.782	0.796	0.798	0.85	0.845	0.852	0.852	0.852	0.857	0.949	0.953	0.956	0.966	0.967	0.963
T130_3	0.801	0.806	0.8	0.795	0.802	0.79	0.807	0.82	0.812	0.87	0.869	0.874	0.878	0.879	0.878	0.929	0.93	0.931	0.948	0.946	0.945
T130_2	0.8	0.797	0.801	0.795	0.803	0.791	0.807	0.809	0.812	0.868	0.867	0.872	0.875	0.876	0.877	0.924	0.925	0.927	0.942	0.943	0.939
T130_1	0.8	0.796	0.8	0.794	0.802	0.79	0.805	0.808	0.811	0.867	0.865	0.87	0.873	0.874	0.875	0.923	0.924	0.921	0.942	0.94	0.939
T140_3	0.814	0.81	0.815	0.806	0.813	0.8	0.799	0.803	0.804	0.887	0.886	0.89	0.89	0.891	0.893	0.933	0.932	0.934	0.944	0.943	0.942
T140_2	0.815	0.811	0.816	0.807	0.815	0.802	0.8	0.804	0.806	0.885	0.88	0.889	0.879	0.89	0.893	0.934	0.933	0.936	0.943	0.943	0.942
T140_1	0.803	0.8	0.804	0.796	0.804	0.791	0.808	0.813	0.815	0.877	0.875	0.88	0.881	0.881	0.883	0.928	0.927	0.93	0.938	0.937	0.937
T168_1	0.803	0.8	0.805	0.796	0.804	0.791	0.793	0.798	0.799	0.881	0.88	0.885	0.886	0.886	0.887	0.938	0.936	0.94	0.949	0.95	0.943
T168_3	0.812	0.809	0.814	0.806	0.814	0.801	0.801	0.805	0.806	0.886	0.886	0.886	0.892	0.892	0.893	0.937	0.934	0.939	0.947	0.948	0.941
T168_2	0.811	0.807	0.812	0.804	0.812	0.799	0.799	0.803	0.805	0.883	0.884	0.879	0.89	0.89	0.891	0.936	0.934	0.938	0.948	0.946	0.941
T182_2	0.815	0.809	0.817	0.807	0.815	0.8	0.804	0.807	0.809	0.887	0.886	0.89	0.889	0.891	0.892	0.941	0.94	0.944	0.951	0.953	0.945
T182_3	0.819	0.814	0.821	0.812	0.819	0.805	0.809	0.812	0.818	0.892	0.89	0.896	0.895	0.897	0.897	0.943	0.942	0.946	0.953	0.96	0.947
T182_1	0.811	0.806	0.812	0.803	0.81	0.796	0.8	0.803	0.804	0.883	0.883	0.887	0.886	0.889	0.889	0.938	0.937	0.942	0.95	0.951	0.943

(To be continued on next page)

(Continued from the last page)

	T24_2	T24_1	T24_3	T50_3	T50_1	T50_2	T70_2	T70_3	T70_1	T130_3	T130_2	T130_1	T140_3	T140_2	T140_1	T168_1	T168_3	T168_2	T182_2	T182_3	T182_1
H2_1	0.839	0.83	0.832	0.797	0.789	0.791	0.766	0.772	0.775	0.801	0.8	0.8	0.814	0.815	0.803	0.803	0.812	0.811	0.815	0.819	0.811
H2_3	0.838	0.837	0.834	0.796	0.789	0.79	0.763	0.771	0.772	0.806	0.797	0.796	0.81	0.811	0.8	0.8	0.809	0.807	0.809	0.814	0.806
H2_2	0.84	0.835	0.835	0.796	0.788	0.79	0.765	0.773	0.774	0.8	0.801	0.8	0.815	0.816	0.804	0.805	0.814	0.812	0.817	0.821	0.812
H3_1	0.833	0.826	0.824	0.786	0.775	0.78	0.754	0.761	0.763	0.795	0.795	0.794	0.806	0.807	0.796	0.796	0.806	0.804	0.807	0.812	0.803
H3_2	0.84	0.834	0.832	0.797	0.789	0.791	0.765	0.772	0.772	0.802	0.803	0.802	0.813	0.815	0.804	0.804	0.814	0.812	0.815	0.819	0.81
H3_3	0.829	0.823	0.819	0.784	0.777	0.778	0.75	0.757	0.759	0.79	0.791	0.79	0.8	0.802	0.791	0.791	0.801	0.799	0.8	0.805	0.796
H1_1	0.848	0.84	0.841	0.801	0.791	0.795	0.773	0.779	0.782	0.807	0.807	0.805	0.799	0.8	0.808	0.793	0.801	0.799	0.804	0.809	0.8
H1_3	0.85	0.842	0.843	0.813	0.805	0.807	0.787	0.794	0.796	0.82	0.809	0.808	0.803	0.804	0.813	0.798	0.805	0.803	0.807	0.812	0.803
H1_2	0.852	0.845	0.845	0.816	0.808	0.809	0.789	0.796	0.798	0.812	0.812	0.811	0.804	0.806	0.815	0.799	0.806	0.805	0.809	0.818	0.804
B_F_2	0.902	0.895	0.901	0.865	0.855	0.857	0.841	0.847	0.85	0.87	0.868	0.867	0.887	0.885	0.877	0.881	0.886	0.883	0.887	0.892	0.883
B_F_1	0.9	0.891	0.897	0.861	0.85	0.852	0.838	0.843	0.845	0.869	0.867	0.865	0.886	0.88	0.875	0.88	0.886	0.884	0.886	0.89	0.883
B_F_3	0.906	0.895	0.902	0.867	0.856	0.857	0.843	0.85	0.852	0.874	0.872	0.87	0.89	0.889	0.88	0.885	0.886	0.879	0.89	0.896	0.887
B_M_2	0.91	0.9	0.906	0.866	0.856	0.857	0.843	0.849	0.852	0.878	0.875	0.873	0.89	0.879	0.881	0.886	0.892	0.89	0.889	0.895	0.886
B_M_3	0.909	0.899	0.905	0.865	0.855	0.855	0.84	0.849	0.852	0.879	0.876	0.874	0.891	0.89	0.881	0.886	0.892	0.89	0.891	0.897	0.889
B_M_1	0.911	0.901	0.908	0.869	0.86	0.861	0.848	0.854	0.857	0.878	0.877	0.875	0.893	0.893	0.883	0.887	0.893	0.891	0.892	0.897	0.889
T10_3	0.975	0.968	0.977	0.953	0.951	0.947	0.945	0.95	0.949	0.929	0.924	0.923	0.933	0.934	0.928	0.938	0.937	0.936	0.941	0.943	0.938
T10_1	0.975	0.968	0.973	0.957	0.954	0.951	0.949	0.954	0.953	0.93	0.925	0.924	0.932	0.933	0.927	0.936	0.934	0.934	0.94	0.942	0.937
T10_2	0.977	0.97	0.978	0.96	0.955	0.953	0.95	0.955	0.956	0.931	0.927	0.921	0.934	0.936	0.93	0.94	0.939	0.938	0.944	0.946	0.942
T15_2	0.986	0.983	0.984	0.973	0.969	0.967	0.963	0.967	0.966	0.948	0.942	0.942	0.944	0.943	0.938	0.949	0.947	0.948	0.951	0.953	0.95
T15_3	0.985	0.981	0.985	0.971	0.97	0.965	0.963	0.967	0.967	0.946	0.943	0.94	0.943	0.943	0.937	0.95	0.948	0.946	0.953	0.96	0.951
T15_1	0.984	0.982	0.987	0.97	0.968	0.965	0.962	0.966	0.963	0.945	0.939	0.939	0.942	0.942	0.937	0.943	0.941	0.941	0.945	0.947	0.943
T24_2	1	0.996	0.998	0.976	0.972	0.971	0.973	0.974	0.971	0.952	0.947	0.947	0.938	0.941	0.936	0.949	0.946	0.945	0.951	0.953	0.948
T24_1	0.996	1	0.997	0.975	0.974	0.972	0.973	0.973	0.971	0.954	0.949	0.948	0.936	0.939	0.934	0.947	0.945	0.944	0.948	0.951	0.946
T24_3	0.998	0.997	1	0.978	0.975	0.972	0.976	0.977	0.973	0.952	0.946	0.945	0.939	0.941	0.936	0.948	0.945	0.944	0.95	0.952	0.947
T50_3	0.976	0.975	0.978	1	0.996	0.996	0.985	0.986	0.986	0.969	0.967	0.965	0.949	0.951	0.948	0.953	0.95	0.949	0.961	0.96	0.956
T50_1	0.972	0.974	0.975	0.996	1	0.995	0.988	0.99	0.986	0.967	0.966	0.964	0.943	0.947	0.945	0.949	0.945	0.946	0.958	0.954	0.955
T50_2	0.971	0.972	0.972	0.996	0.995	1	0.985	0.984	0.983	0.97	0.968	0.969	0.947	0.95	0.948	0.951	0.948	0.947	0.96	0.957	0.954
T70_2	0.973	0.973	0.976	0.985	0.988	0.985	1	0.996	0.995	0.97	0.967	0.965	0.951	0.952	0.951	0.959	0.954	0.953	0.962	0.96	0.957
T70_3	0.974	0.973	0.977	0.986	0.99	0.984	0.996	1	0.996	0.969	0.966	0.963	0.952	0.954	0.952	0.96	0.955	0.955	0.962	0.961	0.958
T70_1	0.971	0.971	0.973	0.986	0.986	0.983	0.995	0.996	1	0.968	0.965	0.962	0.953	0.955	0.951	0.96	0.951	0.955	0.961	0.962	0.958
T130_3	0.952	0.954	0.952	0.969	0.967	0.97	0.97	0.969	0.968	1	0.996	0.997	0.968	0.97	0.967	0.966	0.966	0.964	0.974	0.973	0.97
T130_2	0.947	0.949	0.946	0.967	0.966	0.968	0.967	0.966	0.965	0.996	1	0.995	0.967	0.969	0.965	0.964	0.963	0.962	0.973	0.972	0.969
T130_1	0.947	0.948	0.945	0.965	0.964	0.969	0.965	0.963	0.962	0.997	0.995	1	0.965	0.967	0.964	0.963	0.962	0.96	0.97	0.969	0.968
T140_3	0.938	0.936	0.939	0.949	0.943	0.947	0.951	0.952	0.953	0.968	0.967	0.965	1	0.991	0.99	0.971	0.972	0.968	0.966	0.964	0.96
T140_2	0.941	0.939	0.941	0.951	0.947	0.95	0.952	0.954	0.955	0.97	0.969	0.967	0.991	1	0.992	0.972	0.973	0.969	0.967	0.966	0.962
T140_1	0.936	0.934	0.936	0.948	0.945	0.948	0.951	0.952	0.951	0.967	0.965	0.964	0.99	0.992	1	0.97	0.971	0.968	0.961	0.961	0.956
T168_1	0.949	0.947	0.948	0.953	0.949	0.951	0.959	0.96	0.96	0.966	0.964	0.963	0.971	0.972	0.97	1	0.998	0.997	0.982	0.984	0.981
T168_3	0.946	0.945	0.945	0.95	0.945	0.948	0.954	0.955	0.951	0.966	0.963	0.962	0.972	0.973	0.971	0.998	1	0.996	0.982	0.984	0.981
T168_2	0.945	0.944	0.944	0.949	0.946	0.947	0.953	0.955	0.955	0.964	0.962	0.96	0.968	0.969	0.968	0.997	0.996	1	0.981	0.983	0.98
T182_2	0.951	0.948	0.95	0.961	0.958	0.96	0.962	0.962	0.961	0.974	0.973	0.97	0.966	0.967	0.961	0.982	0.982	0.981	1	0.996	0.996
T182_3	0.953	0.951	0.952	0.96	0.954	0.957	0.96	0.961	0.962	0.973	0.972	0.969	0.964	0.966	0.961	0.984	0.984	0.983	0.996	1	0.997
T182_1	0.948	0.946	0.947	0.956	0.955	0.954	0.957	0.958	0.958	0.97	0.969	0.968	0.96	0.962	0.956	0.981	0.981	0.98	0.996	0.997	1

Table S9. PCA scores of the mouse blood test

The PCA was conducted with the MALDI-TOF mass spectra generated from the mouse blood-circulating exosomes.

ID	PC0 score	PC1 score	PC2 score
Eigenvalue	35.0857	32.9911	25.505
Variance	0.1124	0.1057	0.0818
Cumulative	0.1124	0.2182	0.2999
Healthy#0	-2.845	0.0238	0.5115
Healthy #1	-3.506	-0.6076	0.8602
Healthy #2	-2.577	-0.6106	1.0045
Healthy #3	-2.5073	-0.3133	0.1758
Healthy #4	-3.5222	-0.5861	0.8634
Healthy #5	-2.9575	-0.4617	0.8853
Healthy #6	-2.3827	-0.1228	0.2223
Healthy #7	-2.1278	-0.0231	0.274
Healthy #8	-2.211	-0.0758	0.2248
Black speckles #9	2.8543	-1.9927	-3.9047
Black speckles #10	2.8967	-2.0763	-3.8099
Black speckles #11	2.8384	-1.8751	-3.567
Black speckles #12	3.2152	-2.115	-3.5057
Black speckles #13	3.5637	-2.027	-3.6436
Black speckles #14	3.2517	-2.1104	-3.7089
Early tumor #15	1.9425	2.9715	-1.5136
Early tumor #16	2.9895	2.0178	-0.9105
Early tumor #17	2.4455	1.824	-1.2308
Early tumor #18	1.5592	1.4817	-1.3795
Early tumor #19	2.6029	1.5973	-1.3356
Early tumor #20	2.5536	1.51	-1.9417
Early tumor #21	0.5645	4.1782	-0.7465
Early tumor #22	0.8393	4.0668	-0.8041
Early tumor #23	0.0026	4.4776	-0.5846
Medium-sized tumor #24	0.8488	4.8923	-1.4507
Medium-sized tumor #25	1.2292	4.7409	-1.1084
Medium-sized tumor #26	1.0444	4.8329	-1.4922
Medium-sized tumor #27	1.7531	4.0881	-1.0494
Medium-sized tumor #28	1.9261	4.431	-0.8766
Medium-sized tumor #29	1.7083	4.4121	-0.5944
Metastatic tumor #30	1.7481	4.2987	-0.2469
Metastatic tumor #31	1.5484	4.4456	0.2622
Metastatic tumor #32	1.8388	5.0595	-0.4944
Metastatic tumor #33	4.5161	-0.3519	3.2159
Metastatic tumor #34	4.2136	0.1064	3.235
Metastatic tumor #35	4.3659	-0.1885	2.7912
Metastatic tumor #36	4.1562	0.6183	2.0702
Metastatic tumor #37	4.2358	0.5092	2.2076
Metastatic tumor #38	4.2512	0.4619	2.5514
Metastatic tumor #39	1.3134	2.3977	0.2114
Metastatic tumor #40	1.2279	2.6103	0.2821
Metastatic tumor #41	1.4487	2.5544	0.4454

Table S10. One-way ANOVA statistic of the mouse blood test PCA scores

ID*	PC0 score				PC1 score				PC2 score			
	MeanDiff*	SEM*	F-value	P-value	MeanDiff	SEM	F-value	P-value	MeanDiff	SEM	F-value	P-value
Speckles & Healthy	5.84072	0.5171	31.89527	1.57E-11	-1.72417	0.64491	1.7869	1.52E-01	-4.24794	0.43619	23.71133	8.83E-10
Early T & Healthy	4.45957	0.46251	23.24281	1.15E-09	2.98912	0.57683	6.71331	3.63E-04	-1.71874	0.39014	4.85211	3.01E-03
Early T & Speckles	-1.38116	0.5171	1.78E+00	1.53E-01	4.71329	0.64491	13.35329	7.91E-07	2.5292	0.43619	8.40552	6.28E-05
Medium T & Healthy	4.15571	0.5171	16.14666	9.80E-08	4.87479	0.64491	14.28406	3.84E-07	-1.65326	0.43619	3.59154	1.43E-02
Medium T & Speckles	-1.68502	0.56645	2.21218	8.65E-02	6.59897	0.70647	21.81271	2.59E-09	2.59468	0.47782	7.37201	1.80E-04
Medium T & Early T	-0.30386	0.5171	0.08633	9.86E-01	1.88567	0.64491	2.13733	9.56E-02	0.06548	0.43619	0.00563	1.00E+00
Metastatic T & Healthy	5.64273	0.43264	42.52789	2.35E-13	2.18538	0.53957	4.10104	7.53E-03	0.81961	0.36494	1.26101	3.03E-01
Metastatic T & Speckles	-0.19799	0.49056	0.04072	9.97E-01	3.90955	0.61182	10.20822	1.13E-05	5.06756	0.4138	37.49326	1.53E-12
Metastatic T & Early T	1.18316	0.43264	1.86976	1.36E-01	-0.80374	0.53957	0.55472	6.97E-01	2.53836	0.36494	12.095	2.20E-06
Metastatic T & Medium T	1.48702	0.49056	2.29714	7.73E-02	-2.68942	0.61182	4.83073	3.09E-03	2.47288	0.4138	8.92812	3.76E-05

*MeanDiff: difference in the mean value.

*SEM: standard error of the mean.

*ID. Speckles: Black speckles; Early T: Early tumor; Medium T: Medium-sized tumor; Metastatic T: Metastatic tumor.

Data File S1. Proteomic data for peak assignment on mouse skin surface mass fingerprints

Skin tissues were excised from the tumor region of T130, T168 and T182 mouse, *i.e.* the mouse carrying skin tumor with superficial surface area of 130, 168 and 182 mm^2, respectively. Proteins were extracted from the skin tissues, and afterwards subjected to top-down proteomic analysis. The epidermal MALDI-TOF MS fingerprint peaks were tentatively assigned to proteins by correlation with the top-down proteomic data, according to the measured protein mass. Results obtained from the T182 mouse were shown below as the representative. In order to further confirm the protein identities, the T182 mouse skin tissue was also subjected to bottom-up proteomic analysis, which analyzed the digestion products (peptides) of the tissue proteins using liquid chromatography-tandem mass spectrometry. The peak mass values obtained from MALDI-TOF MS measurements allow a relative mass tolerance of 1,000 ppm. The number label of each peak is consistent with **Figure 3** and **Figure 5** in the main article.

Peak 1. *Tβ4* _ thymosin beta-4 (isoform short) [*Mus musculus* (house mouse)], UniProt accession number P20065-2;

A). MALDI-TOF MS peak: 4,690 *m/z*;

B). Top-down proteomic analysis: precursor monoisotopic mass 4687.421653 Da, adjusted precursor monoisotopic mass 4687.39016 Da, theoretical average mass 4690.232 Da, number of matched fragment ions 15, E value 6.5E-12, P value 6.5E-12, protein sequencing:

M.(S)[Acetyl]DKPDMAEIEKFDKSKLKKTETQEKNPLPSKETIEQEKQA.G

C). According to the UniProt database, the theoretical full protein sequence shall be:

MSDKPDMAEIEKFDKSKLKKTETQEKNPLPSKETIEQEKQAGES

Peak 2. *Vim* _ vimentin [*Mus musculus* (house mouse)], fragment, UniProt accession number P20152;

A). MALDI-TOF MS peak: 7,493 *m/z*;

B). Top-down proteomic analysis: precursor monoisotopic mass 7488.740313 Da, adjusted precursor monoisotopic mass 7489.7282 Da, theoretical average mass 7494.144 Da, number of matched fragment ions 33, E value 2.00E-29, P value 2.00E-29, protein sequencing:

M.(S)[Acetyl]TRSVSSSSYRRMFGGSGTSSRPSSNRSYVTTSTRTYSLGSALRPSTSRSLYSSSPGGAYVTRSSAVR
LR.S

C). Bottom-up proteomic analysis: 100% identification, 58 exclusive unique peptides, 104 exclusive unique spectra, 512 total spectra, 376/466 amino acids (81% coverage), the theoretical full protein sequence shown below (the detected peptide sequences were underlined):

MSTRSVSSSS YRRMFGGSGT SSRPSSNRSY VTTSTRTYSL GSALRPSTSR SLYSSSPGGA YVTRSSAVRL
RSSVPGVRLL QDSVDFSLAD AINTEFKNTR TNEKVELQEL NDRFANYIDK VRFLEQQNKI LLAELEQLKG
QGKSRLGDLY EEEMRELRRQ VDQLTNDKAR VEVERDNLAE DIMRLREKLQ EEMLQREEAE STLQSFRQDV
DNASLARLDL ERKVESLQEE IAFLKKLHDE EIQELQAQIQ EQHVQIDVDV SKPDLTAALR DVRQQYESVA
AKNLQEAEEW YKSKFADLSE AANRNNDALR QAKQESNEYR RQVQSLTCEV DALKGTNESL ERQMREMEEN
FALEAANYQD TIGRLQDEIQ NMKEEMARHL REYQDLLNVK MALDIEIATY RKLLEGEESR ISLPLPTFSS
LNLRETNLES LPLVDTHSKR TLLIKTVETR DGQVINETSQ HHDDLE

Peak 3. *L1-ORF1p* _ LINE-1 retrotransposable element ORF1 protein [*Mus musculus* (house mouse)], fragment, UniProt accession number P11260;

A). MALDI-TOF MS peak: 7,811 *m/z*;

B). Top-down proteomic analysis: precursor monoisotopic mass 7807.923456 Da, adjusted precursor monoisotopic mass 7806.908825 Da, theoretical average mass 7811.677 Da, number of matched fragment ions 13, E value 1.90E-5, P value 1.90E-5, protein sequencing:

K.QENTAKQVMEMNKTILELKGEVDTIKKTQSEATLEIETLGKRSGTIDASISNRIQEMEERISGAEDSIEN.I

C). According to the UniProt database, the theoretical full protein sequence shall be:

MAKGKRKNPT NRNQDHSPSS ERSTPTPPSP GHPNTTENLD PDLKTFLMMM IEDIKKDFHK SLKDLQESTA
KELQALKEKQ ENTAKQVMEM NKTILELKGE VDTIKKTQSE ATLEIETLGK RSGTIDASIS NRIQEMEERI
SGAEDSIENI DTTVKENTKC KRILTQNIQV IQDTMRRPNL RIIGIDENED FQLKGPANIF NKIIEENFPN
IKKEMPMIIQ EAYRTPNRLD QKRNSSRHII IRTTNALNKD RILKAVREKG QVTYKGRPIR ITPDFSPETM
KARRAWTDVI QTLREHKCQP RLLYPAKLSI TIDGETKVFH DKTKFTQYLS TNPALQRIIT EKKQYKDGNH
ALEQPRK

Peak 4. *Actb* _ actin, beta [*Mus musculus* (house mouse)], fragment, UniProt accession number P60710;

A). MALDI-TOF MS peak: 8,712 *m/z*;

B). Top-down proteomic analysis: precursor monoisotopic mass 8707.536708 Da, adjusted precursor monoisotopic mass 8707.510615 Da, theoretical average mass 8713.084 Da, number of matched fragment ions 23, E value 3.97E-15, P value 3.97E-15, protein sequencing:

Y.ANTVLSGGTTMYPGIADRMQKEITALAPSTMKIKIIAPPERKYSVWIGGSILASLSTFQQMWISKQEYDESGPSIVHR
K.C

C). Bottom-up proteomic analysis identified this protein as beta-actin-like protein 2 (alternate ID Actbl2): 100% identification, 2 exclusive unique peptides, 4 exclusive unique spectra, 13 total spectra, 193/376 amino acids (51% coverage), the theoretical full protein sequence shown below (the detected peptide sequences were underlined):

MVDDELTALV VDNGSGMCKA GFGGDDAPRA VFPSMVGRPR HQGVMVGMGQ KDCYVGDEAQ SKRGILTLKY
PIEHGVVTNW DDMEKIWYHT FYNELRVAPD EHPILLTEAP LNPKINREKM TQIMFEAFNT PAMYVAIQAV
LSLYASGRTT GIVMDSGDGV THTVPIYEGY ALPHAILRLD LAGRDLTDYL MKILTERGYN FTTTAEREIV
RDVKEKLCYV ALDFEQEMVT AAASSSLERS YELPDGQVIT IGNERFRCPE AIFQPSFLGI ESRGIHETTF
NSIMKCDVDI RKDLFANTVL SGGSTMYPGI ADRMQKEIVT LAPSTMKIKI IAPPERKYSV WIGGSILASL
STFQQMWISK QEYDEAGPPI VHRKCF

Peak 5. *Atpif1* _ ATPase inhibitor, mitochondrial [*Mus musculus* (house mouse)], UniProt accession number O35143;

A). MALDI-TOF MS peak: 9,366 *m/z*;

B). Top-down proteomic analysis: precursor monoisotopic mass 9361.767326 Da, adjusted precursor monoisotopic mass 9361.739925 Da, theoretical average mass 9367.289 Da, number of matched fragment ions 22, E value 4.04E-15, P value 4.04E-15, protein sequencing:

V.SDSSDSMDTGAGSIREAGGAFGKREKAEEDRYFREKTKEQLAALRKHHEDEIDHHSKEIERLQKQIERHKKKIQQLKN
NH.

C). Bottom-up proteomic analysis: 100% identification, 2 exclusive unique peptides, 3 exclusive unique spectra, 3 total spectra, 12/106 amino acids (11% coverage), the theoretical full protein sequence shown below (the detected peptide sequences were underlined):

MAGSALAVRA RFGVWGMKVL QTRGFVSDSS DSMDTGAGSI REAGGAFGKR EKAEEDRYFR EKTKEQLAAL RKHHEDEIDH HSKEIERLQK QIERHKKKIQ QLKNNH

Peak 7. *S100a8* _ S100 calcium binding protein A8 [*Mus musculus* (house mouse)], UniProt accession number P27005;

A). MALDI-TOF MS peak: 10,165 *m/z*;

B-1). Top-down proteomic analysis: precursor monoisotopic mass 10157.00076 Da, adjusted precursor monoisotopic mass 10157.02537 Da, theoretical average mass 10163.373 Da, number of matched fragment ions 73, E value 3.82E-59, P value 3.82E-59, protein sequencing:

M.PSELEKALSNLIDVYHNYSNIQGNHHALYKNDFKKMVTTECPQFVQNINIENLFRELDINSDNAINFEEFLAMVIKVG VASHKDSHKE.

B-2). Top-down proteomic analysis: precursor monoisotopic mass 10173.04361 Da, adjusted precursor monoisotopic mass 10173.34861 Da, theoretical average mass 10180.292 Da, number of matched fragment ions 37, E value 3.19E-23, P value 3.19E-23, protein sequencing:

M.PSELEKALSNLIDVYHNYSNIQGNHHALYKNDFKKMVTTECPQF(VQNINIENLFRELDINSDNA)[16.91937]IN FEEFLAMVIKVGVASHKDSHKE.

B-3). Top-down proteomic analysis: precursor monoisotopic mass 10191.03962 Da, adjusted precursor monoisotopic mass 10191.16962 Da, theoretical average mass 10197.517 Da, number of matched fragment ions 36, E value 1.53E-22, P value 1.53E-22, protein sequencing:

M.PSELEKALSNLIDVYHNYSNIQGNHHALYKNDFKKMVTTECPQFV(QNINIENLFRELDINSD)[34.14424]NAIN FEEFLAMVIKVGVASHKDSHKE.

C). Bottom-up proteomic analysis: 100% identification, 6 exclusive unique peptides, 12 exclusive unique spectra, 15 total spectra, 77/89 amino acids (87% coverage), the theoretical full protein sequence shown below (the detected peptide sequences were underlined):

MPSELEKALS NLIDVYHNYS NIQGNHHALY KNDFKKMVTT ECPQFVQNIN IENLFRELDI NSDNAINFEE FLAMVIKVGV ASHKDSHKE

Peak 8. (Probably) *S100b* _ S100 calcium binding protein B (S100 protein, beta polypeptide, neural) [*Mus musculus* (house mouse)], UniProt accession number P50114;

A). MALDI-TOF MS peak: 10,598 *m/z*;

B). Top-down proteomic analysis did not detect any protein around 10520-10700 Da. But the bottom-up proteomic analysis detected *S100b* protein around this mass, and this protein was detectable only from the tumor mouse not from the healthy mouse.

C). Bottom-up proteomic analysis: 100% identification, 3 exclusive unique peptides, 7 exclusive unique spectra, 7 total spectra, 37/92 amino acids (40% coverage), the theoretical full protein sequence shown below (the detected peptide sequences were underlined):

MSELEKAMVA LIDVFHQYSG REGDKHKLKK SELKELINNE LSHFLEEIKE QEVVDKVMET LDEDGDGECD FQEFMAFVAM VTTACHEFFEHE

According to the peak *m/z* value, the sequence detected by MALDI-TOF MS could be:

M.SELEKAMVALIDVFHQYSGREGDKHKLKKSELKELINNELSHFLEEIKEQEVVDKVMETLDEDGDGECDFQEFMAFVA MVTTACHEFFEHE. (theoretical monoisotopic mass 10589.998 Da, theoretical average mass 10596.839 Da)

Peak 9. *Hspe1* _ 10 kDa heat shock protein, mitochondrial [*Mus musculus* (house mouse)], UniProt accession number Q64433;

A). MALDI-TOF MS peak: 10,871 *m/z*;

B).Top-down proteomic analysis: precursor monoisotopic mass 10866.82702 Da, adjusted precursor monoisotopic mass 10866.83556 Da, theoretical average mass 10873.510 Da, number of matched fragment ions 21, E value 1.42E-13, P value 1.42E-13, protein sequencing:

M.(A)[Acetyl]GQAFRKFLPLFDRVLVERSAAETVTKGGIMLPEKSQGKVLQATVVAVGSGGKGKSGEIEPVSVKVGD
KVLLPEYGGTKVVLDDKDYFLFRDSDILGKYVD.

C). Bottom-up proteomic analysis: 100% identification, 6 exclusive unique peptides, 7 exclusive unique spectra, 7 total spectra, 44/102 amino acids (43% coverage), the theoretical full protein sequence shown below (the detected peptide sequences were underlined):

MAGQAFRKFL PLFDRVLVER SAAETVTKGG IMLPEKSQGK VLQATVVAVG SGGKGKSGEI EPVSVKVGDK
VLLPEYGGTK VVLDDKDYFL FRDSDILGKY VD

Peak 10. *Actg1* _ actin, gamma, cytoplasmic 1 (also named actin, cytoplasmic 2) [*Mus musculus* (house mouse)], fragment, UniProt accession number P63260;

A). MALDI-TOF MS peak: 11,546 *m/z*;

B).Top-down proteomic analysis: precursor monoisotopic mass 11537.68519 Da, adjusted precursor monoisotopic mass 11537.18019 Da, theoretical average mass 11545.204 Da, number of matched fragment ions 26, E value 3.19E-09, P value 3.19E-09, protein sequencing:

.((M)[Acetyl]EEEI)[-173.08687]AALVIDNGSGMCKAGFAGDDAPRAVFPSIVGRPRHQGVMVGMGQKDSY
VGDEAQSKRGILTLKYPIEH GIVTNWDDMEKIWHHTFYNELRVAPEEHPVLL.T

C). Bottom-up proteomic analysis: 100% identification, 60 exclusive unique peptides, 106 exclusive unique spectra, 478 total spectra, 330/375 amino acids (88% coverage), the theoretical full protein sequence shown below (the detected peptide sequences were underlined):

MEEEIAALVI DNGSGMCKAG FAGDDAPRAV FPSIVGRPRH QGVMVGMGQK DSYVGDEAQS KRGILTLKYP
IEHGIVTNWD DMEKIWHHTF YNELRVAPEE HPVLLTEAPL NPKANREKMT QIMFETFNTP AMYVAIQAVL
SLYASGRTTG IVMDSGDGVT HTVPIYEGYA LPHAILRLDL AGRDLTDYLM KILTERGYSF TTTAEREIVR
DIKEKLCYVA LDFEQEMATA ASSSSLEKSY ELPDGQVITI GNERFRCPEA LFQPSFLGME SCGIHETTFN
SIMKCDVDIR KDLYANTVLS GGTTMYPGIA DRMQKEITAL APSTMKIKII APPERKYSVW IGGSILASLS
TFQQMWISKQ EYDESGPSIV HRKCF

Peak 11. *Hba-a1* _ hemoglobin subunit alpha [*Mus musculus* (house mouse)], UniProt accession number P01942;

A). MALDI-TOF MS peak: 14,975 *m/z*;

B).Top-down proteomic analysis: precursor monoisotopic mass 14971.73697 Da, adjusted precursor monoisotopic mass 14971.75197 Da, theoretical average mass 14980.834 Da, number of matched fragment ions 38, E value 2.81E-10, P value 2.81E-10, protein sequencing:

L.SGEDKSNIKAAWGKIGGHGAEYGAEALERMFASFPTTKTYFPHFDVSHGSAQVKGHGKKVADALA(SAAGHLD)[239
.18462]DLPGALSALSDLHAHKLRVDPVNFKLLSHCLLVTLASHHPADFTPAVHASLDKFLASVSTVLTSKYR

C). Bottom-up proteomic analysis: 100% identification, 25 exclusive unique peptides, 45 exclusive unique spectra, 142 total spectra, 120/142 amino acids (85% coverage), the theoretical full protein sequence shown below (the detected peptide sequences were underlined):

MVLSGEDKSN IKAAWGKIGG HGAEYGAEAL ERMFASFPTT KTYFPHFDVS HGSAQVKGHG KKVADALASA
AGHLDDLPGA LSALSDLHAH KLRVDPVNFK LLSHCLLVTL ASHHPADFTP AVHASLDKFL ASVSTVLTSK YR

Peak 12. *Hbb-b2* _ hemoglobin subunit beta-2 [*Mus musculus* (house mouse)], UniProt accession number P02089;

A). MALDI-TOF MS peak: 15,615 *m/z*;

B).Top-down proteomic analysis: precursor monoisotopic mass 15608.42467 Da, adjusted precursor monoisotopic mass 15608.14285 Da, theoretical average mass 15617.887 Da, number of matched fragment ions 16, E value 1.17E-12, P value 1.17E-12, protein sequencing:

V.HLTDAEKSAVSCLWAKVNPDEVGGEALGRLLVVYPWTQRYFDSFGDLSSASAIMGNPKVKAHGKKVITAFNEGLKNLD
NLKGTFASLSELHCDKLHVDPENFRLLGNAIVIVLGHHLGKDFTPAAQAAFQKVVAGVA (T) [-30.00172]
ALAHKY H.

C). Bottom-up proteomic analysis: 100% identification, 2 exclusive unique peptides, 2 exclusive unique spectra, 2 total spectra, 90/147 amino acids (61% coverage), the theoretical full protein sequence shown below (the detected peptide sequences were underlined):

MVHLTDAEKS AVSCLWAKVN PDEVGGEALG RLLVVYPWTQ RYFDSFGDLS SASAIMGNPK VKAHGKKVIT
AFNEGLKNLD NLKGTFASLS ELHCDKLHVD PENFRLLGNA IVIVLGHHLG KDFTPAAQAA FQKVVAGVAT
ALAHKYH

Data File S2. Quantitative proteomic data of mouse skin tissues

The quantity of each identified protein was compared between skin tumors and healthy skins. The increased or decreased expression of a protein due to the tumor development was conditioned by absolute log2 fold change higher than 1 and the paired t-test statistical significant level (P-value) lower than 0.05. This file lists the differently expressed proteins caused by the growth of melanoma. It is related to the data shown in **Figure 6A** (from Scaffold spectral counting) and **Figure S16A** (from MaxQuant LFQ), respectively. The two quantification procedures shared 795 common up-regulated proteins and 253 common down-regulated proteins, as listed below. The protein names were given in their abbreviations (according to the gene name).

(1) Down-regulated proteins

Aacs	Ak1	Bbox1	Cisd1	Crat	Eci1	Folr2	Hnmt	Krt79	Mcee	Mylpf	Pdlim3	Procr	Serpina3j	Tmod4
Abcc4	Aldh1a1	Bcat2	Ckap4	Cryab	Ecm2	Galm	Hspb1	Lama3	Mcpt4	Myom2	Pdlim5	Prx	Serpinb1a	Tnmd
Abhd5	Aldh1l2	Bgn	Ckm	Csrp3	Eno2	Gcat	Hspb2	Lamb3	Mfap4	Myot	Pdlim7	Pvalb	Serpinb6	Tnnc2
Abi3bp	Aldh3a1	C1qtnf3	Ckmt2	Cthrc1	Eno3	Glt8d2	Hspb6	Lamc2	Mgl2	Myoz1	Pfkm	Pygm	Serpinb6c	Tnnt3
Acadl	Aldh4a1	Ca1	Clec10a	Ctsk	Eppk1	Glul	Idh2	Ldb3	Mgst1	Ndufa2	Pgam2	Rab43	Sh3bgr	Tnxb
Ace	Aldoa	Ca3	Clec11a	Cycs	F13a1	Got1	Idh3a	Lgals3	Mmp3	Ndufa4l2	Pgm1	Rarres2	Sh3bgrl2	Tpi1
Aco2	Amacr	Camk2a	Clec3b	Cyp2b10	Fabp3	Got2	Igkv5-39	Lipe	Mp68	Ndufa5	Pgm5	Retn	Slc25a13	Tpm2
Acot13	Ang	Casq1	Clybl	Cyp2f2	Fabp4	Gpt	Igkv6-32	Lox	Mpz	Ndufb4	Phkg1	Rnase2b	Sncg	Trappc4
Acta1	Angptl2	Ccdc90b	Cnn1	Dcn	Fam213a	Gpx8	Il1rn	Lrrc57	Mrps26	Neb	Pkp3	Rtn2	Sord	Trim29
Actn2	Anxa8	Ccl27a	Col17a1	Des	Far2	Gsta3	Inmt	Lum	Msra	Nefl	Plin1	Ryr1	Srl	Trim72
Actn3	Apobec2	Cd209d	Col1a1	Dhdh	Fbp2	Gstm1	Jsrp1	Ly6c1	Mybpc1	Nefm	Plin2	S100a14	Srpx	Tst
Acyp2	Arg1	Cd34	Col1a2	Dhrs7	Fhl1	Gstt1	Jup	Ly6d	Mybpc2	Neu2	Plin4	Samhd1	Suclg2	Ugt1a1
Adh1	Aspn	Cd36	Col3a1	Dhrs7c	Fkbp14	Gstt3	Klhl41	Ly6g6c	Myh1	Ogn	Podn	Sbsn	Susd2	Uqcrc2
Adh7	Atp2a1	Cdh13	Col5a1	Dpp4	Fkbp9	Gstz1	Klk10	Macrod1	Myh11	Olfml3	Pof1b	Scel	Sypl2	Xdh
Adssl1	Atp2a2	Cenpv	Coq9	Dpt	Flg2	Gys1	Krt10	Maob	Myh2	P4ha2	Ppa1	Scin	Tacstd2	
Aebp1	Atp5f1	Ces1d	Cox6a2	Dusp23	Fmod	Hba	Krt15	Mb	Myh4	Pam16	Ppl	Sdr39u1	Tmed5	
Agl	Atp5j2	Chdh	Cpa3	Echdc1	Fndc1	Hhatl	Krt76	Mbp	Myl1	Pcolce	Prelp	Sec14l4	Tmod1	

(2) Up-regulated proteins

Aars	Get4	Psmc4	Atp2b4	Ilf2	Rock2	Cnn2	Man2a1	Sntb1	Ddx42	Nae1	Tcerg1	Elovl4	Pex11b	Uaca
Abca6	Gfpt1	Psmd1	Atp6v1h	Ilf3	Rp2	Cnn3	Man2c1	Snx1	Ddx58	Naglu	Tecpr1	Emc1	Pfas	Uba2
Abca8a	Ggcx	Psmd12	Atp8a1	Ilk	Rpa1	Cnot1	Manba	Snx27	Degs1	Nap1l1	Tfg	Emc3	Pglyrp2	Uba5
Abca8b	Gid8	Psmd2	Atp9a	Impad1	Rpia	Cnp	Map1b	Snx4	Denr	Nap1l4	Thbd	Eml2	Phldb1	Uba6
Abce1	Git1	Psmd3	Bag6	Inf2	Rpp30	Col12a1	Map1s	Snx7	Dera	Nars	Thoc2	Eml4	Pigu	Ube2e3
Abcg2	Glg1	Psmd4	Bax	Ints1	Rps6ka3	Col14a1	Map2k6	Soat1	Dhcr7	Ncam1	Thrap3	Endod1	Pik3r4	Ube2g1
Abhd12	Gmds	Psmg1	Bche	Ipo4	Rtkn	Col15a1	Map4	Sorbs1	Dhrs1	Ncbp2	Thyn1	Endou	Pla2g4a	Ube2h
Acaca	Gmps	Psmg2	Bcl2l1	Ipo9	Ruvbl2	Col18a1	Map4k4	Sorbs2	Dhx15	Nckap1	Timm44	Enoph1	Plaa	Ube2z
Acin1	Gnb4	Pspc1	Bicd2	Islr	S100b	Col20a1	Mapk3	Sorcs2	Dhx9	Ncln	Timp3	Epb41l2	Plcb3	Ube3c
Acot7	Golga2	Ptk2	Bpgm	Isyna1	Sart3	Col4a1	Mapre2	Sort1	Diaph1	Ncoa5	Tinagl1	Epx	Pld1	Ubqln2
Acox1	Golga3	Ptk7	C4bpa	Itga1	Sbds	Col4a2	Marcks	Spag9	Diaph2	Ndrg3	Tjp1	Erc1	Plek	Ubr4
Acp2	Golgb1	Ptn	Cad	Itga2	Scamp3	Colec12	Marcksl1	Sparcl1	Dip2b	Nek9	Tln2	Esyt2	Plekha6	Uchl3
Acsl4	Golim4	Ptpn1	Calu	Itga5	Scly	Cops6	Mars	Specc1	Dlg3	Nf1	Tm9sf1	Exoc2	Plekho2	Uchl5
Actr10	Gpc1	Ptpn11	Camk1	Itga8	Sdf4	Coro1b	Matn2	Spon1	Dmd	Nhlrc2	Tm9sf2	Exoc4	Plod3	Ugt1a6
Adam10	Gpld1	Ptpn13	Caprin1	Itgav	Sec14l2	Coro7	Matr3	Sppl2b	Dnajc13	Nid1	Tm9sf3	Exoc5	Plp1	Unc119b
Add1	Gpm6b	Ptpn23	Casp14	Itgb1	Sec23ip	Cotl1	Mavs	Sptan1	Dnajc3	Nid2	Tm9sf4	Exoc6b	Plxnb2	Unc45a
Afap1l2	Gpr107	Ptpn9	Casp3	Itih5	Sec24c	Cpd	Mcam	Srp68	Dnajc5	Nip7	Tmed1	Exosc1	Plxnb3	Upf1
Afm	Gps1	Ptpra	Cbfb	Itm2b	Sec61a1	Cpm	Mcts1	Srp72	Dnajc7	Nisch	Tmem165	Fabp7	Pno1	Urm1
Agfg1	Grn	Ptprj	Ccar1	Itpr3	Seh1l	Cpn1	Me2	Srrm1	Dock1	Nmt1	Tmem167	Faf2	Pofut1	Usp14
Agpat3	Gsdmc	Puf60	Ccar2	Jagn1	Sf3a1	Cpne2	Metap2	Srrt	Dock11	Nnmt	Tmem63a	FAM120A	Polr2b	Usp39
Agrn	Gsk3b	Pus7	Ccdc124	Kank2	Sf3a2	Cpsf1	Mgam	Srsf7	Dock7	Nomo1	Tmem87a	Fam129a	Polr2d	Usp4
Ahcyl1	Gspt1	Pxdn	Ccdc47	Kank4	Sf3a3	Cpsf6	Mlec	Srsf9	Dpysl3	Nono	Tmem9b	Fam177a1	Pon2	Usp5
Aif1	Gss	Pxn	Ccl6	Kcnab2	Sf3b1	Cpt1a	Mmgt1	Ssrp1	Dr1	Nop58	Tmlhe	Fam206a	Postn	Usp7
Aip	Gulp1	Qars	Ccnd3	Kif5b	Sf3b2	Crot	Mms19	Stag2	Dscr3	Npc1	Tmod2	Fam49a	Ppfibp1	Usp8
Aldh1a3	Gusb	Qki	Ccs	Klc1	Sf3b3	Crp	Mon2	Stam	Dst	Npepl1	Tmtc3	Fam98b	Ppig	Usp9x
Aldh3b1	H2afy2	Rab12	Cd109	Klkb1	Sf3b5	Crym	Moxd1	Stam2	Dus3l	Nploc4	Tmx4	Fap	Ppil3	Utrn
Ampd3	Hacd3	Rab23	Cd151	Kpna4	Sgcd	Csde1	Mpdu1	Stat3	Dync1h1	Nrbp1	Tnfaip8l2	Farp1	Ppm1b	Vars
Ankfy1	Hbs1l	Rab31	Cd2ap	Kpna6	Sgpp1	Cse1l	Mpp1	Steap4	Dync1li1	Nrd1	Tnks1bp1	Fbln2	Ppp1r12a	Vasp
Ano10	Hcfc1	Rab3gap2	Cdc42bpb	Ktn1	Sgsh	Csf1r	Mprip	Stfa3	Dync1li2	Nsfl1c	Tnpo1	Fbn2	Ppp1r18	Vav1

Ano6	Heatr1	Rab8b	Cdc5l	L1cam	Sh3bp1	Csk	Mrpl11	Stk39	Ear1	Nsun2	Tnpo2	Fcgrt	Ppp1r2	Vcan
Anp32e	Heatr5a	Rabgap1	Cdh19	Lama2	Sh3kbp1	Csnk1a1	Mrpl20	Stom	Ear2	Nucb1	Tnpo3	Fcho2	Ppp2r2a	Vcl
Ap1m1	Hgs	Rad21	Cdh2	Lama4	Sirt2	Cspg4	Mrps23	Strip1	Ear6	Nudcd2	Tns1	Fermt2	Ppp2r5a	Vps13c
Ap2a1	Hip1	Rai14	Cdk2	Lamb1	Sirt5	Ctbp2	Mrto4	Strn	Ecpas	Nudt4	Tns2	Fermt3	Ppp2r5e	Vps16
Ap3d1	Hmbs	Ranbp2	Cdk4	Lars	Slc12a4	Ctnnal1	Msi2	Strn3	Edf1	Nudt9	Tns3	Fgl2	Ppp4c	Vps45
Apip	Hmox1	Ranbp3	Celf2	Lbr	Slc12a9	Ctnnb1	Mta2	Strn4	Eea1	Numa1	Tomm34	Fhl2	Ppp6r3	Vps51
Apon	Hmox2	Rap1gds1	Cers2	Lgals3bp	Slc25a17	Ctnnd1	Mtch1	Sts	Efhd1	Nup155	Top2b	Fhod1	Prcp	Vps8
Appl1	Hnrnpdl	Rap2a	Cfl1	Lgmn	Slc35b2	Cttn	Mthfd1l	Stt3b	Efnb1	Nup205	Tor1aip1	Fkbp15	Prg2	Vrk1
Arap1	Hnrnph3	Rasa1	Chd4	Lima1	Slc39a7	Cul4a	Mtmr6	Stx18	Eftud2	Nup93	Tor1b	Flg	Prg3	Vwa1
Arfip1	Hnrnpul1	Raver1	Chid1	Lims1	Slc3a2	Cul5	Mxra7	Sugt1	Egfl8	Ola1	Tpp2	Flii	Prkaa1	Wars
Arhgef1	Hrnr	Rbm14	Chkb	Lipa	Slc44a1	Cyfip1	Myadm	Sun1	Egflam	Osbp	Tpr	Flot2	Prkacb	Wasl
Arhgef10	Hsdl2	Rbm25	Chl1	Lmf2	Slc9a3r1	Cyp20a1	Mybbp1a	Swap70	Egfr	Osbpl9	Tpsb2	Fmnl2	Prkar1a	Wdfy1
Arhgef2	Hspa12a	Rbm8a	Chmp4b	Lpar1	Slk	Cyp51a1	Myef2	Syk	Eif2a	Oxsr1	Trappc6b	Fmo1	Prkar2b	Wdr11
Arhgef7	Hspg2	Rbms1	Chordc1	Lpcat2	Smad2	Cyth1	Myh10	Syne1	Eif2b1	P2ry12	Trim2	Fn1	Prkra	Wdr6
Armc10	Huwe1	Rbp1	Chtop	Lpp	Smap2	Dag1	Myo18a	Syne2	Eif2s2	Paics	Trim25	Fscn1	Prmt1	Xpo1
Arpin	Hyou1	Rela	Ciapin1	Lrba	Smarca4	Dbn1	Myo1b	Syvn1	Eif2s3x	Pak2	Trim47	Fstl1	Prmt5	Xpo7
Arsb	Iars	Rer1	Ckap5	Lrpprc	Smarcb1	Dcaf8	Myo1e	Tacc1	Eif3c	Palld	Triobp	Fxr1	Pros1	Yars
As3mt	Igbp1	Rftn2	Clasp1	Lrrc15	Smarcc2	Dcakd	Myo1f	Tars	Eif3d	Parva	Trip11	G3bp1	Prpf31	Ythdf1
Asap2	Igf2r	Rheb	Clasp2	Lsamp	Smc3	Dctn2	Myo5a	Tbc1d15	Eif4g1	Pcid2	Trip12	G3bp2	Prpf40a	Ythdf2
Asl	Igfals	Rhoj	Clip2	Lsm1	Snap23	Dctn4	Myo6	Tbc1d8b	Eif4g2	Pdcd5	Tubb4a	Ganc	Prpf8	Zc3hav1
Atp11b	Igfbp7	Ric8a	Clptm1	Ltbp4	Snrnp200	Dcun1d1	Myo9b	Tbcc	Eif4g3	Pdlim1	Txndc12	Gas7	Prps2	Zfpl1
Atp13a1	Igha	Rnmt	Clptm1l	Luc7l2	Snrnp40	Ddrgk1	Myof	Tbcd	Eif5	Pdlim4	Txndc9	Gbf1	Psen1	Zmpste24
Atp1b2	Il1rap	Robo2	Cmpk2	Macf1	Snrnp70	Ddx21	Naa10	Tcaf2	Eif5b	Pds5b	Tyr	Gbp7	Psip1	Znf22
Atp2b1	Il6st	Rock1	Cmtm7	Maged2	Snrpa1	Ddx3y	Naalad2	Tcea1	Elmo2	Pef1	U2af2	Gclm	Psmc3	Zyx

Data File S3. Quantitative proteomic data of melanoma biomarkers

Tissue excised from a normal skin region on a healthy mouse and the tissues excised from the cancerous skin of the T70 mouse, T130 mouse and T182 mouse (*i.e.* the mouse carrying skin tumor with superficial surface area of 70, 130, 182 mm^2, respectively) were conducted quantitative proteomic analysis using liquid chromatography-tandem mass spectrometry. The data obtained for six well-established melanoma biomarkers are summarized below, with the corresponding unique peptides listed. Unique peptides are the distinct peptide sequences unique to a single protein group, regardless of any modification. The file is related to **Figure 6B** and **Figure S16B**.

Biomarker 1: *Pmel* _ premelanosome protein [*Mus musculus (house mouse)*], UniProt accession Q60696;

A). *Pmel* was not detectable from *Healthy Mouse Skins.*

B). *Pmel* detected from *Mouse Skin Tumors*
Protein identification probability: 100%;
Quantitative value (normalized total spectrum count): 2.021±0.621;
Quantitative value (LFQ intensity $\times 10^7$): 2.009±0.516;
Exclusive unique peptides detected for this protein:

(K)YWQVLGGPVSR(L)	(R)LSIATGHAK(L)	(R)SFVYVWK(T)

Biomarker 2: *Tyr* _ tyrosinase [*Mus musculus (house mouse)*], UniProt accession P11344;

A). *Tyr* was not detectable from *Healthy Mouse Skins.*

B). *Tyr* detected from *Mouse Skin Tumors*
Protein identification probability: 100%;
Quantitative value (normalized total spectrum count): 2.401±2.897;
Quantitative value (LFQ intensity $\times 10^7$): 3.135±2.332;
Exclusive unique peptides detected for this protein:

(R)GScQDILLSSAPSGPQFPFK(G)	(R)DTLLGGSEIWR(D)	(K)DLGYDYSYLQESDPGFYR(N)	(K)FFSYLTLAK(H)
(R)NYIEPYLEQASR(I)	(R)DIDFAHEAPGFLPWHR(L)	(R)HPENPNLLSPASFFSSWQIIcSR(S)	

Biomarker 3: S*100b*_ S100 calcium binding protein B [*Mus musculus (house mouse)*], UniProt accession P50114;

A). *S100b* was not detectable from *Healthy Mouse Skins.*

B). *S100b* detected from the *Mouse Skin Tumors*
Protein identification probability: 100%;
Quantitative value (normalized total spectrum count): 6.818±0.366;
Quantitative value (LFQ intensity $\times 10^7$): 6.754±0.386;
Exclusive unique peptides detected for this protein:

(K)AMVALIDVFHQYSGR(E)	(K)ELINNELSHFLEEIK(E)	(K)ELINNELSHFLEEIKEQEVVDK(V)

Biomarker 4: *Cspg4*_ *chondroitin sulfate proteoglycan 4* [*Mus musculus (house mouse)*], UniProt accession Q8VHY0;

A). *Cspg4* detected from *Healthy Mouse Skins*
Protein identification probability: 100%;
Quantitative value (normalized total spectrum count): 4.826±0.879;

Quantitative value (LFQ intensity $\times 10^7$): 4.560±0.722;
Exclusive unique peptides detected for this protein:

(K)ITVAALDAANLLASVPASQR(S)	(K)SYSVALLSVPEAVR(T)

B). *Cspg4* detected from the *Mouse Skin Tumors*
Protein identification probability: 100%;
Quantitative value (normalized total spectrum count): 330.413±55.843;
Quantitative value (LFQ intensity $\times 10^7$): 332.940±48.185;
Exclusive unique peptides detected for this protein:

(H)TFHYELVQAPR(R)	(R)DGQSVTSFSQR(D)	(R)GVLSYLEPR(G)	(R)SQQAPLAFQAGDKR(G)
(K)GLWVPEGQR(A)	(R)DQPGEPATEFScR(E)	(R)HDVLFQVTQFPTR(G)	(R)TGSMPHFR(L)
(K)GQGTMLLR(N)	(R)EEGTLEFTLTTR(S)	(R)HGDLELDILGAQTR(K)	(R)TPNPALR(N)
(K)HDVQVLTAK(P)	(R)EEPDVAYR(L)	(R)HVQPTLDLTEAELR(K)	(R)TSEAADDSFR(F)
(K)HDVQVLTAKPR(N)	(R)ELEVGDIVYVHR(G)	(R)HVQPTLDLTEAELRK(S)	(R)VAPDTEVHR(F)
(K)IYVFQGEAAEIR(R)	(R)ELEVGDIVYVHRG(G)	(R)KMFTLLDVVNR(K)	(R)VTGTLQFGELQK(Q)
(K)KIYVFQGEAAEIR(R)	(R)EVEEQLIR(Y)	(R)KSQVLFSVSQSAR(H)	(T)AGPQWGQLLR(D)
(K)MFTLLDVVNR(K)	(R)FTQEDLR(K)	(R)LEISVDQYPTR(T)	(V)APDTEVHR(F)
(K)MFTLLDVVNRK(A)	(R)FTQEDLRK(K)	(R)LLAGPR(Y)	(Y)AHGGGGTQQDGFR(F)
(K)QALLSLEGTR(K)	(R)GcLHSAILNGR(N)	(R)LTLELWAK(G)	(Y)SVALLSVPEAVR(T)
(K)qALLSLEGTRK(L)	(R)GGPAQDLTFR(V)	(R)NGLAGDTETFR(K)	(R)VSDGMQASAPATLK(V)
(K)SQVLFSVSQSAR(H)	(R)GNFIYVDIFEGHLR(A)	(R)QQLQVISDR(E)	(R)SRHDVLFQVTQFPTR(G)
(K)SYSVALLSVPEAVR(T)	(M)SLAVDVLPSTIEVQLR(A)	(R)NLLRPLTSDVHEGcA(E)	(R)VAIQPVNDHAPVQTISR(V)
(F)SGPHSLAAFPAWSTR(E)	(R)DVNERPPQPQASIPLR(V)	(R)QQLQVISDREEPDVAYR(L)	(V)PPAVALLDFATEPYHAAK(S)
(K)EDHSQDGSLSTFSWR(E)	(R)FTQAQLDSGLVLFSHR(G)	(R)LSDGESFSQSDLQAGR(V)	(R)RGQIYILPIQVNPVNDPPR(I)
(K)STPVTSFTNEDLLHGR(L)	(R)FTQAQLDSGLVLFSHRG(A)	(R)GQIYILPIQVNPVNDPPR(I)	(R)RPYFLQSELAAGQLVYAH(G)
(K)SLNSASYLYEVMEQPHHGK(L)	(R)DLEEGQLGLEVGKPEGR(S)	(R)KDLLFGSIVAMEEPTRPIYR(F)	(R)SGNEVHYHVTAGPQWGQLLR(D)
(K)QGAGGVEGTEWWDTLAFHQR(D)	(P)ASFFGENHLEVPVPSALTR(V)	(K)DLLFGSIVAMEEPTRPIYR(F)	(K)ITVAALDAANLLASVPASQR(S)
(K)ATYGLFVGSSGSLDLPYLK(G)	(R)DQLEVVQEAVLPADIMFSLR(S)	(R)LVYQHDDSETIEDDIPFVATR(Q)	(Y)FLQSELAAGQLVYAHGGGGTQQDGFR(F)
(R)NSVPVADGQPHEVSVHIDVHR(L)	(R)AQLSVVDPDSAPGEIEYEVQR(A)	(R)GTDNDSGPEDLVYTIEQPSNGR(I)	NLLRPLTSDVHEGcAEEFSAGDEVGLGFSGPH(S)
(K)GVPPAVALLDFATEPYHAAK(S)	(R)AHLQGPTGTSVAGPQTSEAFVITVR(D)	(R)LLTTDDVAFSDADSGFSDAQLVLTR(K)	(R)VTSPPHFSPLYTFPIHIGGDPNAPVLTN(V)
(R)RDQLEVVQEAVLPADIMFSLR(S)	(R)GALEGGFHFDLSDGAHTSPGHFFR(V)	(R)KLTVcPESVQPLSSQSLSASSSTGADPR(H)	(R)VTSPPHFSPLYTFPIHIGGDPNAPVLTNVLL(M)
(H)GASAEEPPSLDPVQSFSQEAVNSGR(V)	(R)DLAATLAVMVSFDAAcPQRPSR(L)	(R)NLLRPLTSDVHEGcAEEFSAGDEVGLGFSGPH(S)	(R)RPYFLQSELAAGQLVYAHGGGGTQQDGFR(F)
(K)LTVcPESVQPLSSQSLSASSSTGADPR(H)	(M)VSHGASAEEPPSLDPVQSFSQEAVNSGR(V)	(R)KVEPGQAIPLITVPGQGPPPGGQPDPELLQFcR(T)	(R)TLAPPLVQITGPYFPTLPGLVLQVLEPPQHGALQK(E)
(F)TITILPVNDQPPVLTTNTGLQIWEGAIVPIPPEALR(G)	(N)EDLLHGRLVYQHDDSETIEDDIPFVATR(Q)	(R)LEPLHTQNPHQETLTPAHLEASLEEEEEEGSPQPH(T)	(R)SPPNAGYLVMVSHGASAEEPPSLDPVQSFSQEAVNSGR(V)
(L)TSDVHEGcAEEFSAGDEVGLGFSGPHSLAAFPAWSTR(E)	(R)APHNGFLSLAGDNTGPVTHFTQADVDAGR(L)	(R)NLLRPLTSDVHEGcAEEFSAGDEVGLGFSGPHSLAAFPAWSTR(E)	(R)QSQPVAFTITILPVNDQPPVLTTNTGLQIWEGAIVPIPPEALR(G)

Biomarker 5: *Fn1_* fibronectin 1 [*Mus musculus (house mouse)*], UniProt accession P11276;

A). *Fn1* detected from *Healthy Mouse Skins*
Protein identification probability: 100%;
Quantitative value (normalized total spectrum count): 154.667±5.132;
Quantitative value (LFQ intensity $\times 10^7$): 148.182±0.093;
Exclusive unique peptides detected for this protein:

(R)GFNcESKPEPEETcFDK(Y)	(R)VEVLPVSLPGEHGQR(L)	(R)VTWAPPPSIELTNLLVR(Y)	(R)APITGYIIR(H)
(K)VGDTYERPK(D)	(R)NTFAEITGLSPGVTYLFK(V)	(R)SSPVIIDASTAIDAPSNLR(F)	(K)ATGVFTTLQPLR(S)
(R)GEWAcIPYSQLR(D)	(R)TVLVTWTPPR(A)	(R)EESPPLIGQQATVSDIPR(D)	(R)ITGYIIK(Y)
(K)STATINNIKPGADYTITLYAVTGR(G)	(K)DDKESAPISDTVVPAVPPPTDLR(F)	(R)DLEVIASTPTSLLISWEPPAVSVR(Y)	(R)ITYGETGGNSPVQEFTVPGSK(S)
(R)TFYQIGDSWEK(F)	(R)FLTTTPNSLLVSWQAPR(A)	(K)YEVSVYALK(D)	(R)GVTYNIIVEALQNQR(R)
(K)YIVNVYQISEEGK(Q)	(R)SDNVPPPTDLQFVELTDVK(V)	(K)GLTPGVIYEGQLISIQQYGHR(E)	(K)LTcQcLGFGSGHFR(C)
(K)SEPLIGR(K)	(R)NLQPGSEYTVTLVAVK(G)	(R)VVTPLSPPTNLHLEANPDTGVLTVSWER(S)	

B). *Fn1* detected from the *Mouse Skin Tumors*
Protein identification probability: 100%;
Quantitative value (normalized total spectrum count): 342.680±65.337;
Quantitative value (LFQ intensity $\times 10^7$): 341.255±56.63;
Exclusive unique peptides detected for this protein:

(F)TAQWIAPSVQLTGYR(V)	(K)VGDTYERPK(D)	(R)GNLLQcVcTGNGR(G)	(R)TFYQIGDSWEK(F)
(K)ATGVFTTLQPLR(S)	(K)WcGTTQNYDADQK(F)	(R)HHAEHSVGRPR(Q)	(R)TFYScTTEGR(Q)
(K)ATGVFTTLQPLR(S)	(K)WcHDNGVNYK(I)	(R)IGDQWDK(Q)	(R)TTPPTAATPVR(L)
(K)cDPHEATcYDDGK(T)	(K)YEKPGSPPR(E)	(R)IGDTWSK(K)	(R)TVLVTWTPPR(A)
(K)cDPIDQcQDSETR(T)	(K)YEVSVYALK(D)	(R)IScTIANR(C)	(R)VTYSSPEDGIR(E)
(K)DSmIWDcTcIGAGR(G)	(K)YIVNVYQISEEGK(Q)	(R)ITGYIIK(Y)	(R)WLPSTSPVTGYR(V)
(K)EATIPGHLNSYTIK(G)	(K)YSFcTDHAVLVQTR(G)	(R)LSDAGFK(L)	(R)WSRPQAPITGYR(I)
(K)GEWTcKPIAEK(C)	(L)GVRPSQGGEAPR(E)	(R)RPHETGGY(M)	(R)YQcYcYGR(G)
(K)GLAFTDVDVDSIK(I)	(N)IIVEALQNQR(R)	(R)SISPDVR(S)	(W)NAPEPSHITK(Y)
(K)HYQINQQWER(T)	(N)SFTVHWVAPR(A)	(R)STTPDITGYR(I)	(Y)EKPGSPPR(E)
(K)IAWESPQGQVSR(Y)	(N)SLLVSWQAPR(A)	(R)SYTITGLQPGTDYK(I)	(R)TAIYQPQTHPQPAPY(G)
(K)IHLYTLNDNAR(S)	(R)APITGYIIR(H)	(R)GVTYNIIVEALQNQR(R)	(R)VEVLPVSLPGEHGQR(L)
(K)LGVRPSQGGEAPR(E)	(R)cHEGGQSYK(I)	(R)KYIVNVYQISEEGK(Q)	(R)VTDATETTITISWR(T)
(K)LTcQcLGFGSGHFR(C)	(R)DAPIVNR(V)	(R)PAQGVITTLENVSPPR(R)	(K)EYLGAIcScTcFGGQR(G)
(K)QYNVGPLASK(Y)	(R)FTNIGPDTMR(V)	(R)NLQPGSEYTVTLVAVK(G)	(R)TYLGNALVcTcYGGSR(G)
(K)SEPLIGR(K)	(R)GEWAcIPYSQLR(D)	(R)HALQSASAGSGSFTDVR(T)	(R)VTWAPPPSIELTNLLVR(Y)
(K)TYHVGEQWQK(E)	(R)ESNPLTAQQTTK(L)	(R)NLQPGSEYTVTLVAVKG(N)	(R)TAIYQPQTHPQPAPYGH(C)
(K)VFAVHQGR(E)	(R)GDSPASSKPVSINYK(T)	(R)PYLPNVDEEVQIGHVPR(G)	(N)SHPIQWNAPEPSHITK(Y)
(R)NTFAEITGLSPGVTYLFK(V)	(K)VTImWTPPDSVVSGYR(V)	(R)SDNVPPPTDLQFVELTDVK(V)	(K)EINLSPDSSSVIVSGLMVATK(Y)
(R)QDGHLWcSTTSNYEQDQK(Y)	(R)FLTTTPNSLLVSWQAPR(A)	(R)ITYGETGGNSPVQEFTVPGSK(S)	(K)ESAPISDTVVPAVPPPTDLR(F)
(R)NGESQPLVQTAVTNIDRPK(G)	(R)GFNcESKPEPEETcFDK(Y)	(R)GGNSNGALcHFPFLYNNR(N)	(R)EESPPLIGQQATVSDIPR(D)
(R)SSPVIIDASTAIDAPSNLR(F)	(R)SIPPYNTEVTETTIVITWTPAPR(I)	(R)RPGAAEPSPDGTTGHTYNQYTQR(Y)	(K)FSQVTPTSFTAQWIAPSVQLTGYR(V)
(K)TEIDKPSQMQVTDVQDNSISVR(W)	(K)FGFcPmAAHEEIcTTNEGVmYR(I)	(R)NSITLTNLNPGTEYVVSIIAVNGR(E)	(K)DDKESAPISDTVVPAVPPPTDLR(F)
(K)TETITGFQVDAIPANGQTPVQR(S)	(K)GLTPGVIYEGQLISIQQYGHR(E)	(R)PGVTEATITGLEPGTEYTIYVIALK(N)	(K)DTLTSRPAQGVITTLENVSPPR(R)
(K)TGLDSPTGFDSSDITANSFTVH(W)	(N)LLPGTEYLVSVSSVYEQHESIPLR(G)	(R)PRPGVTEATITGLEPGTEYTIYVIALK(N)	(R)TKTETITGFQVDAIPANGQTPVQR(S)
(K)TGLDSPTGFDSSDITANSFTVH(W)	(R)DLEVIASTPTSLLISWEPPAVSVR(Y)	(R)NTFAEITGLSPGVTYLFKVFAVHQGRESNPLTAQQTTK(L)	(R)TNTNVNcPIEcFMPLDVQADR(D)
(K)STATINNIKPGADYTITLYAVTGR(G)	(R)EVTSDSGSIVVSGLTPGVEYTYTIQVLR(D)	(K)QSLILSTSQTTAPDAPPDPTVDQVDDTSIVVR(W)	(R)VEYELSEEGDEPQYLDLPSTATSVNIPDLLPGR(K)
(K)TGLDSPTGFDSSDITANSFTVHWVAPR(A)	(Q)TYPGTTGPVQVIITETPSQPNSHPIQWNAPEPSHITK(Y)	(K)TGPMKEINLSPDSSsVIVsGLMVATKYEVsVYALK(D)	(R)VEYELSEEGDEPQYLDLPSTATSVNIPDLLPGRK(Y)
(K)TASPDQTEmTIEGLQPTVEYVVSVYAQNR(N)	(R)EEVVTVGNAVSEGLNQPTDDScFDPYTVSHYAIGEEWER(L)	(K)TPFITNPGYDTENGIQLPGTTHQQPSVGQQMIFEEHGFR(R)	(R)VVTPLSPPTNLHLEANPDTGVLTVSWER(S)
(K)TDELPQLVTLPHPNLHGPEILDVPSTVQK(T)	(K)VREEVVTVGNAVSEGLNQPTDDScFDPYTVSHYAIGEEWER(L)	(K)NEEDVAELSISPSDNAVVLTNLLPGTEYLVSVSSVYEQHESIPLR(G)	(R)TAIYQPQTHPQPAPYGHcVTDSGVVYSVGmQWLK(S)
(K)KTDELPQLVTLPHPNLHGPEILDVPSTVQK(T)			

Biomarker 6: *Mcam_* melanoma cell adhesion molecule [*Mus musculus (house mouse)*], UniProt accession Q8R2Y2;

A). *Mcam* detected from *Healthy Mouse Skins*
Protein identification probability: 100%;
Quantitative value (normalized total spectrum count): 23.653±3.20612;
Quantitative value (LFQ intensity $\times 10^7$): 22.634±2.915;
Exclusive unique peptides detected for this protein:

(R)QILIFR(V)	(R)EVATcVGR(N)	(K)APEEPTIQANVVGIHVDR(Q)	(K)VWVEVEPVGLLK(E)
(R)LQDHYVELQVFK(A)	(K)GPVLQLNNVR(R)	(K)QPVPTPDLVEAEVGSTALLK(C)	

B). *Mcam* detected from the *T70 mouse*
Protein identification probability: 100%;
Quantitative value (normalized total spectrum count): 97.715±3.703;
Quantitative value (LFQ intensity $\times 10^7$): 97.369±3.564;
Exclusive unique peptides detected for this protein:

(K)DAQFYcELSYR(L)	(K)QEITLPPTR(K)	(R)YLcMASVPR(V)	(R)TQLVSVGIFGSPWMALK(E)
(K)EGDHVTIR(C)	(K)SEFVVEVK(S)	(K)VWVEVEPVGLLK(E)	(R)VHIQSSQIVESSGLYTLK(S)
(K)EVTVPVFYPAEK(V)	(R)DKTGQLLGK(G)	(R)LQDHYVELQVFK(A)	(R)cLTDGNPQPHFTINK(K)
(K)GPVLQLNNVR(R)	(R)EPGEYEHR(L)	(R)NGYPIPQVLWYK(N)	(R)cLTDGNPQPHFTINKK(D)
(K)GVVIVAVIVcT(L)	(R)EVATcVGR(N)	(K)EDKDAQFYcELSYR(L)	(K)APEEPTIQANVVGIHVDR(Q)
(K)KLPQPESK(G)	(R)KSEFVVEVK(S)	(R)cLTDGNPQPHFTIN(K)	(K)QPVPTPDLVEAEVGSTALLK(C)
(K)LPQPESK(G)	(R)QILIFR(V)	(R)EAGGRYLcMASVPR(V)	(R)LSLQDSVATLALSHVTPHDER(M)
(K)NSLPLQEEENR(V)			

Data File S4. Proteomic data for the assignment of exosomal mass spectral peaks

Intact proteins were extracted from the mouse blood exosomes, and afterwards subjected to top-down proteomic analysis. The exosome fingerprint peaks measured by MALDI-TOF MS were tentatively assigned to proteins by correlation with the top-down proteomic data. Results obtained from the mouse carrying 182 mm^2 tumor (T182 mouse) were shown below as the representative. In order to further confirm the protein identities, the T182 mouse blood exosomes were also subjected to bottom-up proteomic analysis, which analyzed the digestion products (peptides) of the exosome proteins using liquid chromatography-tandem mass spectrometry.

Peak 2. *HC-II* (*Serpind1*) _ heparin cofactor 2 [*Mus musculus* (house mouse)], fragment, UniProt accession number P49182;

A). MALDI-TOF MS peak: 4,190 *m/z*;

B). Top-down proteomic analysis: precursor monoisotopic mass 4187.192343 Da, adjusted precursor monoisotopic mass 4187.181195 Da, theoretical average mass 4189.888 Da, number of matched fragment ions 17, E value 5.49E-17, P value 5.49E-17, protein sequencing:

L.STQVRFTVDRPFLFLVYEHRTSCLLFMGKVTNPAKS.

C). Bottom-up proteomic analysis: 100% identification, 20 exclusive unique peptides, 35 exclusive unique spectra, 117 total spectra, 261/478 amino acids (55% coverage), the theoretical full protein sequence shown below (the detected peptide sequences were underlined):

MKHPLCTLLS LITFMCIGSK GLAEQLTNEN LTTSFLPANF HKENTVTNDW IPEGEEDEDY LDLEKLLGED
DDYIYIIDAV SPTDSESSAG NILQLFQGKS RIQRLNILNA KFAFNLYRVL KDQATTSDNL FIAPVGISTA
MGMISLGLRG ETHEEVHSVL HFRDFVNASS KYEVTTIHNL FRKLTHRLFR RNFGYTLRSV NGLYIQKQFP
IREDFKAAMR EFYFAEAQEA NFPDPAFISK ANNHILKLTK GLIKEALENI DPATQMLILN CIYFKGTWVN
KFPVEMTHNH NFRLNEREVV KVSMMQTKGN FLAANDQELD CDILQLEYVG GISMLIVVPR KLSGMKTLEA
QLTPQVVERW QKSMTNRTRE VLLPKFKLEK NYNLVEVLKS MGITKLFNKN GNMSGISDQR IAIDLFKHQS
TITVNEEGTQ AAAVTTVGFM PLSTQVRFTV DRPFLFLVYE HRTSCLLFMG KVTNPAKS

Peak 1&5. *C3* _ complement component 3 [*Mus musculus* (house mouse)], fragments, UniProt accession number P01027;

A). MALDI-TOF MS peak: 3,419 *m/z*; 8,715 *m/z*;

B-1). Top-down proteomic analysis: precursor monoisotopic mass 3418.815759 Da, adjusted precursor monoisotopic mass 3418.820805 Da, theoretical average mass 3420.847 Da, number of matched fragment ions 21, E value 7.43E-18, P value 7.43E-18, protein sequencing:

R.SEETKQNEAFSLTAKGKGRGTLSVVAVYHAKL.K

B-2). Top-down proteomic analysis: precursor monoisotopic mass 8708.24276 Da, adjusted precursor monoisotopic mass 8708.247625 Da, theoretical average mass 8714.096 Da, number of matched fragment ions 8, E value 1.76E-7, P value 1.76E-7, protein sequencing:

R.SVQLMERRMDKAGQYTDKGLRKCCEDGMRDIPMRYSCQRRARLITQGENCIKAFIDCCNHITKLREQHRRDHV.L

C). Bottom-up proteomic analysis: 100% identification, 244 exclusive unique peptides, 429 exclusive unique spectra, 2964 total spectra, 1358/1663 amino acids (82% coverage), the theoretical full protein sequence shown below (the detected peptide sequences were underlined):

MGPASGSQLL VLLLLLASSP LALGIPMYSI ITPNVLRLES EETIVLEAHD AQGDIPVTVT VQDFLKRQVL
TSEKTVLTGA SGHLRSVSIK IPASKEFNSD KEGHKYVTVV ANFGETVVEK AVMVSFQSGY LFIQTDKTIY
TPGSTVLYRI FTVDNNLLPV GKTVVILIET PDGIPVKRDI LSSNNQHGIL PLSWNIPELV NMGQWKIRAF
YEHAPKQIFS AEFEVKEYVL PSFEVRVEPT ETFYYIDDPN GLEVSIIAKF LYGKNVDGTA FVIFGVQDGD
KKISLAHSLT RVVIEDGVGD AVLTRKVLME GVRPSNADAL VGKSLYVSVT VILHSGSDMV EAERSGIPIV
TSPYQIHFTK TPKFFKPAMP FDLMVFVTNP DGSPASKVLV VTQGSNAKAL TQDDGVAKLS INTPNSRQPL
TITVRTKKDT LPESRQATKT MEAHPYSTMH NSNNYLHLSV SRMELKPGDN LNVNFHLRTD PGHEAKIRYY
TYLVMNKGKL LKAGRQVREP GQDLVVLSLP ITPEFIPSFR LVAYYTLIGA SGQREVVADS VWVDVKDSCI
GTLVVKGDPR DNHLAPGQQT TLRIEGNQGA RVGLVAVDKG VFVLNKKNKL TQSKIWDVVE KADIGCTPGS
GKNYAGVFMD AGLAFKTSQG LQTEQRADLE CTKPAARRRR SVQLMERRMD KAGQYTDKGL RKCCEDGMRD
IPMRYSCQRR ARLITQGENC IKAFIDCCNH ITKLREQHRR DHVLGLARSE LEEDIIPEED IISRSHFPQS
WLWTIEELKE PEKNGISTKV MNIFLKDSIT TWEILAVSLS DKKGICVADP YEIRVMQDFF IDLRLPYSVV
RNEQVEIRAV LFNYREQEEL KVRVELLHNP AFCSMATAKN RYFQTIKIPP KSSVAVPYVI VPLKIGQQEV
EVKAAVFNHF ISDGVKKTLK VVPEGMRINK TVAIHTLDPE KLGQGGVQKV DVPAADLSDQ VPDTDSETRI
ILQGSPVVQM AEDAVDGERL KHLIVTPAGC GEQNMIGMTP TVIAVHYLDQ TEQWEKFGIE KRQEALELIK
KGYTQQLAFK QPSSAYAAFN NRPPSTWLTA YVVKVFSLAA NLIAIDSHVL CGAVKWLILE KQKPDGVFQE
DGPVIHQEMI GGFRNAKEAD VSLTAFVLIA LQEARDICEG QVNSLPGSIN KAGEYIEASY MNLQRPYTVA
IAGYALALMN KLEEPYLGKF LNTAKDRNRW EEPDQQLYNV EATSYALLAL LLLKDFDSVP PVVRWLNEQR
YYGGGYGSTQ ATFMVFQALA QYQTDVPDHK DLNMDVSFHL PSRSSATTFR LLWENGNLLR SEETKQNEAF
SLTAKGKGRG TLSVVAVYHA KLKSKVTCKK FDLRVSIRPA PETAKKPEEA KNTMFLEICT KYLGDVDATM
SILDISMMTG FAPDTKDLEL LASGVDRYIS KYEMNKAFSN KNTLIIYLEK ISHTEEDCLT FKVHQYFNVG
LIQPGSVKVY SYYNLEESCT RFYHPEKDDG MLSKLCHSEM CRCAEENCFM QQSQEKINLN VRLDKACEPG
VDYVYKTELT NIELLDDFDE YTMTIQQVIK SGSDEVQAGQ QRKFISHIKC RNALKLQKGK KYLMWGLSSD
LWGEKPNTSY IIGKDTWVEH WPEAEECQDQ KYQKQCEELG AFTESMVVYG CPN

Peak 3&6. *Fga* _ fibrinogen alpha chain [*Mus musculus* (house mouse)], fragments, UniProt accession number E9PV24;

A). MALDI-TOF MS peak: 4605 *m/z*; 9,320 *m/z*;

B-1). Top-down proteomic analysis: precursor monoisotopic mass 4600.198195 Da, adjusted precursor monoisotopic mass 4600.333195 Da, theoretical average mass 4603.007 Da, number of matched fragment ions 17, E value 2.77E-11 , P value 2.77E-11 , protein sequencing:

K.EFGSKTHSDSDIL(T)[35.09232]NIEDPSSHVPEFSSSSKTSTVKKQVTKT.Y

B-2). Top-down proteomic analysis: precursor monoisotopic mass 9316.284822 Da, adjusted precursor monoisotopic mass 9316.290325 Da, theoretical average mass 9322.150 Da, number of matched fragment ions 53, E value 3.52E-41, P value 3.52E-41, protein sequencing:

T.TDTEDKGEFLSEGGGVRGPRVVERHQSQCKDSDWPFCSDDDWNHKCPSGCRMKGLIDEANQDFTNRINKLKNSLFDFQ
RNN.K

C). Bottom-up proteomic analysis: 100% identification, 141 exclusive unique peptides, 256 exclusive unique spectra, 1763 total spectra, 646/789 amino acids (82% coverage), the theoretical full protein sequence shown below (the detected peptide sequences were underlined):

MLSLRVTCLI LSVASTVWTT DTEDKGEFLS EGGGVRGPRV VERHQSQCKD SDWPFCSDDD WNHKCPSGCR
MKGLIDEANQ DFTNRINKLK NSLFDFQRNN KDSNSLTRNI MEYLRGDFAN ANNFDNTYGQ VSEDLRRRIE
ILRRKVIEKA QQIQALQSNV RAQLIDMKRL EVDIDIKIRS CKGSCSRAVN REINLQDYEG HQKQLQQVIA
KELLPTKDRQ YLPALKMSPV PDLVPGSFKS QLQEAPPEWK ALTEMRQMRM ELERPGKDGG SRGDSPGDSR
GDSRGDFATR GPGSKAENPT NPGPGGSGYW RPGNSGSGSD GNRNPGTTGS DGTGDWGTGS PRPGSDSGNF
RPANPNWGVF SEFGDSSSPA TRKEYHTGKA VTSKGDKELL IGKEKVTSSG TSTTHRSCSK TITKTVTGPD
GRREVVKEVI TSDDGSDCGD ATELDISHSF SGSLDELSER HPDLSGFFDN HFGLISPNFK EFGSKTHSDS
DILTNIEDPS SHVPEFSSSS KTSTVKKQVT KTYKMADEAG SEAHREGETR NTKRGRARAR PTRDCDDVLQ
TQTSGAQNGI FSIKPPGSSK VFSVYCDQET SLGGWLLIQQ RMDGSLNFNR TWQDYKRGFG SLNDKGEGEF
WLGNDYLHLL TLRGSVLRVE LEDWAGKEAY AEYHFRVGSE AEGYALQVSS YRGTAGDALV QGSVEEGTEY

TSHSNMQFST FDRDADQWEE NCAEVYGGGW WYNSCQAANL NGIYYPGGTY DPRNNSPYEI ENGVVWVPFR GADYSLRAVR MKIRPLVGQ

Peak 7. *Hp* _ haptoglobin [*Mus musculus* (house mouse)], fragment, UniProt accession number Q61646;

A). MALDI-TOF MS peak: 9,468 *m/z*;

B). Top-down proteomic analysis: precursor monoisotopic mass 9462.497426 Da, adjusted precursor monoisotopic mass 9462.511675 Da, theoretical average mass 9468.546 Da, number of matched fragment ions 18, E value 5.10E-9, P value 5.10E-9, protein sequencing:

A.VELGNDAMDFEDDSCPKPPEIANGYVEHLVRYRCRQFYRLRAEGDGVYTLNDEKQWVNTVAGEKLPECEAVCGKPKHP VDQVQ.R

C). Bottom-up proteomic analysis: 100% identification, 82 exclusive unique peptides, 140 exclusive unique spectra, 1408 total spectra, 286/347 amino acids (82% coverage), the theoretical full protein sequence shown below (the detected peptide sequences were underlined):

MRALGAVVTL LLWGQLFAVE LGNDAMDFED DSCPKPPEIA NGYVEHLVRY RCRQFYRLRA EGDGVYTLND EKQWVNTVAG EKLPECEAVC GKPKHPVDQV QRIIGGSMDA KGSFPWQAKM ISRHGLTTGA TLISDQWLLT TAKNLFLNHS ETASAKDITP TLTLYVGKNQ LVEIEKVVLH PNHSVVDIGL IKLKQRVLVT ERVMPICLPS KDYIAPGRVG YVSGWGRNAN FRFTDRLKYV MLPVADQDKC VVHYENSTVP EKKNLTSPVG VQPILNEHTF CAGLTKYQED TCYGDAGSAF AIHDMEEDTW YAAGILSFDK SCAVAEYGVY VRATDLKDWV QETMAKN

Peak 8. (Probably) *Saa1* & *Saa2* _ serum amyloid A-1 & A-2 [*Mus musculus* (house mouse)], UniProt accession number P05366 & P05367

A). MALDI-TOF MS peak: 11,660 *m/z*, 11,755 *m/z*;

B). Top-down proteomics did not detect any protein in the mass range of 11-14 kDa. However, the bottom-up proteomics detected a high abundance of *Saa1* and *Saa2* around this mass from the tumor mouse. A total of 149 and 143 normalized total spectra of *Saa1* and *Saa2* were detected from the tumor mouse, while the values from the healthy mouse were only 21 and 4, respectively.

C-1). Bottom-up proteomic analysis for *Saa2*: 100% identification, 8 exclusive unique peptides, 18 exclusive unique spectra, 67 total spectra, 86/122 amino acids (70% coverage), the theoretical full protein sequence shown below (the detected peptide sequences were underlined):

MKLLTSLVFC SLLLGVCHGG FFSFIGEAFQ GAGDMWRAYT DMKEAGWKDG DKYFHARGNY DAAQRGPGGV WAAEKISDAR ESFQEFFGRG HEDTMADQEA NRHGRSGKDP NYYRPPGLPA KY

According to the peak *m/z* value, the sequence detected by MALDI-TOF MS is estimated to be

.GGFFSFIGEAFQGAGDMWRAYTDMKEAGWKDGDKYFHARGNYDAAQRGPGGVWAAEKISDARESFQEFFGRGHEDTMAD QEANRHGRSGKDPNYYRPPGLPAKY (theoretical monoisotopic mass 11655.379 Da, theoretical average mass 11662.647 Da)

C-2). Bottom-up proteomic analysis for *Saa1*: 100% identification, 12 exclusive unique peptides, 21 exclusive unique spectra, 114 total spectra, 85/122 amino acids (70% coverage), the theoretical full protein sequence shown below (the detected peptide sequences were underlined):

MKLLTSLVFC SLLLGVCHGG FFSFVHEAFQ GAGDMWRAYT DMKEANWKNS DKYFHARGNY DAAQRGPGGV WAAEKISDGR EAFQEFFGRG HEDTIADQEA NRHGRSGKDP NYYRPPGLPD KY

According to the peak *m/z* value, the sequence detected by MALDI-TOF MS is estimated to be

G.GFFSFVHEAFQGAGDMWRAYTDMKEANWKNSDKYFHARGNYDAAQRGPGGVWAAEKISDGREAFQEFFGRGHEDTIAD QEANRHGRSGKDPNYYRPPGLPDKY (theoretical monoisotopic mass 11746.450 Da, theoretical average mass 11753.697 Da)

Peak 4&9. *Hba-a1* _ hemoglobin subunit alpha [*Mus musculus* (house mouse)], UniProt accession number P01942;

A). MALDI-TOF MS peak: 5845 *m/z*, 14,975 *m/z*;

B-1).Top-down proteomic analysis: precursor monoisotopic mass 5842.106765 Da, adjusted precursor monoisotopic mass 5842.281765 Da, theoretical average mass 5845.944 Da, number of matched fragment ions 7, E value 5.58E-5, P value 5.58E-5, protein sequencing:

A.(HKLRVDPVNFKLLSHCLLVTLASHHPADFTPAVH)[-36.90064]ASLDKFLASVSTVLTSKY R.

B-2).Top-down proteomic analysis: precursor monoisotopic mass 14971.75934 Da, adjusted precursor monoisotopic mass 14971.68434 Da, theoretical average mass 14981.061 Da, number of matched fragment ions 9, E value 3.39E-9, P value 3.39E-9, protein sequencing:

.MVLSGEDKSNIKAAWGKIGGHGAEYGAEALERMFASFPTTKTYFPHFDVSHGSAQVKGHGKKVADALASAAGHLDDLPG
ALSALSDLHAHKLRVDPVNFKLLSHCLL(VTLASHHPADFTPAVHASLDKFL)[-104.07597]ASVSTVLTSKY R.

C). Bottom-up proteomic analysis: 100% identification, 42 exclusive unique peptides, 61 exclusive unique spectra, 388 total spectra, 120/142 amino acids (85% coverage), the theoretical full protein sequence shown below (the detected peptide sequences were underlined):

MVLSGEDKSN IKAAWGKIGG HGAEYGAEAL ERMFASFPTT KTYFPHFDVS HGSAQVKGHG KKVADALASA
AGHLDDLPGA LSALSDLHAH KLRVDPVNFK LLSHCLLVTL ASHHPADFTP AVHASLDKFL ASVSTVLTSK YR

Peak 10. *Hbb-b2* _ hemoglobin subunit beta-2 [*Mus musculus* (house mouse)], UniProt accession number P02089;

A). MALDI-TOF MS peak: 15,615 *m/z*;

B).Top-down proteomic analysis: precursor monoisotopic mass 15606.13787 Da, adjusted precursor monoisotopic mass 15606.17787 Da, theoretical average mass 15615.986 Da, number of matched fragment ions 6, E value 8.88E-6, P value 8.88E-6, protein sequencing:

M.VHLTDAEKSAVSCLWAKVNPDEVGGEALGRLLVVYPWTQRYFDSFGDLSSASAIMGNPKVKAHGKKVITAFNEGLKNL
DNLKGTFASLSELHCDKLHVDPENFRLLGNAIVIVLGHHLGKDF(TPAAQAAFQKVVAGVAT)[-131.03510]A
LAHKYH.

C). Bottom-up proteomic analysis identified this protein as hemoglobin subunit beta *Hbb-bs* (UniProt accession A8DUK4): 100% identification, 39 exclusive unique peptides, 64 exclusive unique spectra, 800 total spectra, 124/147 amino acids (84% coverage), the theoretical full protein sequence shown below (the detected peptide sequences were underlined):

MVHLTDAEKA AVSGLWGKVN ADEVGGEALG RLLVVYPWTQ RYFDSFGDLS SASAIMGNAK VKAHGKKVIT
AFNDGLNHLD SLKGTFASLS ELHCDKLHVD PENFRLLGNM IVIVLGHHLG KDFTPAAQAA FQKVVAGVAA
ALAHKYH

References

1. Dankort, D.; Curley, D. P.; Cartlidge, R. A.; Nelson, B.; Karnezis, A. N.; Damsky, W. E.; You, M. J.; DePinho, R. A.; McMahon, M.; Bosenberg, M., Braf(V600E) cooperates with Pten loss to induce metastatic melanoma. *Nat Genet* **2009,** *41* (5), 544-552.
2. Cheng, W. C.; Tsui, Y. C.; Ragusa, S.; Koelzer, V. H.; Mina, M.; Franco, F.; Laubli, H.; Tschumi, B.; Speiser, D.; Romero, P.; Zippelius, A.; Petrova, T. V.; Mertz, K.; Ciriello, G.; Ho, P. C., Uncoupling protein 2 reprograms the tumor microenvironment to support the anti-tumor immune cycle. *Nat Immunol* **2019,** *20* (4), 206-217.
3. Zhu, Y. D.; Qiao, L.; Prudent, M.; Bondarenko, A.; Gasilova, N.; Moller, S. B.; Lion, N.; Pick, H.; Gong, T. Q.; Chen, Z. X.; Yang, P. Y.; Loveyf, L. T.; Girault, H. H., Sensitive and fast identification of bacteria in blood samples by immunoaffinity mass spectrometry for quick BSI diagnosis. *Chem Sci* **2016,** *7* (5), 2987-2995.
4. Yang, Y.; Lin, Y.; Chen, Z. X.; Gong, T. Q.; Yang, P. Y.; Girault, H.; Liu, B. H.; Qiao, L., Bacterial Whole Cell Typing by Mass Spectra Pattern Matching with Bootstrapping Assessment. *Anal Chem* **2017,** *89* (22), 12556-12561.
5. Lademann, J.; Jacobi, U.; Surber, C.; Weigmann, H. J.; Fluhr, J. W., The tape stripping procedure - evaluation of some critical parameters. *Eur J Pharm Biopharm* **2009,** *72* (2), 317-323.
6. Weinstein, D.; Leininger, J.; Hamby, C.; Safai, B., Diagnostic and prognostic biomarkers in melanoma. *J Clin Aesthet Dermatol* **2014,** *7* (6), 13-24.
7. Miller, A. J.; Mihm Jr, M. C., Melanoma. *New Engl J Med* **2006,** *355* (1), 51-65.